

SKELETAL MUSCLE STEM CELLS FOR CARDIAC REPAIR

by

Thomas Richard Payne

BS, Benedictine University, 2000

Submitted to the Graduate Faculty of
School of Engineering in partial fulfillment
of the requirements for the degree of
Doctor of Philosophy

University of Pittsburgh

2005

UNIVERSITY OF PITTSBURGH
SCHOOL OF ENGINEERING

This dissertation was presented

by

Thomas Richard Payne

It was defended on

November 29, 2005

and approved by

Bradley B. Keller, MD, Professor, Pediatric Cardiology

Bruno Péault, PhD, Professor, Pediatrics

Sanjeev G. Shroff, PhD, Professor, Bioengineering

William R. Wagner, PhD, Associate Professor, Bioengineering

Dissertation Director: Johnny Huard, PhD, Associate Professor, Orthopedic Surgery and

Bioengineering

Copyright © by Thomas Richard Payne

2005

SKELETAL MUSCLE STEM CELLS FOR CARDIAC REPAIR

Thomas R. Payne, PhD

University of Pittsburgh, 2005

Because current treatments have had limited success in reducing morbidity and mortality associated with heart failure, the transplantation of cells into the heart has emerged as a potential therapy to repair damaged myocardium and reverse end-stage heart failure. While an array of lineage-committed cell types has been evaluated for experimental cardiac cell transplantation, recent studies have focused on adult stem cells due to their capacity for self-renewal and potential for multilineage differentiation. Here we investigated the application of postnatal murine skeletal muscle–derived stem cells (MDSCs) for cardiac cell therapy. We initially tested the ability of MDSCs to regenerate cardiac muscle after intramyocardial injection into the hearts of dystrophin-deficient *mdx* mice, a model of cardiomyopathy and muscular dystrophy. After transplantation, we observed that MDSCs generated large persistent grafts consisting primarily of numerous skeletal muscle myocytes and, to a substantially lesser degree, donor-derived cardiomyocytes, which were primarily located at the graft–host myocardium border. Further experiments revealed that more than half of these donor-derived cardiomyocytes resulted from the fusion of transplanted MDSCs with host cardiomyocytes. Next, we investigated the therapeutic potential of MDSC transplantation for cardiac repair using a mouse model for acute myocardial infarction. We report that in comparison with committed skeletal myoblast– and control saline-injected hearts, MDSCs implanted into infarcted hearts elicited significant improvements in cardiac performance. This beneficial effect was partially attributed to the ability

of MDSCs to induce neovascularization of ischemic myocardium. In the final study, we investigated the mechanism by which transplanted MDSCs contribute to revascularization of ischemic myocardium. To address this issue, we employed a gain- and loss-of-function approach using MDSCs genetically engineered to express the potent angiogenic factor vascular endothelial growth factor (VEGF) or the anti-angiogenic factor soluble Flt1, a VEGF-specific antagonist. When we transplanted MDSCs expressing soluble Flt1, we observed significantly less neoangiogenesis and a significant decrease in cardiac function when compared to the transplantation of control MDSCs and VEGF-engineered MDSCs. These results suggest that the transplantation of MDSCs elicits improvements in cardiac performance by inducing neovascularization of ischemic myocardium through the secretion of VEGF. In conclusion, these results suggest that MDSCs represent a promising cell type for cardiac repair and further translational research is warranted.

TABLE OF CONTENTS

TABLE OF CONTENTS	VI
LIST OF TABLES	XI
LIST OF FIGURES	XII
PREFACE.....	XIV
1.0 INTRODUCTION.....	1
1.1 SIGNIFICANCE.....	1
1.2 CELL THERAPY FOR CARDIAC REGENERATION AND REPAIR.....	2
1.2.1 Cellular Cardiomyoplasty	2
1.2.2 Skeletal Myoblasts for Cardiac Cell Transplantation.....	4
1.2.3 Skeletal Muscle–Derived Stem Cells: Potential for Tissue Regeneration	7
1.3 PROJECT OBJECTIVES	7
1.3.1 Objective #1: Evaluate the Cardiogenic Potential of MDSCs	7
1.3.2 Objective #2: MDSCs for Myocardial Infarct Repair.....	8
1.3.3 Objective #3: Mechanism of Cell Therapy: Role of VEGF.....	9
2.0 FATE OF MDSCS AFTER INTRAMYOCARDIAL TRANSPLANTATION ..	11
2.1 INTRODUCTION	11
2.2 RESULTS.....	12
2.2.1 Characterization of the nLacZ-Expressing MDSCs In Vitro.....	12

2.2.2	Validation of Cardiac and Skeletal Muscle–Specific Markers	15
2.2.3	MDSCs Generate Large Grafts in the <i>mdx</i> Heart	15
2.2.4	Donor-derived Cells Express Cardiac Markers.....	18
2.2.5	Use of <i>LacZ</i> to Validate Donor Origin of Dytrophin ⁺ Cardiomyocytes.	18
2.2.6	Donor Cells with a Hybrid Cardiac and Skeletal Muscle Phenotype	21
2.2.7	Evaluation of Fusion between MDSCs and Host Cardiomyocytes	22
2.2.8	Evaluation of Connexin43 Gap Junction Protein Expression	25
2.2.9	Assessment of Scar Tissue in the Graft Area	26
2.2.10	Donor Cells Contribute to Blood Vessel Structures in the Heart.....	27
2.3	DISCUSSION.....	28
2.3.1	Fusion of MDSCs with Host Cardiomyocytes	29
2.3.2	Evidence for Potential Nuclear Fusion.	29
2.3.3	Cardiac Differentiation of MDSC without Cellular Fusion.....	30
2.3.4	Gap Junction Formation for Electromechanical Coupling	31
2.3.5	Scar Tissue Formation.....	31
2.3.6	Donor Cell Contribution to Blood Vessels in the Graft.....	32
2.4	CONCLUSIONS	32
2.5	METHODS.....	33
2.5.1	Animals	33
2.5.2	Isolation and Culture of MDSCs	34
2.5.3	MDSCs Transduced to Express the nLacZ Reporter Gene.....	34
2.5.4	Intracardiac Cell Transplantation	35
2.5.5	Histology and Trichrome Staining	35

2.5.6	Staining for both Cardiac and Skeletal Muscle–Specific Markers	35
2.5.7	Detection of Cellular Fusion	36
2.5.8	Microscopy.....	37
3.0	CELL THERAPY FOR MYOCARDIAL INFARCTION: SKELETAL MUSCLE STEM CELLS VERSUS COMMITTED SKELETAL MYOBLASTS	38
3.1	INTRODUCTION	38
3.2	RESULTS	40
3.2.1	MDSCs are Less Committed to the Myogenic Lineage than Myoblasts	40
3.2.2	MDSCs Generate Larger Grafts than Myoblasts after Implantation ...	41
3.2.3	MDSCs Improve Cardiac Function More Effectively than Myoblasts..	43
3.2.4	Both MDSCs and Myoblasts Acquired a Cardiac Phenotype	45
3.2.5	Expression of a Hybrid Cardiac and Skeletal Muscle Phenotype.....	45
3.2.6	Size of Donor-derived Cells that Acquired a Cardiac Phenotype.....	47
3.2.7	Donor Cells Acquire a Cardiac Phenotype through Fusion.	47
3.2.8	Donor Cells Express the Gap Junction Protein Connexin43	48
3.2.9	Induction of Neoangiogenesis by the Implanted Cells.....	50
3.2.10	Differentiation of MDSC into New Vasculature.	50
3.2.11	Donor Cells Express Vascular Endothelial Growth Factor (VEGF).....	52
3.3	DISCUSSION.....	53
3.3.1	Cell Engraftment and Persistence	54
3.3.2	Adoption of a Cardiac Phenotype	56
3.3.3	Functional Improvement.....	56
3.3.4	Neovascularization Elicited by Cell Transplantation.....	58

3.4	CONCLUSIONS	59
3.5	MATERIAL AND METHODS	59
3.5.1	Animals	59
3.5.2	Isolation, Characterization, and Expansion of MDSCs and Myoblasts	60
3.5.3	Cell Transduction with the nLacZ Reporter Gene	60
3.5.4	Myocardial Infarction and Cell Transplantation	61
3.5.5	Histology and Immunohistochemistry	61
3.5.6	Estimate of nLacZ[+] Cells in Hearts after Infarction	62
3.5.7	Echocardiography	62
3.5.8	Mouse Y-chromosome Fluorescence In Situ Hybridization	63
3.5.9	Analysis of Angiogenesis	63
3.5.10	Statistical Analysis	64
4.0	TRANSPLANTED MDSCS IMPROVE CARDIAC FUNCTION AFTER MYOCARDIAL INFARCTION BY INDUCING NEOVASCULARIZATION OF ISCHEMIC MYOCARDIUM THROUGH THE SECRETION OF VEGF..	65
4.1	INTRODUCTION	65
4.2	RESULTS	66
4.2.1	Hypoxia and Cyclic Stretch Stimulate VEGF Secretion from MDSCs .	66
4.2.2	In vivo Study Design	69
4.2.3	Secretion of VEGF from MDSCs Induces Neovascularization	71
4.2.4	Effect of VEGF and sFlt1 on the Transplantation Capacity of MDSCs	74
4.2.5	Evaluation of Cardiac Function by Echocardiography	75
4.3	DISCUSSION	78
4.4	CONCLUSIONS	78

4.5	MATERIALS AND METHODS	79
4.5.1	Cell Culture and Transduction with Retroviral Vectors	79
4.5.2	In vitro Stimulation of MDSCs with Hypoxia and Cyclic Stretch	79
4.5.3	Myocardial Infarction and Cell Transplantation	80
4.5.4	Echocardiography	80
4.5.5	Tissue Processing and Immunohistochemical Stainings	81
4.5.6	Image Analysis	81
4.5.7	Statistical Analysis	82
5.0	CONCLUSIONS	83
5.1	FUTURE DIRECTIONS.....	84
5.1.1	Identification of Muscle Stem Cells from Human Skeletal Muscle.....	84
5.1.2	Comparision of Different Adult Stem Cell Types for Cardiac Repair ..	84
5.1.3	Cell Therapy for Chronic Models of Ischemic Cardiomyopathy.....	85
5.1.4	Alternatives to Cell-based Therapies	85
APPENDIX A		86
APPENDIX B		88
APPENDIX C		90
APPENDIX D.....		92
BIBLIOGRAPHY		94

LIST OF TABLES

Table 2.1: Frequency of donor cells expressing a cardiac phenotype in the heart.	20
Table 4.1: Fast sk. MHC graft area (mm ²).....	75

LIST OF FIGURES

Figure 1.1: The autologous cell and gene therapy approach for cardiac repair.	5
Figure 2.1: Validation of donor-specific markers and of cardiac and skeletal muscle-specific antibodies.	14
Figure 2.2: Engraftment and expression of a skeletal muscle phenotype by MDSCs in mdx/SCID hearts.	17
Figure 2.3: Donor-derived dystrophin ⁺ myocytes expressing a cardiac phenotype.	19
Figure 2.4: Colocalization of donor- and cardiac-specific markers in cells within MDSC-injected hearts.	20
Figure 2.5: Expression of hybrid cardiac and skeletal muscle phenotype by donor-derived myocytes.	22
Figure 2.6: Transplanted MDSCs fuse with host cardiomyocytes.	24
Figure 2.7: Connexin43 gap junction staining.	25
Figure 2.8: Presence of scar tissue at the border of the graft and the host myocardium.	27
Figure 2.9: Double staining for CD31, an endothelial-specific marker, and nLacZ.	28
Figure 3.1: MDSCs display superior engraftment in infarcted hearts when compared with myoblasts.	42
Figure 3.2: MDSCs prevent remodeling and improve cardiac function more effectively than myoblasts.	44
Figure 3.3: Donor cells within the injured myocardium adopt a cardiac phenotype.	46
Figure 3.4: Donor cells fusion with host cardiomyocytes.	48
Figure 3.5: Half of the donor cells that acquire a cardiac phenotype express connexin43.	49

Figure 3.6: Analysis of neoangiogenesis within the infarcted hearts.	51
Figure 3.7: Transplanted cells express VEGF in the infarct.	53
Figure 4.1: Hypoxia and cyclic stretch stimulate stem cells to secrete VEGF.	68
Figure 4.2: Experimental design to test the VEGF paracrine effect hypothesis.....	70
Figure 4.3: Expression of human VEGF and human soluble Flt1 (sFlt) by transduced mouse MDSCs.....	70
Figure 4.4: Level of human VEGF secretion in the MDSC-VEGF50 and MDSC-VEGF25 cells	71
Figure 4.5: Donor cell–induced neovascularization is VEGF-dependent.	73
Figure 4.6: Assessment of cardiac function.....	77

PREFACE

I would like to convey genuine appreciation to my dissertation advisor, Johnny Huard, for his guidance and allowing me to work on a project that was of great interest to me. Merci beaucoup.

Sincere thanks are owed to Bradley Keller, Bruno Péault, Sanjeev Shroff and William Wagner for their service on my dissertation committee. I appreciate their time, expertise, and guidance.

I would like to thank every member of the Growth and Development Laboratory. In particular, I would like to thank my partners in the cardiac cell therapy business, Sensei Hideki Oshima and Sensei Masaho Okada. I truly cherish the friendship that we have made while working together on this challenging and exciting project. Arigatou. Special thanks are owed to Burhan Gharaibeh for his extremely dedicated support with FISH. I would like to express sincere gratitude to the administration (R. Sauder, B. Lipari, M. Predis and J. Cummins) and technical support staff (M. Branca, M. Huard, J. Zhou and Y. Tang) of the laboratory. I would also like to thank my trailblazing predecessors and friends Ronald Jankowski and Bridget Deasy for their candid advice. Thanks to all the past and present fellows and the current graduate students for making the laboratory a diverse and fun environment.

I would like to gratefully acknowledge Nobuo Momoi, Kimimasa Tobita and Bradley Keller for their assistance with cardiac function analysis. These projects would not have been complete without this appreciated collaboration.

I would like to give a heartfelt thanks to my parents and family for supporting and encouraging my pursuit of higher education.

Thanks to all the friends that I have met here in Pittsburgh, especially Phil Marascalco, Jonathan Vande Geest, Eric Chen, Dan Debrah, and Ryan Pruchnic, for making graduate school a fun and wonderful experience for me. Additionally, I owe an enormous amount of gratitude to Karin Corsi for her encouragement.

I would like to acknowledge the American Heart Association for supporting me with a Predoctoral Fellowship (0315349). The work presented here was supported and made possible by grants to Johnny Huard from the MDA, the NIH (1U54AR050733-01; R01-HL 069368-02), the Pittsburgh Tissue Engineering Initiative (PTEI), the Donaldson Chair, the Hirtzel Memorial Foundation, and the Henry J. Mankin Chair. This investigation was conducted in a facility constructed with support from the NIH.

Nomenclature:

α -MHC, α -myosin heavy chain

ANOVA, analysis of variance

CCM, cellular cardiomyoplasty

CHF, congestive heart failure

cTnI, cardiac Troponin I

Cx43, connexin43

DAPI, 4, 6'-diamidino-2-phenylindole

DMD, Duchenne muscular dystrophy

DMEM, Dulbecco's modified Eagle medium

EDA, end-diastolic area

EDD, end-diastolic dimensions

ELISA, enzyme-linked immunosorbant assay

ESA, end-systolic area

ESD, end-systolic dimensions

FAC, fractional area change

Fast sk. MHC, fast skeletal myosin heavy chain

FISH, fluorescent *in situ* hybridization

FS, fractional shortening

LV, left ventricle

MDSC, muscle-derived stem cell

MDSC-FLT, MDSCs genetically engineered to express sFlt1

MDSC-LacZ, MDSCs genetically engineered to express *LacZ*

MDSC-VEGF, MDSCs genetically engineered to express VEGF

MI, myocardial infarction

O₂, oxygen

PBS, phosphate-buffered saline

SCID, severe combined immune deficiency

sFlt1, soluble Flt1

VEGF, vascular endothelial growth factor

1.0 INTRODUCTION

1.1 SIGNIFICANCE

Heart disease is the leading cause of death for both men and women. It is estimated that 865,000 people in the United States will experience a new or recurrent myocardial infarction (MI) (i.e., heart attack) every year [1]. A MI occurs when one or more of the coronary arteries supplying blood to the heart are blocked. Due to a lack of oxygen and nutrients, muscle cells in the infarcted region of the heart suffer irreversible ischemic injury and die. Because the mammalian heart possesses only a limited capacity to regenerate new cardiac muscle after injury, noncontractile scar tissue eventually replaces the ischemic myocardium. Many MI patients eventually develop congestive heart failure (CHF), a condition in which the debilitated heart can no longer effectively pump blood.

CHF affects about 4.9 million living Americans and is responsible for more than 51,546 deaths per year; an additional 550,000 new CHF cases are diagnosed each year [1]. In 2002, an estimated \$24.3 billion was spent on direct and indirect costs associated with CHF diagnosis and treatment in the United States alone [2]. Pharmaceutical therapies, surgical procedures, and mechanical devices have proven to be effective in improving cardiac function, but they have had limited effect on preventing mortality in patients with CHF [3]. Heart transplantation has been shown to be highly effective, but this procedure is dependent upon organ donor availability and

requires long term immune suppression in patients who receive transplants [3]. Only 2,202 heart transplants were performed in 2001 and that number has not significantly increased from the previous year (2,198 transplants were performed in 2000) [2, 4]. Consequently, the development of novel alternative treatments for this costly and deadly condition is still warranted. Cell transplantation is one such promising alternative therapy.

1.2 CELL THERAPY FOR CARDIAC REGENERATION AND REPAIR

1.2.1 Cellular Cardiomyoplasty

Cellular cardiomyoplasty (CCM) is a procedure that involves the transplantation of exogenous cells into damaged myocardium as a means to regenerate new myocardium (i.e., new cardiomyocytes and vasculature) and reverse heart failure [5-8]. This procedure was initially investigated using experimental models of heart failure, and these studies have led to multiple ongoing human clinical trials [9-21]. Various cell types including embryonic, neonatal and adult cardiomyocytes [22-30], smooth muscle cells [31], autologous adult atrial cells [32], dermal fibroblasts [33], and skeletal muscle-derived cells (i.e., myofibers, myoblasts, and satellite cells) [8, 11-14, 21, 33-61], have been studied as potential cell sources for CCM. Recent interest in stem cell research has helped to identify some potential, alternative cell sources for CCM, including murine embryonic stem cells [30, 62, 63], bone marrow-derived mesenchymal stem cells [64-71], purified (enriched) hematopoietic stem cells [72-81], blood- and bone marrow-derived endothelial progenitor cells [82-86], and cardiac muscle-derived stem cells [87-89].

The efficacy of CCM as a treatment for end-stage heart failure will rely strongly upon the identification of a cell source with a marked capacity for myocardial regeneration and repair. A suitable cell population also would exhibit several other fundamental characteristics, including long-term survival, the capacity to contribute to contractile function in the heart, and the appropriate responsiveness to various factors present in the cardiac microenvironment [5]. To identify the optimal cell population for cardiac repair, several fundamental issues must be addressed, including 1) cell survival after transplantation and the longevity of cell engraftment, 2) the ability of the injected cells to differentiate into cardiomyocytes and blood vessel structures, 3) the capacity of the transplanted cells to undergo electromechanical integration with the host myocardium through the formation of gap junctions and intercalated discs and contribute to contractile function, 4) the ability of the cells to induce neovascularization and reduce adverse remodeling within the infarct [83], and 5) the response of the engrafted cells to physiologic and pathologic stimuli associated with diseased and ischemic myocardium [5, 7]. Although most cell populations mentioned above have demonstrated some beneficial characteristics when used in experimental animal models, various ethical, biological, or technical limitations have hindered their suitability for use in human patients [5]. Currently, progenitor and stem cells derived from skeletal muscle, bone marrow or circulating blood are considered to be highly suitable for clinical use, because these cells can be harvested with relative ease from patients, readily expanded in culture, and transplanted in an autologous manner thereby eliminating the need for immunosuppressive drugs. Indeed, cells derived from these tissue sources are already being investigated in clinical trials for cardiac repair [9, 13-15, 21, 35, 36, 43, 90].

1.2.2 Skeletal Myoblasts for Cardiac Cell Transplantation

Many research groups using animal models have reported that mononucleated skeletal muscle-derived cells (i.e., myoblasts and satellite cells) can engraft in the heart and improve cardiac performance [6, 38]. These groundbreaking animal studies paved the way for skeletal myoblasts to be the first cell type used in clinical trials for cardiac cell therapy [13]. Myoblasts are currently being investigated in multiple clinical trials for cardiac repair [12-14, 21, 35, 36, 44]. Skeletal myoblasts, which have a committed myogenic fate [91], are located between the basal lamina and sarcolemma of myofibers, where they remain during postnatal life. Myoblasts are generally quiescent, but upon stimulation (i.e., injury, mechanical stretch) will differentiate and fuse to form new regenerating myofibers [91]. Skeletal muscle-derived cells (myoblasts, satellite cells and skeletal muscle-derived stem cells [MDSCs]) are attractive for clinical use because they can be harvested by a simple muscle biopsy, readily expanded *in vitro*, transplanted in an autologous manner, and after implantation can differentiate into skeletal muscle that is highly resistant to ischemia (Figure 1.1). Additionally, these isolated cells could be used in an *ex vivo* gene therapy approach to deliver therapeutic factors that would enhance the effect of cell transplantation (Figure 1.1). In the *ex vivo* gene therapy approach, the cells would be genetically engineered before implantation using non-viral or viral vectors that would contain genes encoding therapeutic proteins (Figure 1.1).

Cardiac Cell Therapy Autologous Approach

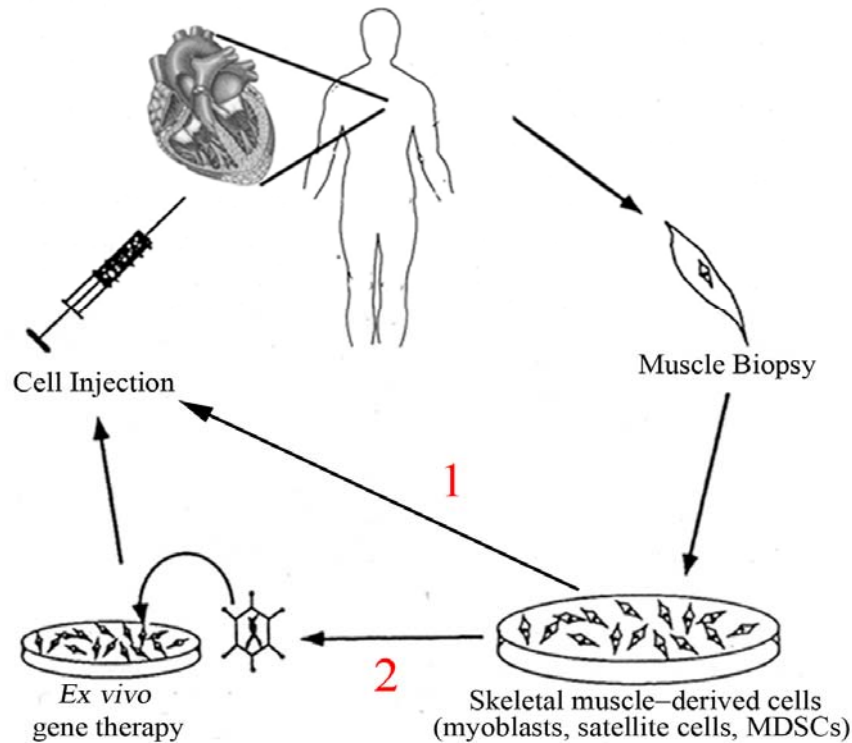


Figure 1.1: The autologous cell and gene therapy approach for cardiac repair.

A simple muscle biopsy would be taken from the patient and processed to isolate skeletal muscle-derived cells (myoblasts, satellite cells and skeletal muscle-derived stem cells [MDSCs]). Then the cells would be expanded to obtain a sufficient number for clinical use. (1) For an autologous cell therapy approach, the cells would be packaged for direct injection back into the same patient. (2) In an *ex vivo* gene therapy approach, the isolated cells would then be genetically engineered with non-viral and viral vectors to express a therapeutic protein, such as VEGF or dystrophin. Following this step, the genetically modified cells would be injected into the heart.

In animal models, successful delivery of skeletal myoblasts into the heart has been achieved by both direct intra-myocardial injection and intra-arterial delivery [8, 11-14, 21, 33-61]. Various studies have shown that the engrafted myoblasts can adapt within the cardiac microenvironment and improve cardiac performance in animal models of cardiac injury [33, 52, 58, 61, 92-94]. Some of these studies suggest that myoblasts can undergo cardiac differentiation [8, 37, 61, 95, 96], while others do not [46, 97]. Overall, none of the studies suggesting cardiac-differentiation employed a combination of molecular markers specific for the donor cells and the

cardiac phenotype that is sufficiently rigorous to provide convincing evidence of cardiac differentiation of skeletal muscle-derived cell types [97]. When Reinecke and colleagues used a combination of specific molecular markers to assess cardiac differentiation of skeletal myoblasts transplanted in rat myocardium, no donor cell differentiation was observed [97]. In skeletal and cardiac muscle, the transplantation of myoblasts has been limited by poor cellular survival rates and limited dissemination of the injected cells throughout the muscle [98-105]. For these reasons, many groups have attempted to isolate a population of skeletal muscle-derived stem cells that would enhance the success of myogenic-derived cell transplantation in both skeletal and cardiac muscle [106-109].

Numerous studies have demonstrated that myoblast transplantation into skeletal muscle is a feasible therapeutic approach for inherited myopathies, including Duchenne muscular dystrophy (DMD). However, myoblast transplantation into skeletal muscle [98, 102, 110] and into cardiac muscle [11, 12, 59, 61, 111] has proven inefficient and continues to be hindered by the very low survival rate and poor engraftment of the transplanted cells. Research performed to follow the fate of myoblasts after transplantation into skeletal muscle has revealed that most of the cells die shortly after implantation and that only a small subpopulation plays a role in new muscle regeneration [103, 110]. These results suggest that myoblasts constitute a heterogeneous population that may contain a subpopulation of cells with stem cell-like characteristics and a high capacity to promote and participate in muscle regeneration. We propose that the identification and isolation of this myogenic subpopulation with a high regenerative capacity would improve the efficacy of myoblast transplantation into the heart.

1.2.3 Skeletal Muscle–Derived Stem Cells: Potential for Tissue Regeneration

Using various techniques, we and others have identified populations of skeletal muscle-derived stem cells (MDSCs) and confirmed that their existence is distinct from myoblasts [112, 113]. We have fractionated various myogenic cell populations from skeletal muscle of normal wild-type mice based on their adhesion characteristics using a modified version of the preplate technique [113, 114]. In particular, we have isolated populations of myoblasts as well as a unique population of MDSCs using this technique [113, 114]. On the basis of their marker profile, these MDSCs appear to be less committed to the myogenic lineage than are myoblasts [113]. These MDSCs can differentiate toward various lineages (i.e., muscle, bone, neural, endothelial, and haematopoietic lineages) [113-115]. More importantly, when we transplanted the same number of myoblasts and MDSCs into the skeletal muscle of dystrophic *mdx* mice, we found that the MDSCs efficiently generated large grafts of new skeletal muscle while the myoblasts formed only a few new muscle fibers [113]. These results indicate that MDSCs may be a better population of myogenic cells for muscle regeneration than myoblasts.

1.3 PROJECT OBJECTIVES

1.3.1 Objective #1: Evaluate the Cardiogenic Potential of MDSCs

It is postulated that the optimal cell type for cardiac cell transplantation would be a cell with the capacity to undergo cardiogenic differentiation. We have previously shown that MDSCs can undergo differentiation toward muscle, bone, neural, endothelial, and hematopoietic lineages

[113-115]. However, their capacity for differentiation into the cardiomyocyte lineage is unknown. Once MDSCs have been transplanted into the myocardium, it will be of interest to understand their fate. Will these immature stem cells differentiate into cardiomyocytes, skeletal myocytes and/or blood vessels? In many cases, the environment into which the cells are transplanted into will dictate the lineage that they will differentiate into. Will the microenvironment of the heart induce transplanted MDSCs to differentiate into cardiomyocytes? We hypothesized that factors present in the local environment could have a significant influence on the differentiation of the implanted cells. However, thus far, myoblasts have displayed a minimal ability to differentiate into new cardiomyocytes both *in vitro* and *in vivo* [48, 97]. In contrast to committed skeletal myoblasts, MDSCs may be more amenable to differentiate since they are considered to be immature. In this objective, we assessed the cardiogenic potential and fate of MDSCs after injection into the hearts of dystrophin-deficient *mdx* mice, a model for cardiomyopathy and muscular dystrophy. In addition, we evaluated the ability of MDSCs for long-term survival and dystrophin delivery after intramyocardial transplantation.

1.3.2 Objective #2: MDSCs for Myocardial Infarct Repair

Before the advent of myoblast transplantation for cardiac repair, numerous studies demonstrated that myoblast transplantation into skeletal muscle is a feasible therapeutic approach for inherited myopathies, including Duchenne muscular dystrophy. Here, we hypothesized whether the identification and isolation of this myogenic subpopulation with a high regeneration capacity would enhance the therapeutic benefit of myoblast transplantation for cardiac repair.

Although our characterization of MDSCs indicates that they possess an enhanced capacity for skeletal muscle regeneration, their potential effect when used for myocardial infarct

repair is unknown. In this objective, we evaluated this application by transplanting MDSCs into the hearts of adult SCID mice injured by acute myocardial infarction. In addition, we investigated whether MDSCs and committed skeletal myoblasts would exhibit differential abilities to engraft and improve cardiac function after myocardial infarction. We also assessed the ability of each cell population to adopt a cardiac phenotype, undergo electromechanical coupling, and promote angiogenesis after implantation.

1.3.3 Objective #3: Mechanism of Cell Therapy: Role of VEGF

Despite the failure of most cell types to extensively regenerate new myocardium (i.e., de novo differentiation of implanted cells into cardiomyocytes and blood vessels), cell therapy has still elicited improvements in cardiac performance after myocardial infarction [6, 7]. Instead, therapeutic benefit has been attributed to cell types that induce elevated levels of neovascularization in ischemic myocardium [7, 83]. Our preliminary data indicates that MDSCs promote neoangiogenesis when transplanted into the infarcted heart. Yet, it remains unknown how MDSCs promote revascularization in the ischemic heart and how this neovascularization affects cardiac function. One possible explanation is that MDSCs secrete angiogenic growth factors which stimulate blood vessel formation in the infarct regions of the heart. Because vascular endothelial growth factor (VEGF) is the most potent inducer of angiogenesis [116, 117], we have immunostained MDSC-injected hearts for the expression of VEGF. Indeed, the grafts in these hearts displayed a strong reactivity with antibodies specific for VEGF (see section 3.2.11 and Figure 3.7). In addition, we have observed that cyclic stretch and hypoxia stimulate the expression of VEGF by MDSCs *in vitro* (see section 4.2.1 and Figure 4.1). Taken together, these results suggest that VEGF is a potent angiogenic factor that MDSCs could secrete in response to

the microenvironment of ischemic hearts. In this objective, we investigated the significance of VEGF in the intracardiac transplantation of MDSCs for cardiac repair. We assessed this by conducting a gain- and loss-of-function experiment in which we genetically modify MDSCs to overexpress either VEGF (gain-of-function) or the VEGF antagonist soluble Flt1 (loss-of function), which is also known as the soluble VEGF-receptor 1 (sVEGF-R1). The data generated from these experiments will help to elucidate the therapeutic and mechanistic role that VEGF plays in MDSC-mediated cardiac repair. In a broader sense, the findings gained from these experiments would reveal how cell transplantation into ischemic myocardium mediates neovascularization.

2.0 FATE OF MDSCS AFTER INTRAMYOCARDIAL TRANSPLANTATION

2.1 INTRODUCTION

Duchenne muscular dystrophy (DMD) is a degenerative muscle disease characterized by a lack of dystrophin expression in the sarcolemma, a condition that leads to progressive muscle weakness [118]. In the heart, the reduced levels or absence of dystrophin in patients causes cardiac muscle degeneration and the gradual development of dilated cardiomyopathy [119]. Dystrophin-deficient myocardium is the result of either a mutation in the X-linked dystrophin gene (as in DMD) [119] or a virus-mediated cleavage of the dystrophin protein [120, 121]. The functional loss of the dystrophin protein compromises the structural integrity of the sarcolemma, resulting in progressive and irreversible degeneration of cardiomyocytes [122, 123]. To date, researchers using cell or gene therapy have made only a few attempts to correct dystrophin deficiency in the hearts of dystrophic animals [124-127].

Cellular cardiomyoplasty, a procedure involving the transplantation of exogenous cells into the heart, is a possible approach by which to regenerate diseased myocardium, deliver therapeutic genes, and improve cardiac function [3]. Researchers have investigated the use of various cell types for cardiac repair, including cardiomyocytes, fibroblasts, embryonic stem cells, endothelial progenitor cells, bone marrow-derived cells, hematopoietic stem cells, mesenchymal stem cells, smooth muscle cells, skeletal muscle-derived cells [5], and the recently identified

cardiac stem cells [87-89, 128, 129]. Notably, numerous research groups have found that skeletal muscle-derived cells can successfully engraft in the heart and improve cardiac performance in animals models [33, 52, 61, 72, 92, 94]. Currently, autologous skeletal myoblasts are being used in clinical trials for cardiac repair [13-15, 36, 44, 130, 131].

Our research group has isolated populations of murine skeletal muscle-derived stem cells (MDSCs) by using a modified preplate technique [113, 114]. MDSCs exhibit stem cell-like properties and appear to be distinct from later-stage myogenic cell populations such as satellite cells and myoblasts [113]. In addition, MDSCs can undergo differentiation toward muscle, bone, neural, endothelial, and hematopoietic lineages [113-115]. By transplanting MDSCs into the dystrophic skeletal muscle of *mdx* mice, we have previously shown that MDSCs generate large grafts containing numerous dystrophin-positive myofibers [113]. Here, we transplanted MDSCs into the dystrophin-deficient hearts of adult *mdx* mice. We sought to determine if the MDSCs could (a) engraft and persist in the heart, (b) regenerate donor-derived myocytes that express both reporter (*nLacZ*) and therapeutic (dystrophin) genes, and (c) acquire a cardiac-specific phenotype after transplantation.

2.2 RESULTS

2.2.1 Characterization of the *nLacZ*-Expressing MDSCs In Vitro

We transduced MDSCs with a retrovirus containing a nuclear *LacZ* (*nLacZ*) reporter gene. We then stained these cells *in vitro* with X-gal substrate to confirm expression of the *nLacZ* reporter

gene (Figure 2.1a). Approximately 50% of the MDSCs expressed *nLacZ in vitro* immediately before delivery by intracardiac injection.

Because we isolated the MDSCs from normal skeletal muscle for injection into dystrophin-deficient myocardium, we tested the cells' ability to express dystrophin after differentiation into myotubes. In low serum-containing medium, MDSCs were able to differentiate into dystrophin-expressing myotubes (Figure 2.1b).

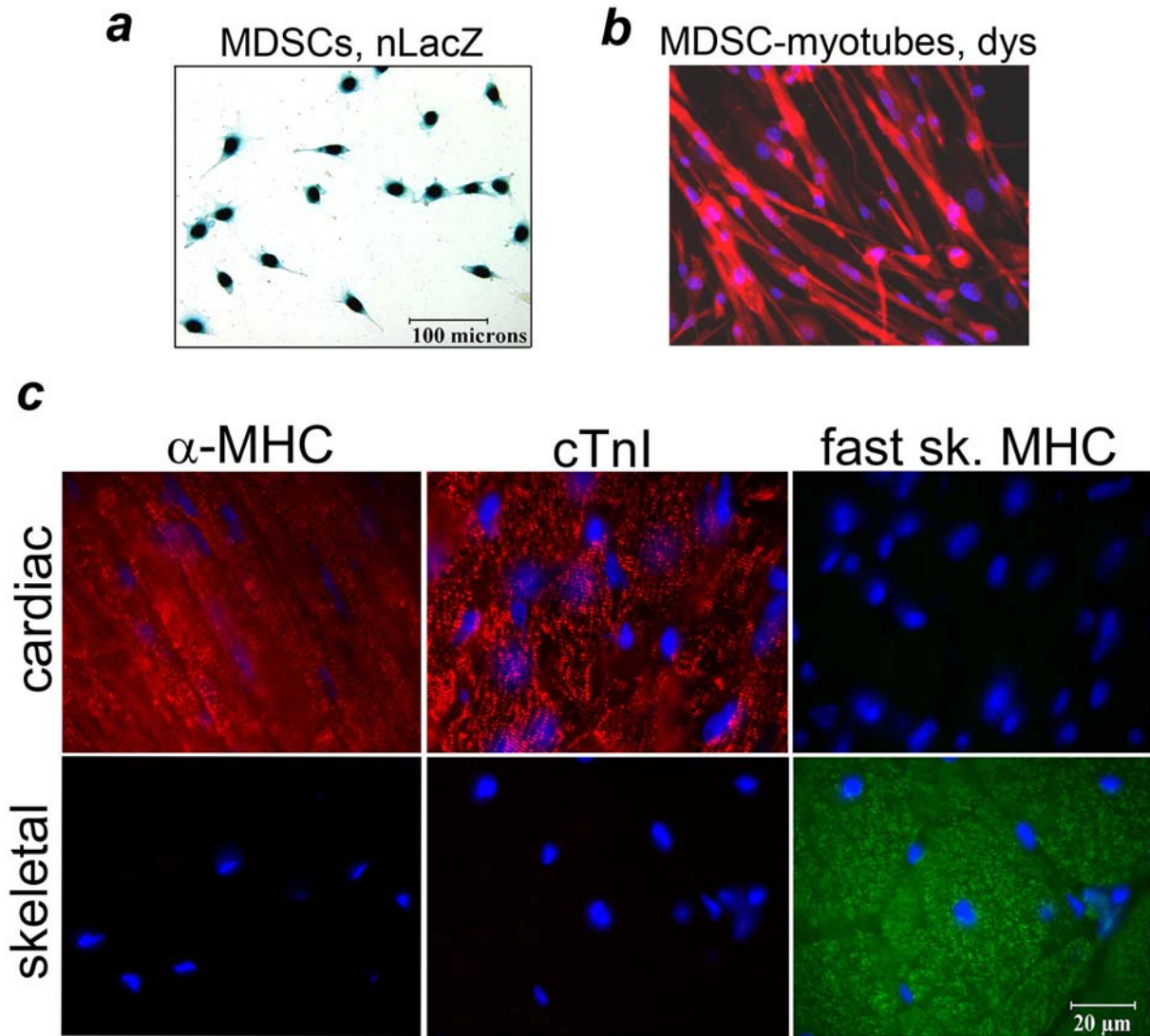


Figure 2.1: Validation of donor-specific markers and of cardiac and skeletal muscle-specific antibodies.

(a) A population of MDSCs was genetically engineered to express the *nLacZ* reporter gene. Positive staining (blue) is localized to the nucleus of the cells *in vitro*. (b) When cultured in low serum-containing medium *in vitro*, the MDSCs differentiated into multinucleated myotubes expressing dystrophin (red). (c) Cardiac-specific antibodies against α -myosin heavy chain (α -MHC) and cardiac Troponin I (cTnI) are reactive with cardiac muscle (red, top row “cardiac”); however, they do not cross-react with skeletal muscle (bottom row “skeletal”). Antibodies against fast skeletal myosin heavy chain (fast sk. MHC) react exclusively with skeletal muscle (green, bottom row “skeletal”) and not cardiac muscle (top row “cardiac”). Nuclei were revealed with DAPI stain (blue). Scale bars equal 100 μ m (a, b) and 20 μ m (c).

2.2.2 Validation of Cardiac and Skeletal Muscle–Specific Markers

The cardiac α -myosin heavy chain (α -MHC) and cardiac Troponin I (cTnI) antibodies reacted specifically to cardiac muscle (Figure 2.1c, top row, red) and not skeletal muscle (Figure 2.1c, bottom row). These results, which confirm the cardiac specificity of the α -MHC and cTnI antibodies in murine tissue, validate the use of these markers to indicate any cardiac-phenotypic changes of the transplanted MDSCs, particularly because the injected MDSCs were of skeletal muscle origin. In addition, an antibody (MY32) against fast skeletal myosin heavy chain (fast sk. MHC) reacted specifically to skeletal muscle (Figure 2.1c, bottom row, green) and not cardiac muscle (Figure 2.1c, top row).

2.2.3 MDSCs Generate Large Grafts in the *mdx* Heart

We injected MDSCs into the left ventricular myocardium of dystrophic *mdx* mice. After injecting the MDSCs, we tracked their fate by observing expression of the *nLacZ* reporter gene and dystrophin protein. Two weeks after implanting the cells, we observed that the injected cells had formed a graft within the myocardium containing numerous myocytes expressing *nLacZ* (blue) (Figure 2.2a, top row). We validated the persistence of the graft 4 and 8 weeks after implantation (Figure 2.2a, top row). On serial sections of the same hearts, dystrophin expression (green) was visible (Figure 2.2a, bottom row) and colocalized with the *nLacZ*-expression observed 2, 4, and 8 weeks after injection (Figure 2.2a, top row); this finding indicates that the MDSCs differentiated into numerous dystrophin-expressing myocytes within the dystrophic myocardium. We observed fewer *nLacZ*[+] nuclei than dystrophin-positive myocytes (Figure 2.2a): Approximately 50% of the MDSCs expressed *nLacZ* *in vitro* immediately before injection,

whereas every MDSC contained the normal dystrophin gene. The *nLacZ*[-] region (i.e., the host myocardium) surrounding the graft was negative for dystrophin, as one would expect to be the case in a dystrophic host (Figure 2.2a). The dystrophin-positive grafts consisted primarily of terminally differentiated skeletal myofibers as indicated by their expression of fast skeletal muscle myosin heavy chain (fast sk. MHC) (red, Figure 2.2b). In addition, these fast sk. MHC-positive donor-derived cells formed multinucleated myofibers (Figure 2.2c).

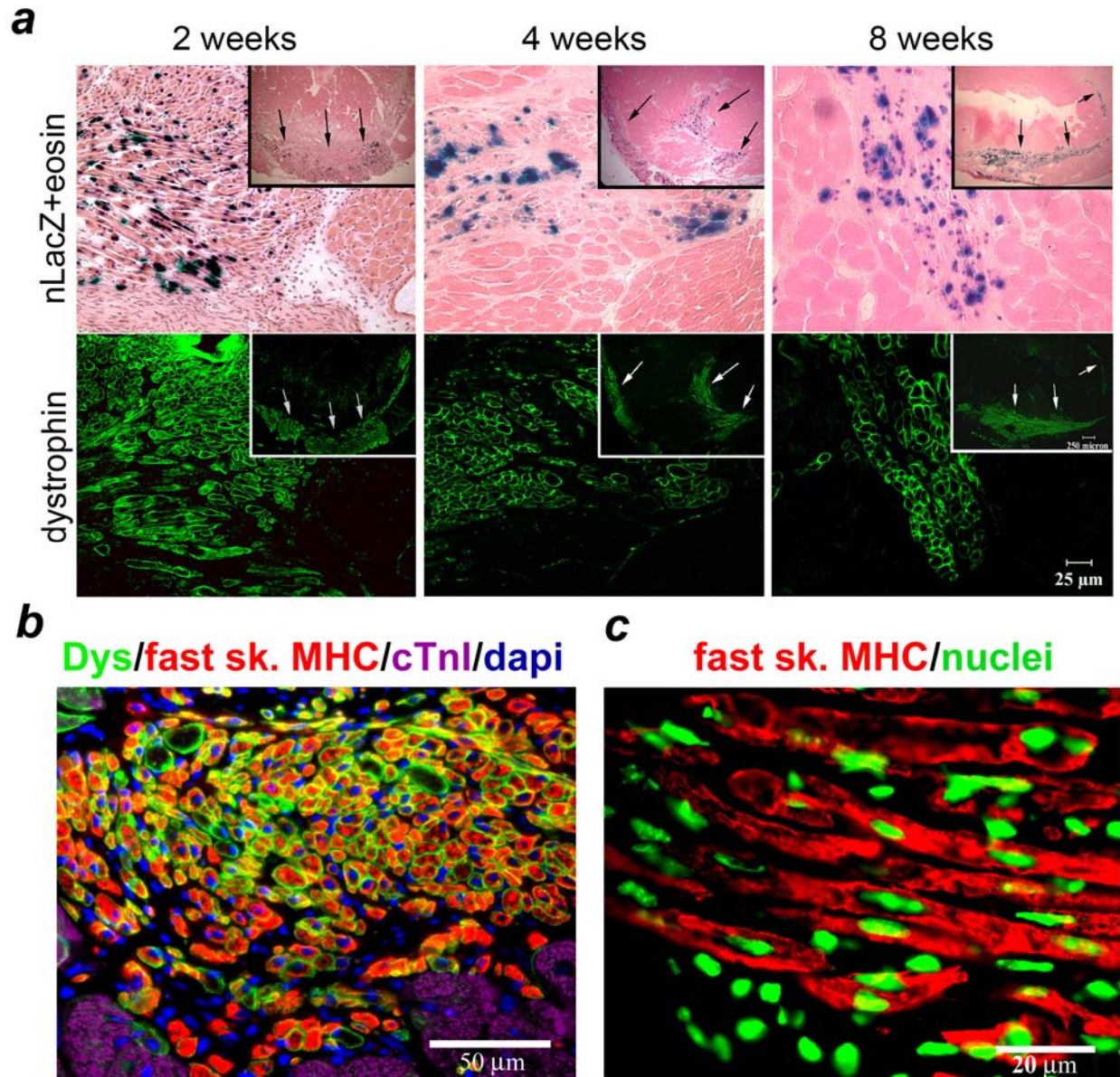


Figure 2.2: Engraftment and expression of a skeletal muscle phenotype by MDSCs in mdx/SCID hearts.

(a) After implanting MDSCs within the *mdx*/SCID hearts, we visualized engraftment by performing stainings for both *nLacZ* (blue) and dystrophin (green). In the myocardium of the left ventricles, large grafts expressing both *nLacZ* (top row, top right corner inserts) and dystrophin (bottom row, top right corner inserts) were visible 2, 4, and 8 weeks after injection (arrows highlight the grafts). High-power magnification revealed *nLacZ*-expressing myocytes colocalized with dystrophin-expressing myocytes, demonstrating that the dystrophin-expressing myocytes originated from the donor (*nLacZ*[+]) MDSCs. Scale bar for inserts, 250 μm ; scale bar for high-power magnification, 25 μm . (b) Quadruple staining for dystrophin (green), fast sk. MHC (red), cTnI (purple), and DAPI (blue) revealed that most dystrophin-positive myocytes within the graft were terminally differentiated skeletal myofibers, as indicated by their expression of fast sk. MHC. Scale bar, 50 μm . (c) The transplanted MDSCs fused to create multinucleated (green) fast sk. MHC[+] myotubes/myofibers (red). Scale bar, 20 μm .

2.2.4 Donor-derived Cells Express Cardiac Markers

We sought to determine whether these donor-derived grafts expressed cardiac-specific markers. After double staining for both dystrophin and cardiac α -MHC at various time points after transplantation, we found that the majority of the dystrophin-expressing (green) myocytes located within the center of the graft did not express cardiac α -MHC (red) (Figure 2.3, “graft” column). However, we did observe colocalization of dystrophin and cardiac α -MHC in a few cells located at the border of the graft and the host myocardium (Figure 2.3; see arrows in “graft-host border” columns).

2.2.5 Use of *LacZ* to Validate Donor Origin of Dystrophin⁺ Cardiomyocytes

Because the presence of colocalized myocytes expressing dystrophin and cardiac α -MHC could be attributable to the presence of revertant dystrophin-positive host cardiomyocytes in the mdx mouse [132], we used nLacZ expression to validate the donor origin of these myocytes. Specifically, we repeated the dystrophin/cardiac α -MHC double staining on cryosections pre-stained in X-gal substrate to enable colocalization of the immunostains with donor-specific nLacZ expression. We observed donor cells containing a nLacZ[+] nucleus and co-expressing both dystrophin and cardiac α -MHC at the border of the graft and host myocardium (Figure 2.4). To quantitatively evaluate the nLacZ and cardiac α -MHC colocalization, we counted both the nLacZ[+] nuclei that colocalized with cardiac α -MHC and the total number of nLacZ[+] nuclei in the 5 sections containing the largest grafts in each MDSC-injected heart. It is important to note here that we used nLacZ instead of dystrophin as the primary marker to identify and quantify the donor cells that did and did not colocalize with cardiac α -MHC (Figure 2.4 and Table 2.1) to

exclude any revertant dystrophin-positive host cardiomyocytes [132]. Using these data, we determined the percentage of nLacZ and cardiac α -MHC colocalization within each heart (n=10) 2, 4, 8, and 12 weeks after implantation (Table 2.1). The percent averages indicate that 3.0% of the donor cells expressed cardiac α -MHC at 2 weeks after transplantation (n=3), 4.0% at 4 weeks (n=3), 5.1% at 8 weeks (n=3), and 0.6% at 12 weeks (n=1) (Table 2.1).

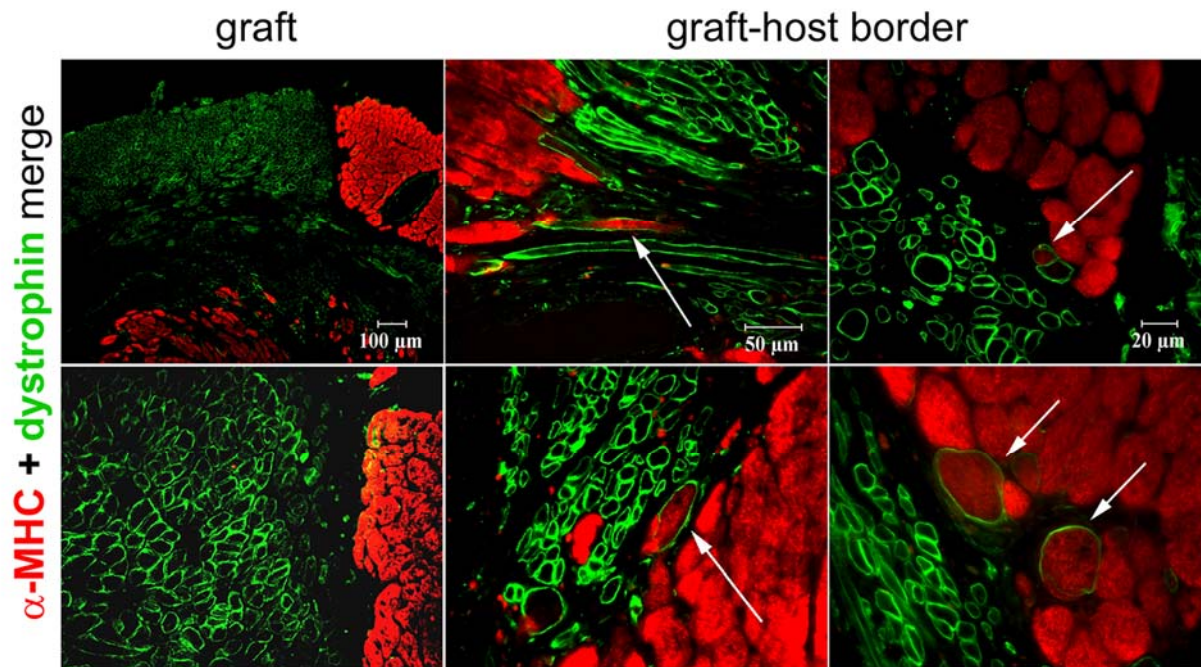


Figure 2.3: Donor-derived dystrophin⁺ myocytes expressing a cardiac phenotype.

Double staining for both cardiac-specific α -MHC (red) and dystrophin (green) revealed very little colocalization throughout most regions of the grafts (as shown in 1st column labeled “graft”). However, we observed some colocalization (see arrows) of dystrophin (green) and α -MHC (red) at the border of the graft and the host myocardium (as shown in 2nd and 3rd columns labeled “graft-host border”). Scale bar for images in first column (“graft”), 100 μ m; scale bar for second column, 50 μ m; scale bar for third column, 20 μ m.

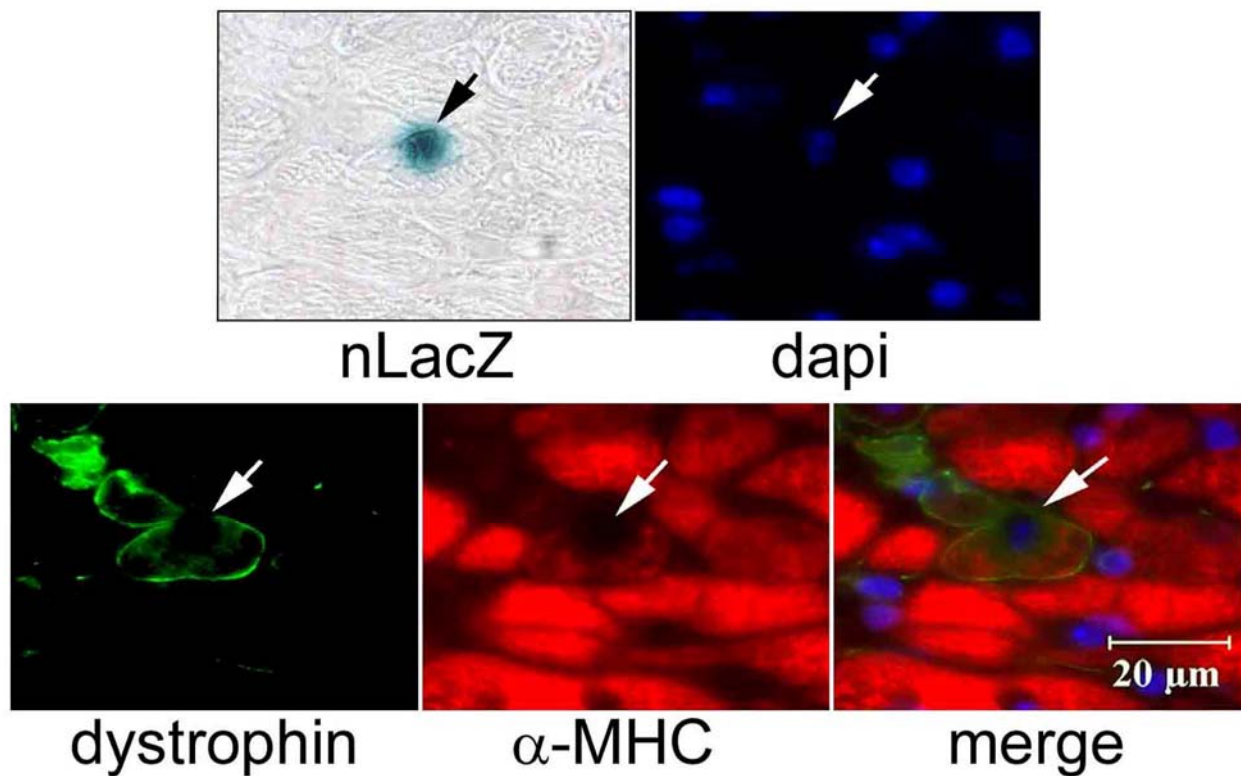


Figure 2.4: Colocalization of donor- and cardiac-specific markers in cells within MDSC-injected hearts. Shown is one donor-derived cell expressing *nLacZ* (brightfield blue, arrows), DAPI (fluorescent blue, arrows), dystrophin (green, arrows), and cardiac-specific α -MHC (red, arrows). Colocalization of cardiac α -MHC, dystrophin, and DAPI is visible in the merged image (arrows). Scale bar equals 20 μ m. (c) Quantification of the number of *nLacZ*[+] cells expressing cardiac α -MHC.

Table 2.1: Frequency of donor cells expressing a cardiac phenotype in the heart.

Time-Point	Mouse	Total <i>nLacZ</i> [+]	<i>nLacZ</i> [+], α -MHC[+]	Percent α -MHC[+]	Percent average \pm s.e.m.
2 weeks	1	5,775	132	2.3%	$3.0 \pm 1.3\%$
	2	334	4	1.2%	
	3	1,257	71	5.6%	
4 weeks	4	4,015	197	4.9%	$4.0 \pm 0.9\%$
	5	1,987	99	5.0%	
	6	6,246	138	2.2%	
8 weeks	7	4,223	129	3.1%	$5.1 \pm 3.1\%$
	8	2,630	26	1.0%	
	9	1,404	157	11.2%	
12 weeks	10	3,946	24	0.6%	—

2.2.6 Donor Cells with a Hybrid Cardiac and Skeletal Muscle Phenotype

To further investigate the cardiac and/or skeletal muscle phenotype of the donor-derived *nLacZ*[+] cells after implantation, we performed additional multilabel stainings to detect cells co-expressing the cardiac-specific marker cTnI and the skeletal muscle-specific marker fast sk. MHC within sections of the MDSC-injected hearts. Similar to our finding in Figure 2.2b and 2.2c, our observations at all time points revealed that most of the *nLacZ* donor cells were expressing fast sk. MHC and were negative for cTnI, which indicates again that the majority of the graft was composed of skeletal muscle myofibers. However, each heart contained a few *nLacZ*[+] cells that expressed cTnI and, like the α -MHC[+] cells observed in the earlier study (Figures 2.3 and 2.4), many of these *nLacZ*[+]/cTnI[+] cells were visible at the border of the graft and the host myocardium (Figure 2.5a). This staining also revealed *nLacZ*[+] donor cells expressing either cTnI alone (Figure 2.5a; “cardiac” row) or both cTnI and fast sk. MHC (Figure 2.5a; “hybrid” row) at all time points. We counted the *nLacZ*[+] nuclei that colocalized with either a cell displaying a hybrid cardiac and skeletal muscle phenotype (i.e., cTnI[+] and fast sk. MHC[+]) or a cell displaying a non-hybrid phenotype (i.e., cTnI[+] and fast sk. MHC[-]) (Figure 2.5b). Notably, the total number of cells containing a *nLacZ*[+] nucleus and expressing cTnI (Figure 2.5b and detailed in Appendix A) was largely comparable to the total number of donor cells expressing α -MHC (as shown in Table 2.1). The resultant findings indicate that more than half of the *nLacZ*[+] nucleated cells that expressed a cardiac phenotype existed in a hybrid cardiac-skeletal state (Figure 2.5b and Appendix A).

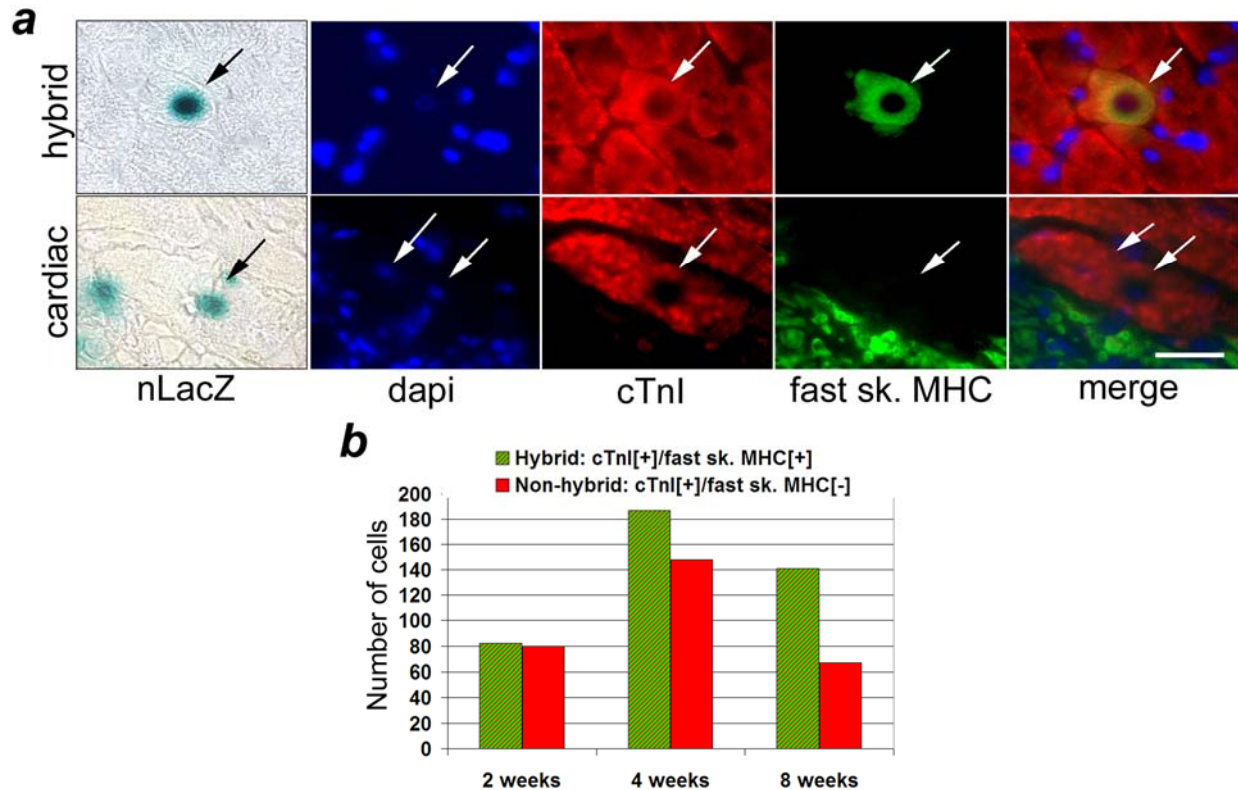


Figure 2.5: Expression of hybrid cardiac and skeletal muscle phenotype by donor-derived myocytes.

(a) A double staining for cTnI (red) and fast sk. MHC (green) revealed the presence of *nLacZ*[+] cells expressing either 1) a hybrid cardiac and skeletal phenotype (i.e., cTnI[+] and fast sk. MHC[+]; arrows, top row “hybrid”) or 2) a cardiac-only phenotype (i.e., cTnI[+] and fast sk. MHC[-]; arrows, bottom row “cardiac”). Scale bar equals 20 μ m. (b) Quantification of the number of *nLacZ*[+] hybrid cells (i.e., cTnI[+] and fast sk. MHC[+]) and non-hybrid cells (i.e., cTnI[+] and fast sk. MHC[-]) in the hearts 2, 4, and 8 weeks after cell transplantation.

2.2.7 Evaluation of Fusion between MDSCs and Host Cardiomyocytes

To determine if the acquisition of the cardiac phenotype by the implanted MDSCs was the result of fusion with host cardiomyocytes, we transplanted female *nLacZ*[+] MDSCs into the hearts of male *mdx*/SCID (immunodeficient) recipient mice. This approach is similar to the one used by Wang and associates to determine if bone marrow–derived hepatocytes formed via cell fusion [133]. We used fluorescence *in situ* hybridization (FISH) with a Y-chromosome probe, *nLacZ* staining, and immunofluorescence staining with cardiac-specific antibodies to identify female *nLacZ*[+] donor-derived cells that had undergone fusion with host male cardiomyocytes. We

identified numerous donor-derived cells that expressed cTnI and contained both an *nLacZ*[+] nucleus and a Y-chromosome-bearing nucleus (Figure 2.6a; top row labeled “Y-chromosome[+]”). We also observed cTnI[+] cells that contained a nucleus expressing *nLacZ* and bearing a Y-chromosome (data not shown). In contrast, some female donor-derived cells that expressed cTnI showed no evidence of fusion with host cardiomyocytes; such cells contained a single *nLacZ*[+]/Y-chromosome[-] nucleus (Figure 2.6a; bottom row labeled “Y-chromosome[-]”). We counted all the *nLacZ*[+]/cTnI[+] cells that were Y-chromosome[+] or [-] in each injected mouse heart. In total, 50 *nLacZ*[+]/cTnI[+] cells contained a Y-chromosome-bearing nucleus and 75 *nLacZ*[+]/cTnI[+] cells lacked a Y-chromosome-bearing nucleus (Figure 2.6b and detailed in Appendix A). Of the 50 *nLacZ*[+]/cTnI[+] cells that contained a Y-chromosome-bearing nucleus, 10 cells displayed colocalization of *nLacZ* in the same Y-chromosome-bearing nucleus. The apparent absence of a Y-chromosome-bearing nucleus in the remaining *nLacZ*[+]/cTnI[+] cells may be attributable to technical limitations associated with this system *in situ*. Specifically, we may have been unable to detect a host Y-chromosome-bearing nucleus in these cells because of a) the plane of the section or b) the hybridization efficiency of the Y-chromosome probe. However, a small number of donor cells in each injected heart exhibited evidence of fusion with host cardiomyocytes.

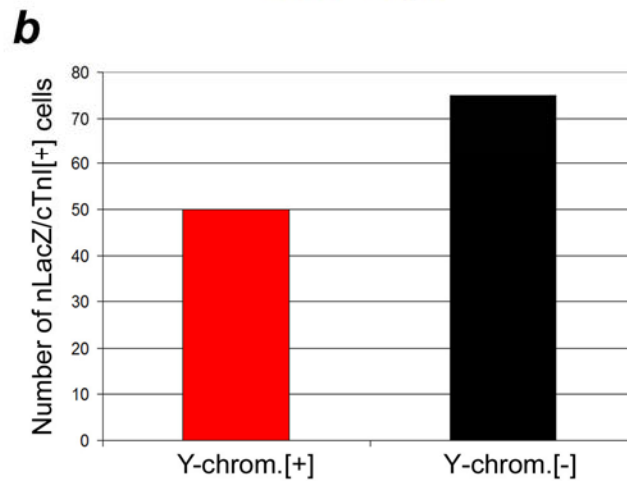
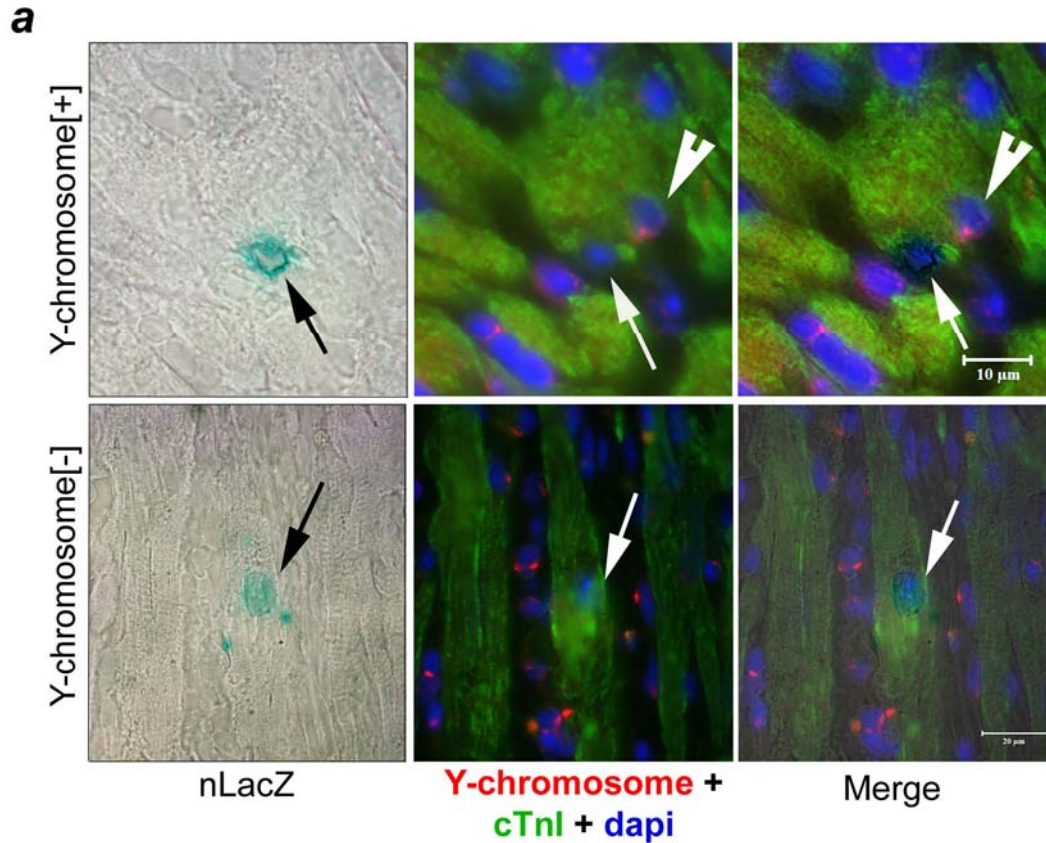


Figure 2.6: Transplanted MDSCs fuse with host cardiomyocytes.

(a) The top row of images displays a representative, multinucleated, donor-derived myocyte that fused with a host cardiomyocyte. An *nLacZ*[+] nucleus (blue, arrows) and a Y-chromosome-bearing nucleus (red, arrowheads) are visible in a cell expressing cTnI (green). The bottom row of images displays a representative donor-derived myocyte that did not display evidence of fusion with host cardiomyocytes. A single *nLacZ*[+] nucleus (blue, arrow) is located within a cTnI[+] cell (green) that does not contain a Y-chromosome-bearing nucleus (red). Overlays of the *nLacZ* brightfield images and the fluorescent images are shown in the third column. Scale bar for images in top row (“Y-chromosome[+]”), 10 μ m; scale bar for bottom row (“Y-chromosome[-]”), 20 μ m. (b) Quantification of the total number of donor (*nLacZ*[+]) cells, present within the cardiac muscle sections of all *mdx*/SCID hearts injected with MDSCs, that expressed cTnI and were either Y-chromosome[+] or [-].

2.2.8 Evaluation of Connexin43 Gap Junction Protein Expression

We stained the cell-injected hearts with antibodies specific for the connexin43 gap junction protein, which is a molecular attribute of electrical coupling between cardiomyocytes. The host myocardium displayed a typical expression pattern of connexin43 (green) between cardiomyocytes, identified by cTnI staining (red) (Figure 2.7a). In contrast, the donor-derived fast sk. MHC[+] myocytes (purple) within the graft did not express connexin43 (Figure 2.7b). In addition, fast sk. MHC[+] myofibers (purple) did not form connexin43 gap junctions (green) with host cardiomyocytes (red) ('graft-host myocardium border', Figure 2.7c).

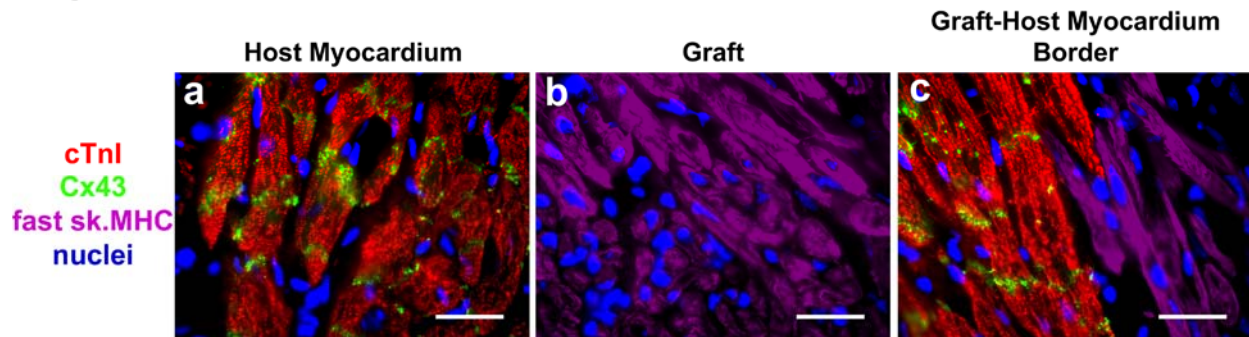


Figure 2.7: Connexin43 gap junction staining.

(a) Connexin43 gap junction proteins (green) were present in the host myocardium, as identified by cTnI staining (red). (b) However, connexin43 gap junctions were absent in the graft tissue, as identified by fast sk. MHC staining (purple). (c) In this representative image, the host cTnI[+] cardiomyocytes (red) do not appear to form connexin43 gap junctions (green) with donor fast sk. MHC[+] myofibers (purple) at the graft-host myocardium border. Scale bars equal 25 μ m.

2.2.9 Assessment of Scar Tissue in the Graft Area

Numerous donor-labeled cells that acquired a cardiac phenotype through fusion with host cardiomyocytes were visible at the border of the graft and the host myocardium. However, the presence of scar tissue at this interface may have hindered the fusion and coupling of additional donor cells with host cardiomyocytes. To assess scar tissue formation (as indicated by the accumulation of collagen) in the graft region, we used the Masson Trichrome stain to label collagen (blue), myofibers (red), and nuclei (black). The graft (GR) in the Trichrome stained sections (Figure 2.8b, e) was identified by colocalization with serial sections stained for *nLacZ* expression (Figure 2.8a, d). We observed minimal collagen (blue) expression in the host myocardium (HM), but observed collagen expression throughout the grafts (GR) at both 4 (Figure 2.8b, top row) and 8 weeks after implantation (Figure 2.8e; bottom row, see arrows). Moreover, higher magnification revealed collagen overgrowth at the border of the graft and the host myocardium, indicating a potential barrier to the fusion of MDSCs with host cardiomyocytes (Figure 2.8c, f; see yellow arrows). We hypothesize that the formation of collagen may occur because of an inflammatory response to myocardial after cell injection.

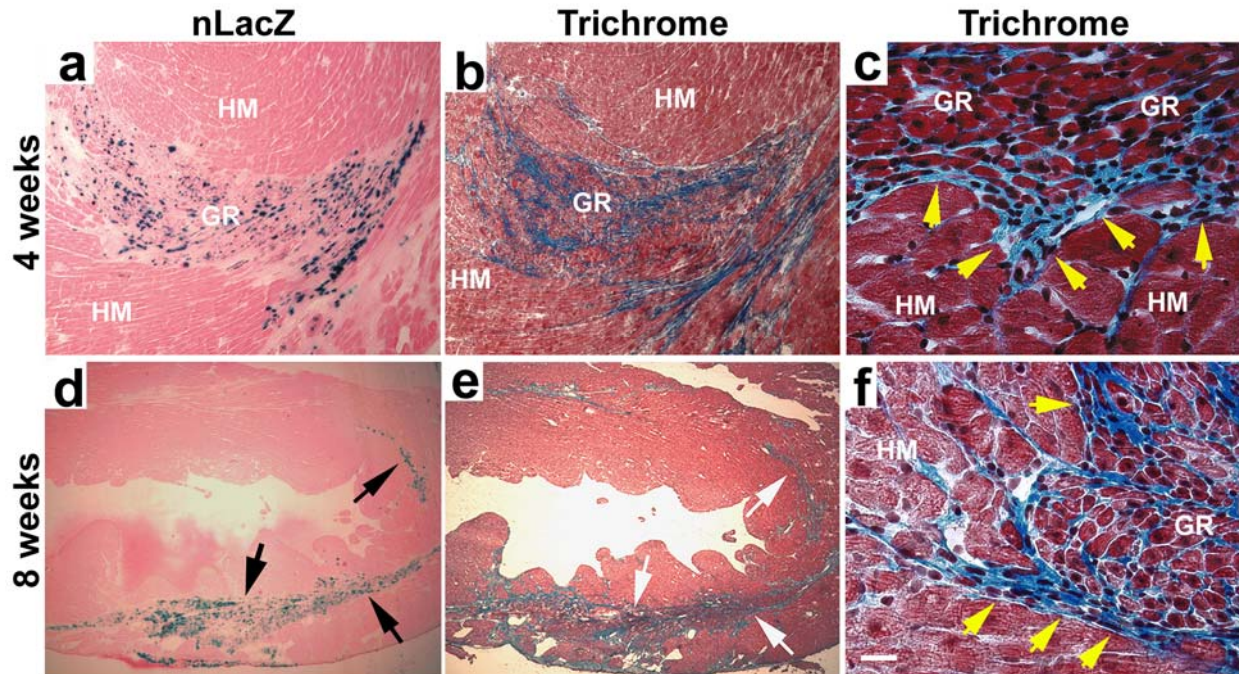


Figure 2.8: Presence of scar tissue at the border of the graft and the host myocardium.

The MDSC grafts (GR)—identified in serial sections by *nLacZ* expression (a, d; blue)—displayed collagen deposition (blue) 4 weeks (b, see GR) and 8 weeks (e; see arrows) after implantation. In contrast, almost no collagen deposition was found within the noninjected area of the host myocardium (HM). At higher magnification, collagen was observed at the border of the graft and the host myocardium (c, f; see yellow arrows), resulting in a distinct separation of the graft (GR) from the host myocardium (HM) at both 4 and 8 weeks after transplantation. Scale bar equals 250 μm (d, e), 100 μm (a, b), and 20 μm (c, f).

2.2.10 Donor Cells Contribute to Blood Vessel Structures in the Heart

To determine whether some donor cells participated in the formation of blood vessel structures in the heart, we double stained for both *nLacZ* and CD31 (also known as PECAM), a marker expressed by endothelial cells (Figure 2.9a–c). We used *nLacZ* rather than dystrophin to identify donor cells, because nonmyocytes such as endothelial cells typically do not express dystrophin. The majority of CD31[+] capillary structures (brown) within the graft did not colocalize with *nLacZ* (blue) and thus appeared to be host derived (Figure 2.9a, b). However, we did observe a few donor cells that displayed colocalization of both *nLacZ* (blue) and CD31 (brown) (Figure 2.9c).

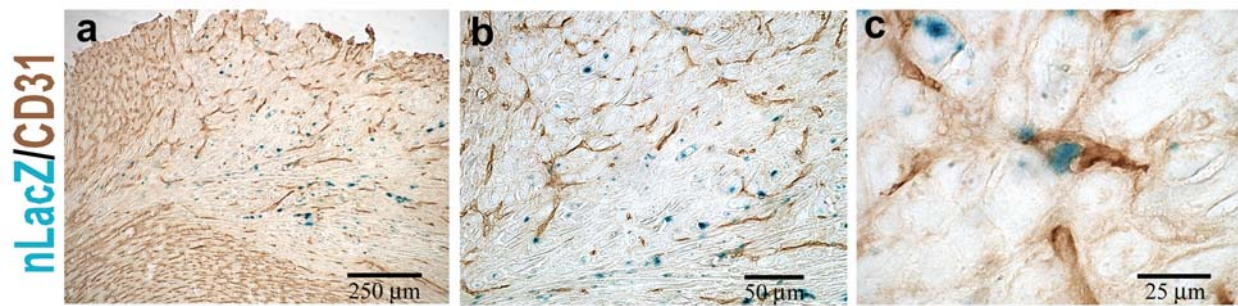


Figure 2.9: Double staining for CD31, an endothelial-specific marker, and nLacZ.

(a) There were significantly fewer CD31[+] capillary structures (brown) within the graft area than within the host myocardium. (b) A representative higher magnification image taken within the graft area shows that most CD31[+] capillary structures (brown) did not colocalize with the donor cell-specific marker *nLacZ*. (c) One representative *nLacZ*[+] donor cell (blue) found within the graft colocalized with CD31 (brown). Scale bars equal 250 μm (a), 50 μm (b), and 25 μm (c).

2.3 DISCUSSION

The data from this study demonstrate that MDSCs can generate numerous dystrophin-positive myocytes after intracardiac transplantation within the dystrophic hearts of *mdx* mice. These dystrophin-positive grafts persisted for at least 12 weeks. It is apparent from these grafts that MDSCs primarily fuse with each other and generate numerous dystrophin-positive skeletal myofibers even when injected into the heart. Our results also suggest that a few donor-derived cells contributed to the formation of blood vessel-like structures in the graft perhaps through differentiation or fusion with existing blood vessel structures. Because the *mdx* heart displays only very mild cardiomyopathy, this study did not allow us to determine if the regeneration of dystrophin-expressing myocytes as a product of the MDSC transplantation could significantly improve global cardiac function.

2.3.1 Fusion of MDSCs with Host Cardiomyocytes

In addition to exhibiting the ability to fuse and create numerous multinucleated skeletal myofibers in the *mdx* heart, the injected MDSCs demonstrated cellular fusion with host cardiomyocytes located at the border of the graft and the host myocardium. Our observations of a) donor cells expressing a hybrid cardiac and skeletal muscle phenotype (Figure 2.5) and b) numerous donor cells expressing a cardiac phenotype and containing host Y-chromosome-bearing nuclei (Figure 2.6) provide evidence of fusion between MDSCs and host cardiomyocytes located in this region. Various *in vitro* and *in vivo* studies have shown that different donor cell populations (e.g., hematopoietic stem cells, bone marrow cells, neuronal cells, and cardiac stem cells) can spontaneously fuse with the cells of recipients and adopt the recipient cells' phenotype [89, 133-138]. Our results regarding the identification of MDSC fusion with host cardiomyocytes are in agreement with two recent studies using myoblasts [48, 51]. These studies have reported that C₂C₁₂ myoblasts [48] and primary myoblast cultures [51] implanted into mouse hearts also display the ability to fuse with host cardiomyocytes at the border of the graft and the host myocardium.

2.3.2 Evidence for Potential Nuclear Fusion.

It is interesting to note that of the 50 nLacZ⁺/cTnI⁺ donor cells that contained a Y-chromosome-bearing nucleus, 10 cells displayed nLacZ⁺ and Y-chromosome⁺ signals in the same nuclei. Because the nLacZ⁺ MDSC population contained only female cells, the colocalization of both nLacZ and the Y-chromosome in a single nuclei likely originated from either a) the migration of the nuclear LacZ marker from a female donor nLacZ⁺ nucleus to a

male host nucleus located in close proximity within a multinucleated fused cell or b) the nuclear fusion of an nLacZ[+] donor nucleus with a male host nucleus. Our experimental setup could not distinguish between these two events. Nonetheless, because cytoplasmic fusion is a prerequisite for either of these events to occur, the presence of an nLacZ[+]/Y-chromosome[+] nucleus in a cTnI[+] cell provides further proof of cellular fusion between donor cells and host cardiomyocytes. Although the other 40 “fused” cells contained one nLacZ[+] nucleus and another Y-chromosome[+] nucleus that did not stain positive for nLacZ, we still considered these hybrid cells to be the product of fusion between donor cells and host cardiomyocytes. In these 40 “fused” cells, the lack of nLacZ in the Y-chromosome-bearing nuclei is explainable on the basis of the nuclear domain theory, which proposes that products from an individual nucleus within a multinucleated fused cell will only migrate a limited distance [139]. Thus, the donor nucleus and host nucleus in these fused cells might not have been located in sufficient proximity for the donor nLacZ gene product to migrate into the host nucleus.

2.3.3 Cardiac Differentiation of MDSC without Cellular Fusion

The primary goal of the sex-mismatched donor and host transplantation experiment was to detect fusion of donor MDSCs with host cardiomyocytes. While analyzing our results, however, we observed numerous *nLacZ* donor-derived myocytes that expressed cTnI but did not contain the Y-chromosome-bearing nucleus indicative of a fusion event (Figure 2.6b). Although these donor-derived myocytes could have arisen via differentiation of MDSCs into cardiomyocytes, the inability to detect Y-chromosome-bearing nuclei in these cells might also be attributed to technical limitations associated with the detection of the Y-chromosome *in situ*. Further

experimentation is necessary to determine if MDSCs are capable of undergoing true cardiac differentiation.

2.3.4 Gap Junction Formation for Electromechanical Coupling

We did not observe connexin43 gap junction connections between donor myocytes or between donor and host myocytes at the graft-myocardial border. The lack of gap junction complexes may signify both electrical isolation of the graft from the myocardium and the potential for cardiac arrhythmias [51, 140], and therefore could be a major limitation associated with the use of MDSCs and other muscle-derived cell types for cardiac repair. We did not monitor for arrhythmias in this study; however, a previous study using surface electrocardiogram did not detect arrhythmias in murine hearts engrafted with C2C12 myoblasts [41]. Future studies will investigate the potential of engrafted MDSCs to induce arrhythmias.

2.3.5 Scar Tissue Formation

Gap junction connections and fusion of transplanted MDSCs with host cardiomyocytes require intimate interaction of the donor cells with the host cardiomyocytes. Our results revealed scar tissue present at the graft and host myocardium interface and within the graft itself. We posit that the scar tissue forms a barrier between the graft and the host myocardium and, in so doing, may prevent donor cells from potentially fusing or coupling via gap junctions with host cardiomyocytes. The use of antifibrosis agents in combination with intracardiac cell transplantation may help to block scar tissue formation in the graft and enhance the integration of the graft with the host myocardium.

2.3.6 Donor Cell Contribution to Blood Vessels in the Graft

The potential of transplanted MDSCs to form new blood vessels may help to promote vascularization of the graft and long-term survival of donor cells. Our results revealed numerous blood vessel structures within the graft area; however, we observed only a few donor cells that adopted an endothelial phenotype (Figure 2.9), indicating that most of the blood vessel structures in the graft region were host-derived. In this study, we could not determine whether the donor-derived cells that incorporated into blood vessel structures in the heart were the result of donor cell differentiation into a new blood vessel or donor cell fusion with host-derived blood vessel. In future studies, we will investigate whether MDSCs could differentiate into an endothelial phenotype after injection into the heart by genetically engineering MDSCs with a vector encoding green fluorescent protein (GFP) that is under the control of endothelial cell-specific promoter. If transplanted MDSCs differentiate into endothelial cells, then GFP will be expressed by the MDSCs. Nevertheless, because only a few donor cells incorporated into new blood vessel structures, we hypothesize that the transplanted MDSCs likely induced the formation of numerous host-derived blood vessels in the graft region through the release of angiogenic factors.

2.4 CONCLUSIONS

In conclusion, this study establishes that MDSCs implanted into dystrophic *mdx* hearts can generate large grafts containing numerous dystrophin-expressing myocytes. Although the graft consisted primarily of skeletal muscle myofibers, a small number of donor-derived myocytes

located at the border of the graft and the host myocardium expressed a hybrid cardiac-skeletal phenotype and fused with host cardiomyocytes. Most donor-derived myocytes did not form connexin43 gap junctions with each other or with host cardiomyocytes. In addition to the ability of the transplanted MDSCs to differentiate into numerous dystrophin-positive myocytes, a few donor-derived cells within the graft also expressed an endothelial cell phenotype, indicating that the donor cells may be capable of differentiation into blood vessel structures. Scar tissue that developed at the graft-host myocardium interface may impede the fusion and coupling of MDSCs with host cardiomyocytes and the vascularization of the graft from pre-existing vasculature (i.e., angiogenesis). In conclusion, this study provides insight into the biology and behavior of MDSCs after intramyocardial transplantation in the *mdx* heart and their potential application for the treatment of DMD-induced cardiomyopathy.

2.5 METHODS

2.5.1 Animals

The Institutional Animal Care and Use Committee, Children's Hospital of Pittsburgh, has approved the use of animals and surgical procedures performed in this study (Protocol no. 6/02). The MDSCs were isolated from the skeletal muscle of female normal neonatal (3–5-day-old) mice (C57BL/6J; Jackson Laboratory, Bar Harbor, Maine) as previously described [113]. These cells were injected into the hearts of 10–12-week-old male *mdx*/SCID mice (n=10, C57BL/10ScSn-*Dmd*^{*mdx*} crossed with C57BL/6J-*Prkdc*^{*scid*}/SzJ). These mice are mutant for both the dystrophin and *Prkdc* genes, and therefore possess an *mdx* and SCID phenotype (*mdx*/SCID).

We used this dystrophic mouse model with a SCID background because the donor MDSCs were derived from allogeneic muscle and were genetically engineered to express the bacterial β -galactosidase protein, a potential immunogen.

2.5.2 Isolation and Culture of MDSCs

MDSCs were isolated via the previously described modified preplate technique [98, 113, 114]. MDSCs were cultured in proliferation medium (PM), which contained DMEM, 10% fetal bovine serum, 10% horse serum (HS), 1% penicillin/streptomycin, and 0.5% chick embryo extract [113]. Low serum-containing medium containing DMEM, 5% HS, and 1% penicillin/streptomycin was used to induce MDSCs to form myotubes *in vitro*. Dystrophin expression by the myotubes *in vitro* was determined by immunocytochemistry, as described previously [141].

2.5.3 MDSCs Transduced to Express the nLacZ Reporter Gene

To enable tracking of the cells after injection into the heart, the MDSCs were genetically engineered to express the *nLacZ* reporter gene. MDSCs were infected with the retroviral vector MFG-NB containing a modified *LacZ* gene (*nls-LacZ*) (gift from Dr. P. Robbins), which includes a nuclear-localization sequence cloned from the simian virus 40 (SV40) large tumor antigen and is transcribed from the long terminal repeat. Retroviral infection of MDSCs was performed 3 times, and the transduced cells were assayed for *nLacZ* expression, as described previously [113].

2.5.4 Intracardiac Cell Transplantation

Mice were anesthetized with a gaseous mixture of isoflurane and oxygen and were mechanically ventilated. The heart was exposed via a left thoracotomy, and a 30G needle was used to inject 10 μ l of PBS solution containing 300,000 MDSCs into the left ventricular free wall. Aseptic technique was maintained throughout the procedure. At various time points after transplantation, mice were sacrificed and their hearts were harvested and frozen in 2-methylbutane precooled in liquid nitrogen. The frozen tissue was then serially cryosectioned into 8 μ m-thick sections.

2.5.5 Histology and Trichrome Staining

Previously described techniques were used to stain sections for both *nLacZ* and eosin [113]. The Masson Modified IMEB Trichrome Stain Kit (IMEB), which stains collagen (blue), muscle fibers (red), and nuclei (black), was used according to the manufacturer's instructions to stain additional sections.

2.5.6 Staining for both Cardiac and Skeletal Muscle-Specific Markers

Cryosections were fixed in 2% formaldehyde (Sigma, St. Louis, Missouri) and then multi-label stained for cardiac α -MHC/dystrophin, *nLacZ*/cardiac α -MHC/dystrophin, *nLacZ*/cTnI/fast sk. MHC, *nLacZ*/dystrophin/fast sk. MHC/cTnI, *nLacZ*/cTnI/Cx43/fast sk. MHC, or *nLacZ*/CD31. Each step of these double and triple stains was performed as follows and is detailed in Appendix D. Sections were stained for *nLacZ* expression in X-Gal solution overnight at 37 °C. The MOM Kit (Vector) was used according to the manufacturer's instructions to apply mouse anti-cardiac

α -MHC antibody (1:2 hybridoma supernatant; ATCC) to the sections. Rabbit anti-dystrophin antibody (1:1000; gift from T. Partridge) was incubated overnight at 4 °C and subsequently reacted with FITC-conjugated anti-rabbit IgG (1:100; Sigma) for 90 minutes at room temperature (RT). Goat anti-cTnI antibody (1:25000; Scripps, La Jolla, California) was incubated for 2 hours at RT and then reacted with Cy3-conjugated anti-goat IgG antibody (1:100; Sigma) for 60 minutes. The MOM Kit was used according to the manufacturer's instructions to stain mouse anti-fast sk. MHC antibodies (1:400; Sigma). Rabbit anti-connexin43 antibody (1:250; Chemicon, Temecula, California) was applied for 2 hours and then reacted with donkey anti-rabbit IgG-AlexaFluor 488 conjugated (1:200; Molecular Probes) for 60 minutes. Rat anti-CD31 (1:100; BD Pharmingen) was stained using Vectastain ABC Kit for Rat IgG (Vector). Nuclei were revealed with 4',6-diamidino-2-phenylindole (DAPI) stain (100 ng/ml; Sigma), and all sections were mounted with Vectashield medium (Vector). Detailed immunohistochemistry protocols (step by step) can be found in Appendix D.

2.5.7 Detection of Cellular Fusion

Cryosections from male hearts injected with female MDSCs were fixed with cold 4% formalin (Sigma), rinsed with PBS, and incubated in X-Gal Solution overnight at 37 °C. After being rinsed in PBS, sections were blocked in 10% rabbit serum (Vector) for 60 minutes at RT, and then were incubated with goat anti-cardiac Troponin I antibody (Scripps) for 2 hours at RT. After several rinses in PBS, biotinylated anti-goat IgG antibody (Vector) was applied to the sections for 60 minutes at RT. Streptavidin, Oregon Green™ 488 conjugate (Molecular Probes) was subsequently applied for 10 minutes. Following the immunostaining for cTnI, we used FISH on these same sections to detect the murine Y-chromosome. A mouse Y-chromosome-specific

probe labeled with digoxigenin (gift from Dr. R. Stanyon) and a hybridization mixture were denatured at 75 °C for 10 minutes and allowed to re-anneal for 60–90 minutes at 37 °C. This mixture was applied for 18–24 hours at 37 °C. The hybridized Y-chromosome-specific probe was detected fluorescently by incubating the sections with sheep anti-digoxigenin FAB fragments coupled with Rhodamine (Roche, Basel, Switzerland) for 45 minutes at 37 °C. Nuclei were revealed with DAPI stain (100 ng/ml; Sigma), and all sections were mounted with Vectashield medium (Vector).

2.5.8 Microscopy

All fluorescent and bright-field microscopy was performed with either a) a Nikon Eclipse E800 microscope equipped with a Spot digital camera and software system (v. 3.0.4; Diagnostic Instruments) or b) a Leica DMIRB microscope equipped with a Retiga 1300 digital camera (Q Imaging, Burnaby, Canada) and Northern Eclipse software system (v. 6.0; Empix Imaging, Inc., Cheektowaga, New York).

3.0 CELL THERAPY FOR MYOCARDIAL INFARCTION: SKELETAL MUSCLE STEM CELLS VERSUS COMMITTED SKELETAL MYOBLASTS

3.1 INTRODUCTION

Because cardiac tissue has a limited ability to regenerate after myocardial injury, many patients diagnosed with certain myocardial diseases develop heart failure. As an alternative to heart transplantation, cellular cardiomyoplasty—the transplantation of exogenous cells into heart tissue—has been investigated as a way to regenerate diseased myocardium and improve the performance of failing hearts [3]. Researchers have used various types of cells to investigate cardiac repair [5-7]. In particular, many research groups have reported that mononucleated skeletal muscle-derived cells (i.e., myoblasts and satellite cells) can engraft in the heart and improve cardiac performance [38, 61, 92, 93]. Indeed, some myoblast and satellite cell populations are currently being investigated in clinical trials for cardiac repair [13-15, 36, 44, 130, 131]. Skeletal myoblasts are attractive for clinical use because they can be readily harvested, expanded *in vitro*, and transplanted in an autologous manner.

Before the advent of myoblast transplantation for cardiac repair, numerous studies demonstrated that myoblast transplantation into skeletal muscle is a feasible therapeutic approach for inherited myopathies, including Duchenne muscular dystrophy. However, studies have revealed that most of the cells die shortly after implantation [98, 102, 110] and that only a

small subpopulation plays a role in muscle regeneration [103, 142]. These results suggest that myoblasts constitute a heterogeneous population that may contain a subpopulation of cells with stem cell-like characteristics and a high capacity to promote and participate in muscle regeneration. Recently Tremblay's and Grounds' groups have achieved better engraftment of myoblasts transplanted into skeletal muscle by modifying transplantation techniques and strategies [143-145] or by using a purified fraction of skeletal muscle-derived cells [146]. Myoblast transplantation into cardiac muscle [11, 12, 59, 61, 111] has also led to inefficient engraftment, which is believed to be hindered by the very low survival rate of the transplanted cells. In this study, we posit that the identification and isolation of a myogenic subpopulation with a high regeneration capacity may improve the efficacy of myoblast transplantation into cardiac muscles.

Using various techniques, we and others have identified populations of skeletal muscle-derived stem cells (MDSCs) and have confirmed that they appear to be distinct from satellite cells and myoblasts [112]. Using a modified version of the preplate technique, our research group has fractionated various myogenic cell populations, including satellite cells, myoblasts and MDSCs, from skeletal muscle of normal wild-type mice (C57BL/6J) on the basis of the cells' adhesion characteristics [113, 114]. The marker profile of MDSCs indicates that they are less committed to the myogenic lineage than are satellite cells and myoblasts [113]. These MDSCs can differentiate toward various lineages (i.e., muscle, bone, neural, endothelial, and haematopoietic lineages) [113-115]. More importantly, when we transplanted the same number of myoblasts and MDSCs into the skeletal muscle of dystrophic *mdx* mice, the MDSCs generated a large number of dystrophin-expressing muscle fibers, whereas the myoblasts regenerated only

a few muscle fibers [113]. These results indicate that MDSCs promote muscle regeneration more effectively than myoblasts.

Although our characterization of MDSCs indicates that they possess an enhanced capacity for skeletal muscle regeneration, their potential effect when used for cardiac repair is unknown. Here we explored this application by transplanting both MDSCs and a population of myoblasts into the hearts of adult SCID mice injured by acute myocardial infarction. Our primary objectives were to determine if these 2 myogenic cell subpopulations, MDSCs and myoblasts, would exhibit differential abilities to engraft and improve cardiac function. We also assessed each cell types' ability to adopt a cardiac phenotype, express a gap junction protein, and promote angiogenesis after implantation.

3.2 RESULTS

3.2.1 MDSCs are Less Committed to the Myogenic Lineage than Myoblasts

Because satellite cells and myoblasts are the classic myogenic population used in many basic and clinical research studies focused on cardiac repair, we compared their capacity for cardiac repair with that of MDSCs. The population of myoblasts used for these experiments expressed both Pax7 [147] and desmin, which are both myogenic cell markers. In contrast, the MDSC population displayed low expression of both Pax7 and desmin (Figure 3.1A). These results indicate that the MDSCs exhibited less commitment to the myogenic lineage than did myoblasts.

3.2.2 MDSCs Generate Larger Grafts than Myoblasts after Implantation

We transplanted the same number of myoblasts and MDSCs into the border zone and the central portion of the infarct of adult male SCID mice immediately after myocardial infarction. We then analyzed the extent of cell engraftment and the cardiac function in the cell-treated groups (myoblasts, $n=22$ mice; MDSCs, $n=17$) and the control group (PBS only, $n=16$). We counted the $nLacZ[+]$ cells in serial sections of the infarcted hearts of mice sacrificed at different time points after cell implantation (Figure 3.1B, C, and Appendix B). Comparisons at all time points revealed that the MDSC-treated group contained significantly more $nLacZ[+]$ cells than the myoblast-treated group ($P<0.01$). Observations 1 week after treatment revealed that the myoblast-injected hearts contained a relatively low number of $nLacZ[+]$ cells when compared with the MDSC-injected hearts. Our examination of MDSC-injected hearts at subsequent time points revealed persistent grafts containing high, stable numbers of $nLacZ[+]$ cells. In contrast, the myocardium of myoblast-injected hearts contained very small grafts comprising only a few $nLacZ[+]$ cells at time points subsequent to 1 week after implantation.

On the basis of these data, we estimate that $50.0 \pm 11.8\%$, $59.0 \pm 33.3\%$, $45.1 \pm 12.0\%$, and $25.2 \pm 12.7\%$ of the original number of injected MDSCs (3×10^5) remained 1, 2, 6, and 12 weeks after implantation, respectively. In contrast, only $4.7 \pm 4.6\%$, $0.06 \pm 0.04\%$, $0.13 \pm 0.19\%$, and $0.01 \pm 0.01\%$ of the original number of injected myoblasts remained 1, 2, 6, and 12 weeks after implantation, respectively.

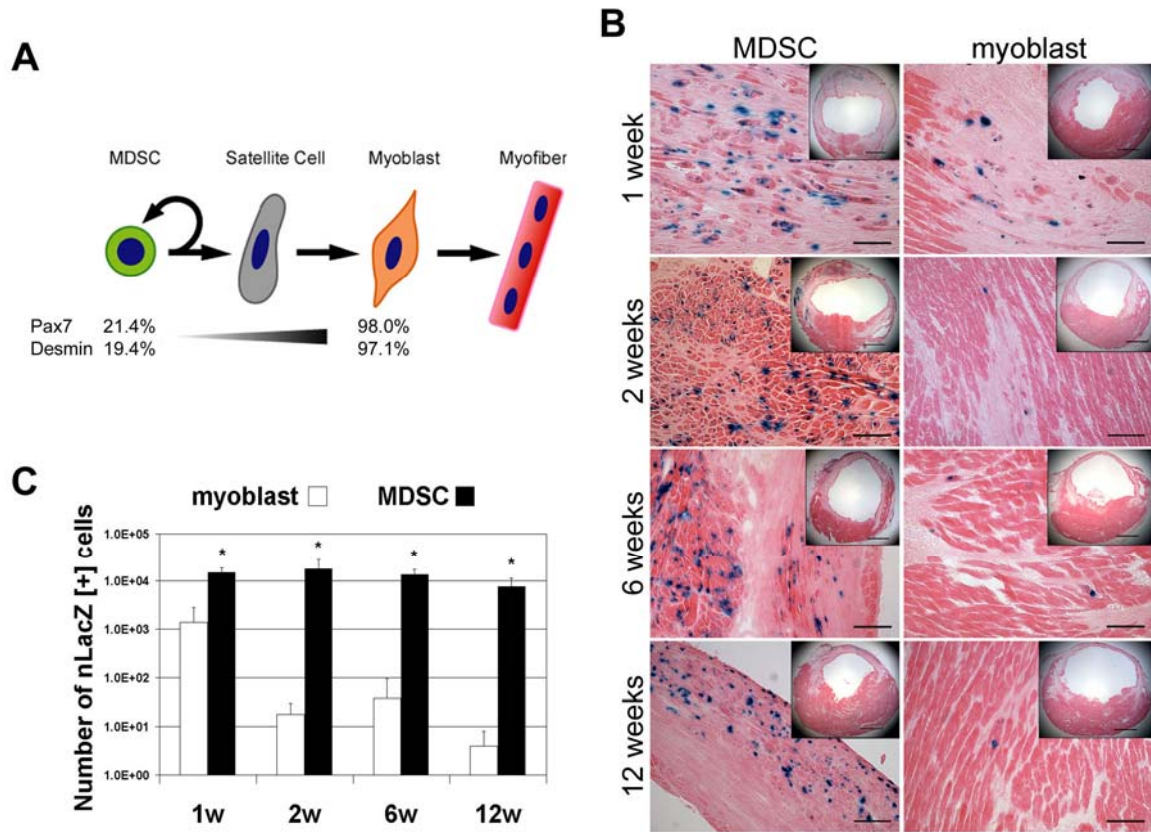


Figure 3.1: MDSCs display superior engraftment in infarcted hearts when compared with myoblasts.

(a) Multipotent muscle-derived stem cells (MDSCs) are less committed to the myogenic lineage than are myoblasts. Characterization of MDSCs and myoblasts by immunocytochemistry revealed a low level of Pax7 and desmin expression in the MDSC population and a high level of Pax7 and desmin expression in the myoblast population. These results suggest that MDSCs are progenitor cells that are less committed to the myogenic lineage than are myoblasts. (b) MDSCs showed excellent engraftment at all time points after implantation in the infarcted hearts, as indicated by the presence of numerous *nLacZ*[+] (blue) myocytes (first column). Although some *nLacZ*[+] cells were visible in the myoblast-injected hearts 1 week after implantation, we observed only a very few *nLacZ*[+] myocytes in the border zone of the graft or within the host myocardium 2, 6, and 12 weeks after implantation (second column). Inset panels are representative images of the infarcted hearts viewed at low-power magnification. Scale bars on insets, 1 mm; scale bars at high-power magnification, 100 μ m. (c) Quantification of the *nLacZ*[+] cells in both the myoblast- and MDSC-injected hearts revealed significantly more *nLacZ*[+] cells in the MDSC-injected hearts than in the myoblast-injected hearts at all time points. (* $P < 0.01$, MDSC vs. myoblast at each time point)

3.2.3 MDSCs Improve Cardiac Function More Effectively than Myoblasts

In the MDSC-injected hearts examined 12 weeks after implantation, the engrafted *nLacZ*[+] donor cells populated primarily the border zone of the infarct and the epicardial side of the infarcted left ventricular free wall (Figure 3.2A, B); very few donor cells were present in these areas within the myoblast-injected hearts (Figure 3.2C, D). To compare the effects of both donor cell populations on left ventricle (LV) remodeling and function, we performed echocardiography 2, 6, and 12 weeks after infarction.

As assessed by LV end diastolic diameter (EDD), progressive LV cavity enlargement occurred in the hearts injected with PBS (control group), and modest enlargement occurred in the myoblast group over time (Figure 3.2E and Appendix B). In contrast, no progressive dilatation of the LV occurred in the MDSC group; the dimensions of the LV cavity remained constant throughout the entire study period (Figure 3.2E and Appendix B; MDSC vs. PBS at 6 and 12 weeks, $P<0.05$; MDSC vs. myoblast at 6 and 12 weeks, $P<0.05$).

We also assessed systolic function in terms of fractional area change (FAC) (Figure 3.2E and Appendix B). Both cell treatment groups showed significantly better systolic function relative to that of the PBS group at all time points (myoblast vs. PBS, $P<0.01$; MDSC vs. PBS, $P<0.01$). Furthermore, FAC in the MDSC group was significantly preserved during the entire study period compared to FAC in the myoblast group ($P<0.01$). Thus, implanted MDSCs appear to have attenuated both ventricular dilatation and dysfunction after acute myocardial infarction more effectively than did myoblasts.

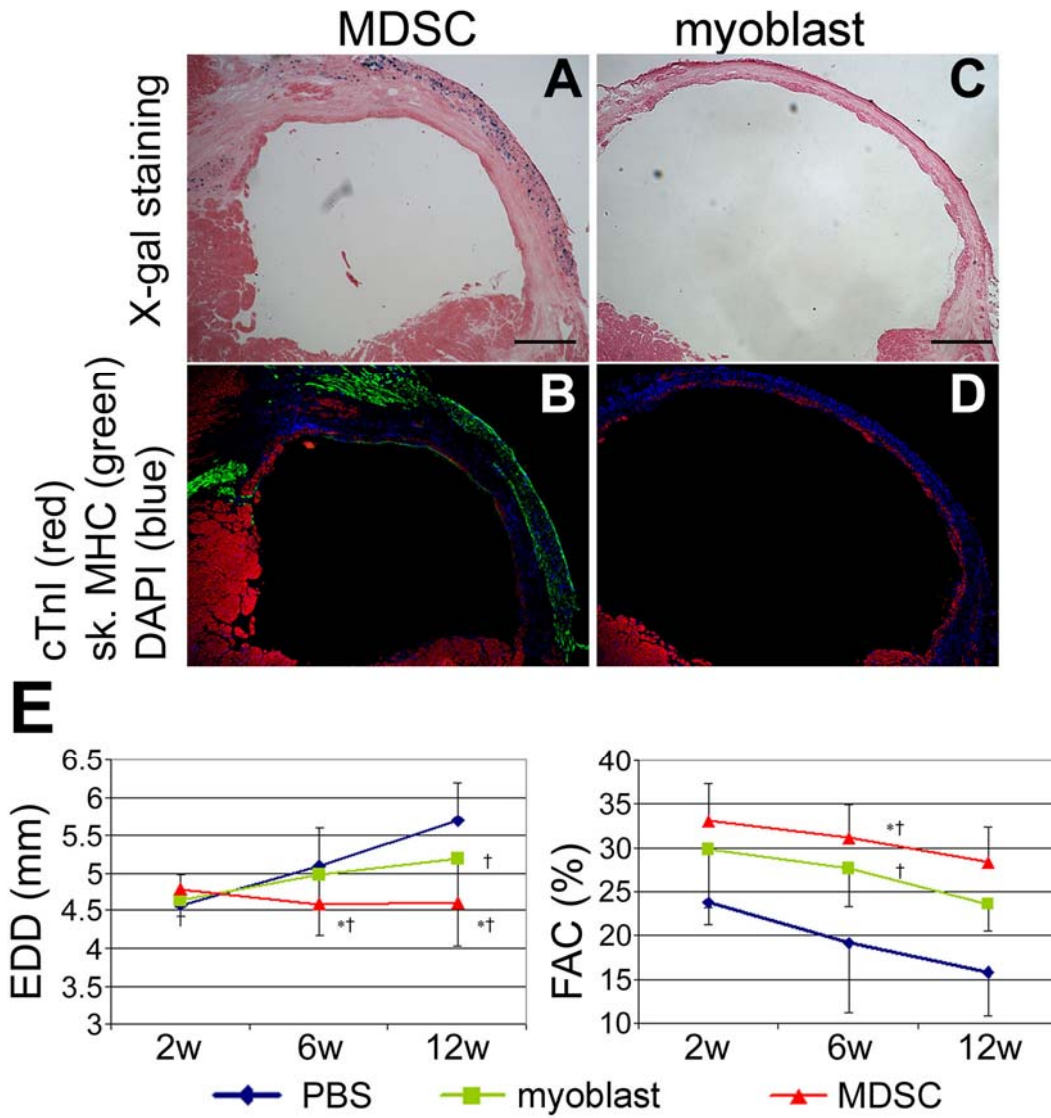


Figure 3.2: MDSCs prevent remodeling and improve cardiac function more effectively than myoblasts.

(a–d) Representative hearts 12 weeks after cell implantation. (a) In this representative section of an MDSC-injected heart, numerous *nLacZ*[+] myocytes are distributed throughout the border zone and the LV free wall regions; in contrast, (c) very few *nLacZ*[+] (blue) cells and poor engraftment are evident in the infarcted LV free wall of this representative section of a myoblast-injected heart. (b, d) Using serial sections from these same hearts, we performed multi-label immunofluorescent stainings for cardiac troponin I (cTnI) (red), fast skeletal myosin heavy chain (fast sk. MHC) (green), and DAPI (nuclear staining) (blue). (b) We detected numerous fast sk. MHC[+] (green) myocytes in the border zone and free wall regions of the MDSC-injected hearts, but (d) none were evident in corresponding regions of the myoblast-injected hearts. Scale bar, 500 μ m. (e) Implantation of MDSCs attenuated LV remodeling and improved cardiac function after acute myocardial infarction. Only MDSC injection significantly inhibited the progressive enlargement of EDD (* $P < 0.05$ MDSC vs. myoblast at 6 and 12 wks, † $P < 0.05$ MDSC vs. PBS at 6 and 12 wks, † $P < 0.05$ myoblast vs. PBS at 12 wks). At all time points, FAC was significantly higher in the cell-injected hearts (MDSC and myoblast groups) than in the PBS-injected hearts († $P < 0.01$, MDSC and myoblast groups vs. PBS group). In comparison with the myoblast group, the MDSC group exhibited significantly improved function at all time points (* $P < 0.01$, MDSC group vs. myoblast group).

3.2.4 Both MDSCs and Myoblasts Acquired a Cardiac Phenotype

We determined the phenotype of MDSCs and myoblasts after implantation into the infarcted hearts. Most of the MDSCs and myoblasts that survived implantation into the heart differentiated toward a skeletal muscle lineage (i.e., they expressed fast skeletal myosin heavy chain [fast sk. MHC]); however, some of the injected cells located at the graft-host myocardium border expressed cardiac Troponin I (cTnI) (Figure 3.3A). We counted many *nLacZ*[+]/cTnI[+] cells in the MDSC-implanted hearts (Figure 3.3B and Appendix B). In contrast, the myoblast-implanted hearts contained a significantly smaller number of donor-derived cells expressing cTnI (Figure 3.3B and Appendix B). These cells also were located in the border zone or within the host myocardium.

3.2.5 Expression of a Hybrid Cardiac and Skeletal Muscle Phenotype.

We next investigated if the donor-derived cells expressing a cardiac phenotype in both the MDSC- and the myoblast-implanted hearts displayed a hybrid cardiac and skeletal muscle phenotype (i.e., fast sk. MHC[+]/cTnI[+]) or a cardiac-only phenotype (i.e., fast sk. MHC[-]/cTnI[+]). We observed donor cells that expressed either a cardiac-only phenotype (Figure 3.3A, C) or a hybrid phenotype in both the MDSC- (Figure 3.3A, C) and myoblast-injected hearts (not illustrated). Fewer than half of the *nLacZ*[+]/cTnI[+] cells in the MDSC-implanted hearts existed in a hybrid state (at 2 weeks, $P < 0.01$), whereas more than half of the *nLacZ*[+]/cTnI[+] cells in the myoblast-implanted hearts existed in a hybrid state (Figure 3.3C and Appendix B).

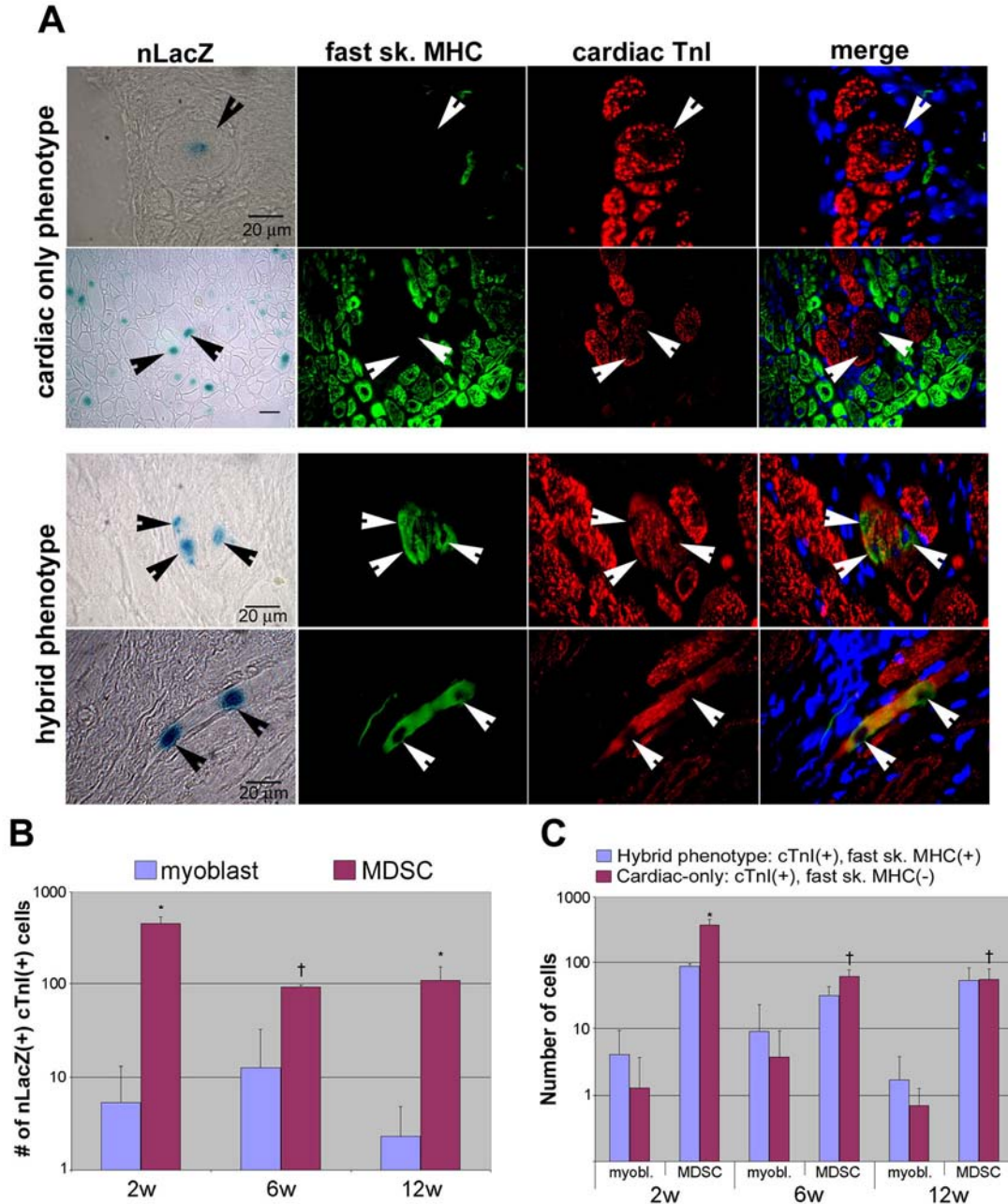


Figure 3.3: Donor cells within the injured myocardium adopt a cardiac phenotype.

(a) Representative cells exhibiting a cardiac only or hybrid phenotype—found within the MDSC-injected hearts—that expressed cTnI (immunofluorescent staining; red) and LacZ (blue) with or without the expression of fast sk. MHC (green). (b) Quantification of cells expressing both *nLacZ* and cTnI in the myoblast- and MDSC-injected hearts at each time point. The MDSC-implanted hearts contained significantly more *nLacZ*[+]/cTnI[+] cells at all time points than the myoblast-implanted hearts (* $P < 0.01$ MDSC vs myoblast at 2 and 12 wks, † $P < 0.05$ MDSC vs. myoblast at 6 wks). (c) Quantification of the *nLacZ*[+] (donor-labeled) cells exhibiting a hybrid cardiac and skeletal muscle phenotype or a cardiac-only phenotype in myoblast- and MDSC-injected hearts at each time point. There was a significant difference between the number of hybrid phenotype cells and the number of cardiac-only phenotype cells in the MDSC-implanted hearts at the 2-week time point (* $P < 0.01$ hybrid phenotype vs. cardiac-only phenotype at 2 wks). The number of cell exhibiting a cardiac-only phenotype in the MDSC-implanted hearts significantly decreased over time († $P < 0.01$ MDSC group ‘cardiac-only phenotype’ at 6 and 12 wks vs. MDSC group ‘cardiac-only phenotype’ at 2 wks).

3.2.6 Size of Donor-derived Cells that Acquired a Cardiac Phenotype.

We also analyzed the size of the myoblasts and MDSCs that expressed a cardiac phenotype. The diameter of myoblasts that expressed a hybrid phenotype was $18.8 \pm 5.6 \mu\text{m}$, and the diameter of myoblasts that expressed a cardiac-only phenotype was $18.7 \pm 4.8 \mu\text{m}$. Likewise, the diameter of MDSCs that expressed a hybrid phenotype was $19.0 \pm 4.5 \mu\text{m}$, and the diameter of MDSCs that expressed a cardiac-only phenotype was $18.2 \pm 5.3 \mu\text{m}$. We did not observe a significant difference in the size of the *nLacZ*-positive donor cells that expressed cardiac markers in the MDSC-injected hearts and the size of those in the myoblast-injected hearts. In addition, we did not observe a significant difference in the size of the donor cells that expressed a cardiac-only phenotype and the size of those that expressed a hybrid phenotype. Moreover, the size of the donor-derived myocytes that expressed a cardiac phenotype in both the myoblast-injected hearts and the MDSC-injected hearts was not significantly different from the size of native cardiomyocytes ($17.9 \pm 3.6 \mu\text{m}$).

3.2.7 Donor Cells Acquire a Cardiac Phenotype through Fusion.

We also performed sex-mismatched transplantation experiments involving the implantation of female donor cells into male recipient mice. To determine if the donor cells adopted a cardiac phenotype through fusion, we counted the *nLacZ*[+]/*cTnI*[+] cells that contained a nucleus bearing a Y-chromosome (Y-chromosome[+]) or lacked one (Y-chromosome[-]) (Figure 3.4A). We examined 345 *nLacZ*[+]/*cTnI*[+] cells in the MDSC group and 42 *nLacZ*[+]/*cTnI*[+] cells in the myoblast group. In the MDSC group, 148 of the *nLacZ*[+]/*cTnI*[+] cells contained a Y-chromosome[+] nucleus; in the myoblast group, 19 of the *nLacZ*[+]/*cTnI*[+] cells contained a Y-

chromosome[+] nucleus (Figure 3.4B). These results suggest that some donor cells (in both MDSC- and myoblast-injected hearts) adopted a cardiac phenotype via fusion with host cardiomyocytes.

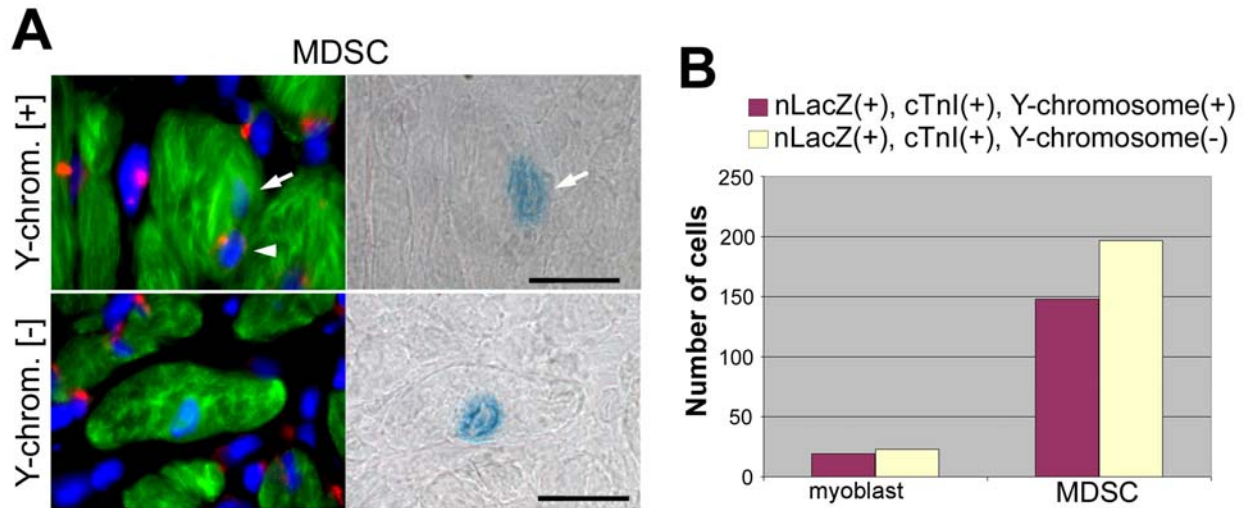


Figure 3.4: Donor cells fusion with host cardiomyocytes.

Fluorescent *in situ* hybridization with a Y-chromosome probe was used to determine the presence of donor nuclei within the cells expressing a cardiac-specific marker. (a) Shown in the top row is a representative cell, found within the MDSC-injected hearts, that expressed cTnI (immunofluorescent staining; green) and contained both an *nLacZ*[+] nucleus (brightfield; blue, arrow) and a Y-chromosome-bearing nucleus (immunofluorescent staining; red, arrowhead). Shown in the bottom row is a representative cell that expressed cTnI (immunofluorescent staining; green) and contained an *nLacZ*[+] nucleus (brightfield; blue) but no Y-chromosome-bearing nucleus (immunofluorescent staining; red). Scale bar, 20 μ m. (b) Quantification of the *nLacZ*[+] (donor-labeled) cells that expressed cTnI and contained a Y-chromosome-bearing nucleus (Y-chromosome[+]) or lacked one (Y-chromosome[-]) in both the myoblast- and MDSC-injected hearts.

3.2.8 Donor Cells Express the Gap Junction Protein Connexin43

We also investigated whether the implanted cells expressed the gap junction protein connexin43, one of the molecular components involved in intercellular electrical communication by cardiomyocytes. In the MDSC- (Figure 3.5) and the myoblast-implanted hearts (data not shown), no donor-derived cells within the graft that were negative for cTnI expressed connexin43. However, approximately 50% of the implanted MDSCs that adopted a cardiac or hybrid

phenotype (cTnI[+]) expressed connexin43 (Figure 3.5A, B). We evaluated all myoblast-implanted hearts and found only 3 donor-derived cells that expressed connexin43 (data not shown), a result likely attributable to the overall poor engraftment of the implanted myoblasts.

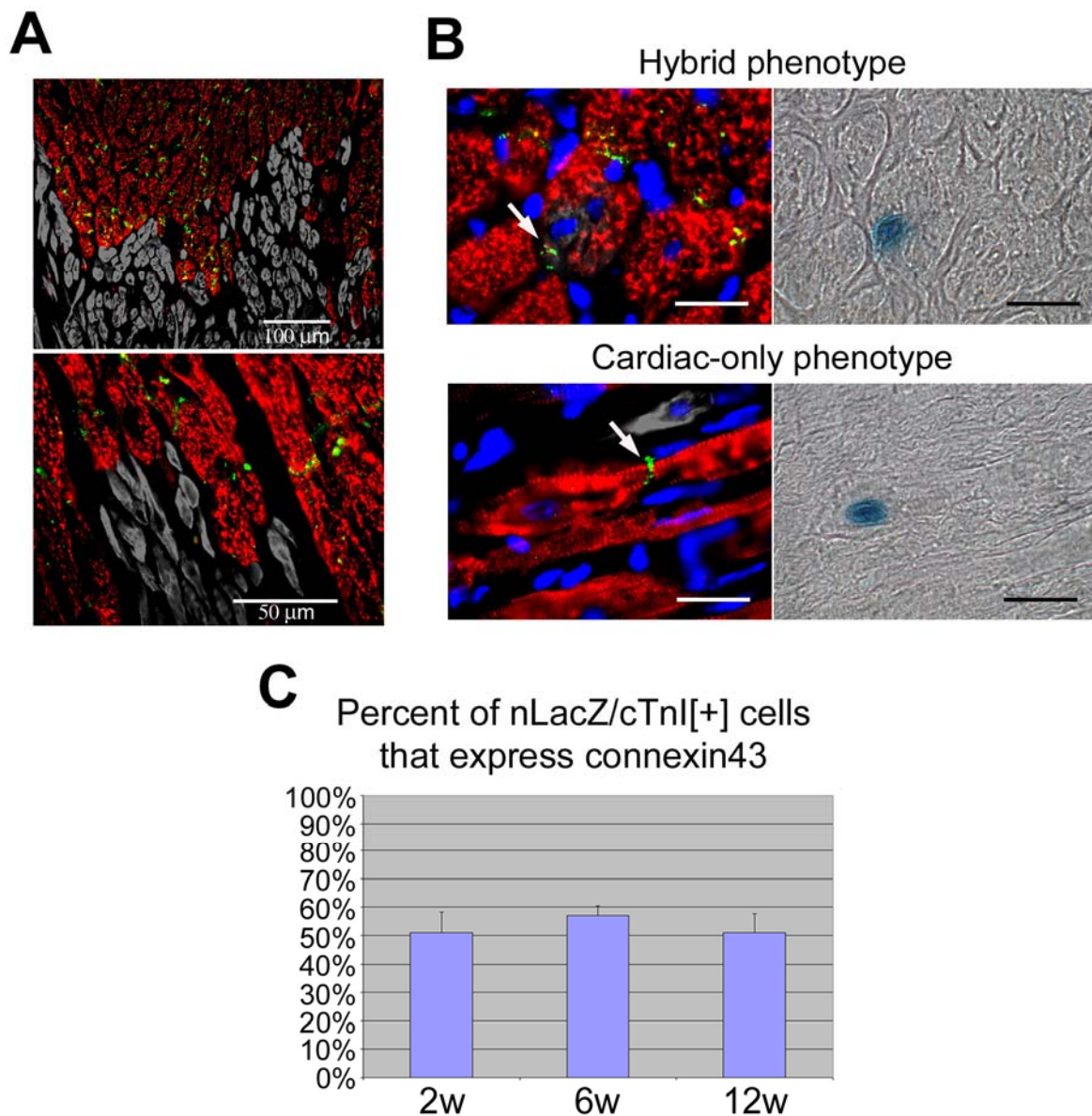


Figure 3.5: Half of the donor cells that acquire a cardiac phenotype express connexin43.

(a) Multi-label staining for cTnI (red), connexin43 (green), and fast sk. MHC (gray) shows that most of the graft (fast sk. MHC[+]/cTnI[-] region) was negative for connexin43. (b) However, some *nLacZ*[+] (donor-labeled) cells that exhibited either a hybrid phenotype or a cardiac-only phenotype and were located at the periphery of the graft

co-expressed connexin43 (green, see arrows). Scale bar, 20 μm . (c) The percentage of implanted MDSCs that expressed cTnI and colocalized with connexin43 at each time point (mean \pm SD).

3.2.9 Induction of Neoangiogenesis by the Implanted Cells

To investigate the mechanism underlying the cardiac functional improvement, we assessed capillary density in the infarct region of hearts injected with PBS, myoblasts, or MDSCs. Capillary density in both the myoblast group and the MDSC group was significantly greater at all time points than capillary density in the PBS group (myoblast vs. PBS, $P < 0.01$ at 2 and 12 weeks, $P < 0.05$ at 6 weeks; MDSC vs. PBS, $P < 0.01$ at 2, 6, and 12 weeks) (Figure 3.6A, B, and Appendix B). Capillary density in the PBS group and the myoblast group decreased significantly over time (2 weeks vs. 6 and 12 week, $P < 0.05$ in both groups) (Figure 3.6A, B, and Appendix B). In contrast, capillary density in the MDSC group increased significantly over time (2 weeks vs. 6 and 12 weeks, $P < 0.01$). Furthermore, capillary density in the MDSC group at 6 and 12 weeks was significantly higher than that in the myoblast group ($P < 0.01$) (Figure 3.6A, B, and Appendix B).

3.2.10 Differentiation of MDSC into New Vasculature.

To investigate if the injected cells promoted angiogenesis by differentiating toward endothelial cells, we analyzed the donor cells' expression of the endothelial cell marker CD31. We counted the *nLacZ*[+]/CD31[+] cells in each heart and found that $0.25 \pm 0.03\%$ of the *nLacZ*[+] cells in MDSC-injected hearts expressed CD31 (Figure 3.6C), but no *nLacZ*[+] cells in the myoblast-injected hearts expressed CD31. These results indicate that more than 99.7% of capillaries in the

infarct zone in MDSC-injected hearts were of host origin, and all capillaries in the infarct zone of the myoblast-injected hearts were of host origin. These findings suggest that muscle cell injection induced neoangiogenesis in the infarct zone; however, this angiogenesis was not primarily due to donor cell differentiation into endothelial cells.

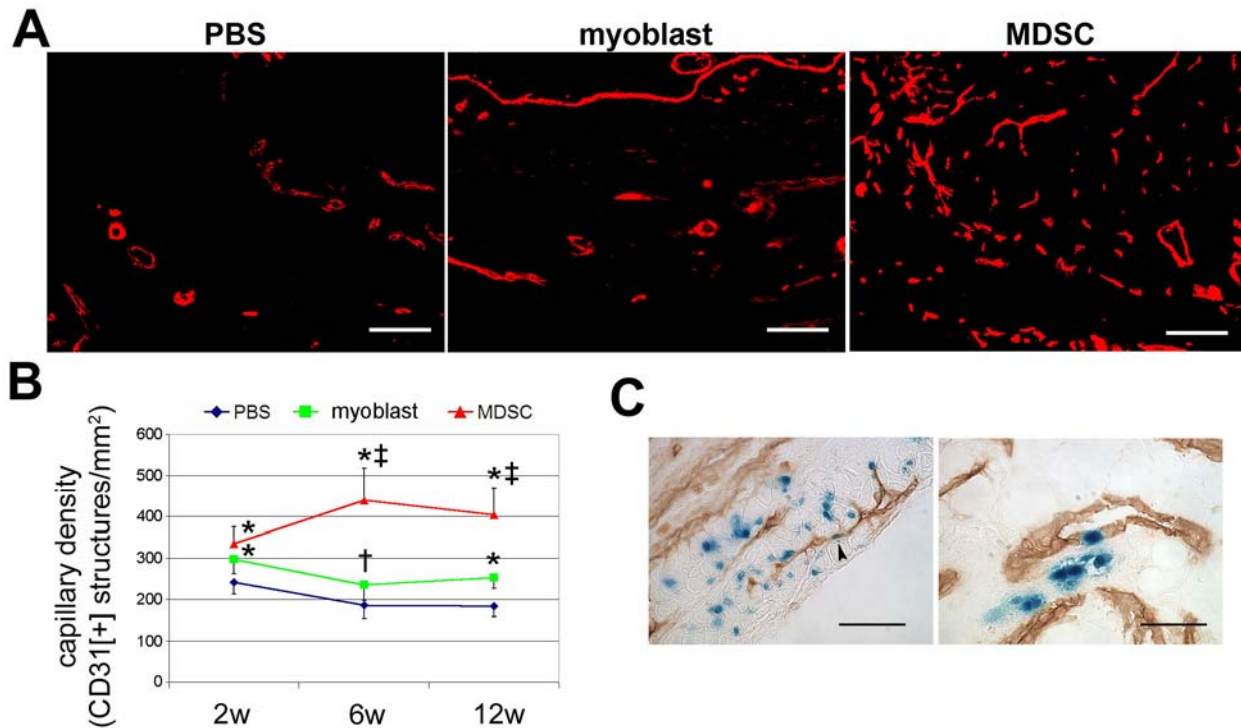


Figure 3.6: Analysis of neoangiogenesis within the infarcted hearts.

(a) Representative images of capillary density, as determined by CD31 immunostaining of the infarct regions within PBS-, myoblast-, and MDSC-injected hearts 6 weeks after implantation. Scale bar, 100 μm . (b) Both myoblast- and MDSC-injected hearts exhibited significantly greater capillary density than PBS-injected hearts at all time points (* $P < 0.01$, † $P < 0.05$). Furthermore, MDSC-injected hearts exhibited significantly greater capillary density than did myoblast-injected hearts 6 and 12 weeks after implantation (‡ $P < 0.01$). (c) Representative images of the colocalization of nLacZ[+] (donor-labeled) nuclei (blue) and CD31 (brown) in small capillaries (left panel, arrowhead) and vessels (right panel) of the MDSC-injected hearts indicate that few donor cells adopted an endothelial cell phenotype. Scale bar, 50 μm .

3.2.11 Donor Cells Express Vascular Endothelial Growth Factor (VEGF)

To further characterize the mechanism underlying the observed enhancement of angiogenesis in the infarct zone, we investigated whether the implanted cells expressed VEGF. As expected on the basis of prior findings, we did not detect VEGF expression in the normal myocardium [148] or in the myofibers of normal tibialis anterior skeletal muscle [149]. Our examination of the PBS-injected hearts 3 days after infarction revealed low VEGF immunoreactivity, but only in endothelial cells lining the small vessels in the infarct region and not in cardiomyocytes (data not shown) [148]. Immunohistochemistry revealed VEGF expression (red) by the donor-derived cells co-expressing LacZ (blue) and fast sk. MHC (green) in both myoblast- and MDSC-injected hearts (Figure 3.7A). Our examination of MDSC-injected hearts from 1 to 12 weeks after cell implantation revealed VEGF expression (green) by many donor cells within the grafts but not by host cardiomyocytes (Figure 3.7B). Our examination of myoblast-injected hearts from 1 to 12 weeks after cell implantation revealed VEGF-positive signals only in the donor cells at the 1-, 2-, and 6-week time point; we observed no VEGF expression 12 weeks after implantation (Figure 3.7B). In addition, very few of these VEGF-positive donor-derived cells were visible 2 and 6 weeks after cell implantation, because the total number of engrafted cells decreased over time in the myoblast-injected hearts (as described earlier). Thus the injection of MDSCs led to significantly more neoangiogenesis (CD31 staining, red) in the infarct region than did the injection of myoblasts, and it is plausible that the persistent VEGF expression (green) by the implanted MDSCs contributed to this promotion of angiogenesis.

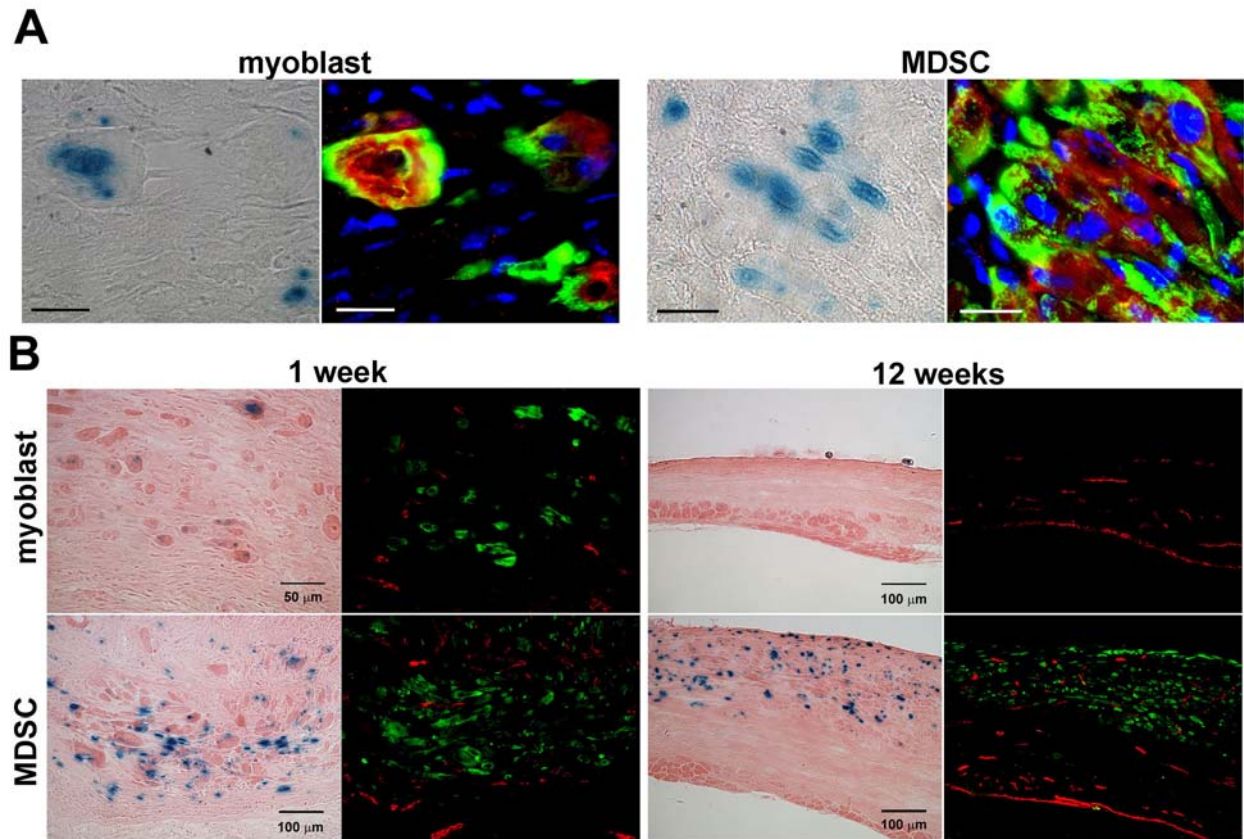


Figure 3.7: Transplanted cells express VEGF in the infarct.

(a) Shown are representative *nLacZ*[+] cells (blue), found within the MDSC- and myoblast-injected hearts, that expressed both VEGF (red) and fast sk. MHC (green). Scale bar, 20 μ m. (b) Representative pictures of VEGF expression (green) and angiogenesis (CD31 staining, red) by the implanted muscle cells. One week after implantation, the donor cells in the infarct region of myoblast- and MDSC-injected hearts expressed VEGF; however, few capillaries were visible within the graft at this time point. We observed no donor cells expressing VEGF in myoblast-injected hearts 12 weeks after implantation. In contrast, observation of the MDSC-injected hearts at the same time point (12 weeks after implantation) revealed persistent grafts that exhibited VEGF expression (green staining) and a greater capillary density (red staining).

3.3 DISCUSSION

This study generated several key findings: (a) In comparison with transplanted myoblasts, transplanted MDSCs exhibited superior engraftment and persistence within injured hearts potentially due to their ability to resist stresses associated with ischemic myocardium; (b) Injected MDSCs attenuated LV remodeling and improved cardiac function after acute

myocardial infarction more effectively than did injected myoblasts; (c) MDSCs induced more angiogenesis in the infarct zone than did myoblasts. These results indicate that the transplantation of MDSCs rather than myoblasts could optimize the benefits of myogenic cell transplantation in the heart.

3.3.1 Cell Engraftment and Persistence

Several studies [11] have demonstrated that a distressingly high percentage of cells die after transplantation into the heart; observations of such behavior by myoblasts (satellite cells) [12, 59, 61], cardiomyocytes [150], haematopoietic stem cells [73, 78], and mesenchymal stem cells [66, 68] are well documented. Our results indicate that MDSCs can more effectively overcome the hurdle of cell death after implantation in infarcted hearts than can myoblasts.

The degree to which MDSCs and myoblasts display myogenic commitment may also affect their regeneration capabilities *in vivo*. Research has shown that muscle-specific gene expression by myogenic precursor cells promotes cell cycle arrest and progression toward terminal skeletal muscle differentiation [151]. Our *in vitro* studies indicate that myoblasts under normal growth culture conditions exhibit a significantly longer division time than MDSCs (data not shown). We also have previously demonstrated that myogenic progenitor cells that display less commitment to the myogenic lineage have a significantly higher regeneration capacity after transplantation into skeletal muscle of mdx mice than do cells that exhibit stronger myogenic commitment [113, 152]. On the basis of these related findings, we hypothesize that, in comparison with MDSCs, the myoblasts used in the current study exhibited lower proliferation *in vitro* and poorer regeneration *in vivo* due to the myoblasts' higher expression of myogenic-

specific genes, which may induce premature cell cycle withdrawal and limit their regenerative potential.

Although they have observed inconsistent rates of engraftment [61], numerous research groups have shown that transplanted myoblasts/satellite cells generate grafts of skeletal muscle in the heart. These findings are at odds with our results, which show numerous donor myoblasts 1 week after implantation in the heart but only a very small number of surviving myoblasts 2, 6, and 12 weeks after implantation. There are at least 2 possible explanations for this apparent discrepancy between our results and those reported by other investigators.

The first possible explanation involves the timing of cell injection after injury to the heart. We injected both cell types immediately after ligation of the coronary artery. The acute myocardial infarction model used in our study produces a more severe environment for implanted cells than does the chronic model of myocardial infarction used in many animal studies and clinical trials focused on cardiac repair. Researchers using the chronic model usually wait at least 1 week after injury before injecting the cells. The increased severity associated with the acute model might explain why the myoblasts in our study exhibited lower levels of engraftment than observed in other studies [8, 46, 61, 153].

Secondly, our study involved the use of a relatively pure population of myoblasts (98.0% Pax7[+], 97.1% desmin[+]) that we isolated via the modified preplate technique. Most other researchers working in this area have transplanted heterogeneous myoblast populations. As mentioned previously, these heterogeneous populations may contain a subpopulation, like MDSCs, that exhibits stem cell-like characteristics and is potentially responsible for the majority of muscle regeneration observed after cell implantation in skeletal muscle [103]. The purified,

mononucleated myoblast population used in our study may have been depleted of any such stem cell-like subpopulation.

3.3.2 Adoption of a Cardiac Phenotype

Most of the implanted MDSCs and myoblasts differentiated into skeletal muscle cells within the infarct. However, at the border between the graft and host myocardium, we observed a small percentage of implanted cells that acquired a cardiac phenotype. In this study, the presence of (a) donor cells expressing a hybrid cardiac and skeletal muscle phenotype and (b) donor cells containing a Y-chromosome-bearing nucleus indicate that some of the donor cells acquired a cardiac phenotype via fusion with host cardiomyocytes. Our findings are in agreement with those of other researchers who have recently reported a low level of fusion of transplanted C2C12 myogenic cells [48] and primary culture myoblasts [51] with host cardiomyocytes. Although some donor cells may have acquired a cardiac phenotype through differentiation, this study was not designed to determine whether MDSCs and myoblasts differentiated into cardiomyocytes. Our future studies will address this issue by incorporating techniques such as the Cre-Lox system.

3.3.3 Functional Improvement

The injection of either population of cells improved the function of the infarcted hearts when compared with PBS injection. However, the injection of MDSCs attenuated LV remodeling and improved the systolic function more than did the injection of myoblasts. Although both myoblasts and MDSCs acquired a cardiac phenotype, the incidence was not high and is not likely

to be the reason for the functional improvement. Aside from the presence of connexin43 in only those donor cells that adopted a cardiac phenotype, the majority of the graft did not express connexin43, which suggests an electrical disconnect between most of the engrafted cells and the host myocardium [51, 140]. Thus, it is unlikely that a significant number of donor cells directly participated in the formation of functional syncytium with the host myocardium [38]. Other researchers have hypothesized that engrafted myocytes may respond to the intrinsic mechanical stretch encountered during diastole with a passive mechanical contraction and thereby may attenuate ventricular dilatation and prevent scar thinning [61, 92, 93, 153].

Functional improvement and attenuation of LV dilatation may be dependent on the size of the graft. The larger grafts within the MDSC-injected hearts correlated with greater improvements in cardiac function and attenuation of LV dimensions than observed in the satellite cell-injected hearts, which contained extremely small grafts at all time points during functional assessment. Our observations are in agreement with those reported in a study by Tambara et al. [111], which showed that larger graft sizes correlated with greater improvements in cardiac function and a reversal in LV remodeling after myoblast transplantation into rat hearts exhibiting chronic infarction. However, Tambara et al. [111] found that the generation of a large graft in the rat model of chronic infarction required a massive dose of myoblasts (5×10^7); lower doses (5×10^6 or 5×10^5) produced very small grafts. Thus the results reported by Tambara et al. [111] also reflect the high engraftment variability often associated with conventional myoblast transplantation in the heart, especially when different numbers of cells are injected.

3.3.4 Neovascularization Elicited by Cell Transplantation

The finding that the injection of myoblasts limited LV dilatation and improved cardiac function despite extremely poor engraftment of the cells indicates that the development of large grafts cannot fully account for the functional improvements observed in our study. Again, this finding closely parallels those of Tambara et al., which showed that even very small grafts generated by implanted myoblasts attenuated LV remodeling [111].

Many previous studies have proposed the expression of certain growth factors by implanted cells as a possible mechanism for functional improvement [11, 12, 38, 57] and it has been previously demonstrated that myogenic cells expressed VEGF after acute ischemia in skeletal muscle [154, 155]. Indeed, we found that the grafts in both myoblast- and MDSC-injected hearts expressed VEGF, which is likely to have induced neoangiogenesis within the infarct zone. This expression of VEGF could explain the higher capillary density observed in the infarct zone of the cell-injected hearts when compared with the infarct zone in PBS-injected hearts. Even though all the donor myoblasts died within 2 weeks after injection, the presence and expression of VEGF 1 week after injection may have contributed to the higher capillary density observed in the infarct zone at later time points (2, 6, and 12 weeks after implantation) upon comparison of the myoblast-injected hearts with the control (PBS-injected) hearts. Thus, the mechanism by which myoblast-injected hearts elicited an improvement in cardiac function likely involved the expression of VEGF and possibly other growth factors that induced neoangiogenesis within the infarct zone. In comparison with the myoblast-injected hearts, the MDSC-injected hearts exhibited a higher capillary density in the infarct zone, probably due to the presence of large grafts expressing VEGF at all time points after transplantation. This enhanced angiogenesis in the infarct zone was likely another major contributor to the functional

improvement and attenuation of LV dimensions observed in the MDSC-injected hearts when compared with myoblast- and PBS-injected hearts.

3.4 CONCLUSIONS

In conclusion, this study demonstrates that MDSCs and myoblast progenitors from skeletal muscle display differential abilities for cardiac repair. When compared with transplanted myoblasts, transplanted MDSCs elicited significantly greater improvements in the function of infarcted hearts. This finding is due in part to the MDSCs' ability to generate larger and more persistent grafts that expressed VEGF, which likely promoted a higher level of angiogenesis in the infarct zones. Our findings suggest that the identification and use of MDSC-like myogenic subpopulations in human skeletal muscle would significantly aid efforts to enhance the efficacy of skeletal muscle-derived cell transplantation for human cardiac repair [11].

3.5 MATERIAL AND METHODS

3.5.1 Animals

The Institutional Animal Care and Use Committee, Children's Hospital of Pittsburgh, approved the animal and surgical procedures performed in this study (Protocol no. 7/03). MDSCs and myoblasts were isolated from the skeletal muscle of female neonatal (3–5-day-old) wild-type mice (C57BL/6J; Jackson Laboratory, Bar Harbor, Maine) [113]. Coronary ligation and cell

transplantation into infarcted hearts were performed in SCID mice (C57BL/6J-*Prkdc*^{scid}/SzJ; Jackson Laboratory).

3.5.2 Isolation, Characterization, and Expansion of MDSCs and Myoblasts

MDSCs ('LTP' fraction) and myoblasts ('PP2' fraction) were isolated via the modified preplate technique [98, 113, 114]. MDSCs were cultured in proliferation medium, which contained Dulbecco's modified Eagles medium (DMEM), 10% fetal bovine serum, 10% horse serum, 1% penicillin/streptomycin, and 0.5% chick embryo extract [113]. Myoblasts were cultured in proliferation media supplemented with basic FGF (6 ng/mL; R&D Systems, Minneapolis, Minnesota). Antibodies specific for Pax7 (Developmental Studies Hybridoma Bank, Iowa City, Iowa) and desmin (Sigma, St. Louis, Missouri) were used as myogenic lineage-specific markers [113]. All Pax7[+] cells or desmin[+] cells were counted in both cell populations.

3.5.3 Cell Transduction with the nLacZ Reporter Gene

To track the cells after implantation into the heart, both cell populations were genetically engineered to express the *nLacZ* reporter gene. Cells were transduced with the retroviral vector MFG-NB containing a modified *LacZ* gene (*nls-LacZ*) (gift from Dr. P. Robbins), which includes a nuclear-localization sequence.

3.5.4 Myocardial Infarction and Cell Transplantation

We anesthetized the mice during the surgical procedure with 1.0–1.5% isoflurane (Abbott Laboratories, North Chicago, Illinois) in 100% O₂ gas. Myocardial infarction was induced via ligation of the left anterior descending coronary artery 2 mm from the tip of the normally positioned left auricle. Immediately after ligation, a 30 µl solution containing 3x10⁵ MDSCs or myoblasts in PBS was injected into the anterior and lateral aspects of the contracting wall bordering the infarct and into the center of the infarct (10 µl per region). In control mice, 30 µl of PBS was injected into the same locations (10 µl per region) after infarction. The investigator was blinded regarding the contents of the injected solutions (i.e., PBS only, myoblasts, or MDSCs).

3.5.5 Histology and Immunohistochemistry

Mice were sacrificed and their hearts were harvested, frozen in 2-methylbutane precooled in liquid nitrogen, and serially cryosectioned (from the apex to the base of each heart) into sections 5–10 µm thick. Previously described techniques were used to stain sections for both *nLacZ* and eosin [113]. Stainings for cardiac- and skeletal-specific markers, donor-derived cell markers, connexin43, CD31, and VEGF were performed according to the multi-label immunohistochemical staining protocols described in Appendix D. Nuclei were revealed with 4,6'-diamidino-2-phenylindole (DAPI) stain (100 ng/ml; Sigma). All fluorescent and brightfield microscopy was performed using either a Nikon Eclipse E800 microscope equipped with a Retiga EXi digital camera (Q Imaging, Burnaby, Canada) or a Leica DMIRB microscope equipped with a Retiga 1300 digital camera (Q Imaging, Burnaby, Canada). Images were acquired with Northern Eclipse software (v. 6.0; Empix Imaging, Inc., Cheektowaga, New York)

for both microscope setups. The *nLacZ*[+]/*cTnI*[+] cells and donor cells that expressed a cardiac-only or hybrid skeletal-cardiac phenotype were counted in the myoblast-injected hearts and MDSC-injected hearts ($n=3$ mice at 2, 6, and 12 weeks after cell implantation). The size of myocytes was analyzed using NIH image software, as previously described [66].

3.5.6 Estimate of *nLacZ*[+] Cells in Hearts after Infarction

Sections were obtained from MDSC-treated mice and myoblast-treated mice ($n=3$ hearts per time point 1, 2, 6, and 12 weeks after cell implantation). *nLacZ*[+] cells were counted within serial sections (10 μm in thickness) cut from the apex to the base of the infarcted hearts. Because the serial sections were obtained every 100 μm , an estimate of the total number of *nLacZ*[+] cells per heart was made by multiplying the number of *nLacZ*[+] cells counted in all serial sections by a factor of 10; this method of estimation has been used in other studies [73].

3.5.7 Echocardiography

Echocardiography was performed by a blinded investigator using a Sequoia C256 system (Acuson, Mountain View, California) equipped with a 13 MHz linear-array transducer (15L8). Mice were anesthetized with isoflurane gas (3% isoflurane for 1 minute induction and 1.25–1.5% isoflurane for maintenance) and restrained in the supine position. Echocardiography was performed 15 minutes after isoflurane induction was begun on each mouse. Although we are aware that isoflurane gas may have a slight variable cardiodepressant effect, a recent report indicates that echocardiographic assessment of cardiac function in mice anesthetized with isoflurane gas was comparable to that in non-anesthetized conscious mice [156]. Two-dimensional images were

obtained at the mid-papillary muscle level. EDD was measured from at least 6 consecutive beats using the M-mode tracing. FAC was calculated as: $FAC (\%) = [(EDA - ESA) \div EDA] \times 100$. Both end-systolic area (ESA) and end-diastolic area (EDA) were determined from short-axis images of the LV.

3.5.8 Mouse Y-chromosome Fluorescence In Situ Hybridization

A mouse Y-chromosome-specific probe labeled with digoxigenin (gift from Dr. R. Stanyon) and a hybridization mixture were denatured at 75 °C for 10 min and allowed to re-anneal for 60–90 min at 37 °C. This mixture was applied for 18–24 hrs at 37 °C. The hybridized Y-chromosome-specific probe was detected fluorescently by incubating the sections with sheep anti-digoxigenin FAB fragments coupled with Rhodamine (Roche, Basel, Switzerland) for 45 min at 37 °C. We measured the number of *nLacZ*[+]/*cTnI*[+] cells that contained a nucleus bearing a Y-chromosome or lacked one in the MDSC group ($n=6$ hearts; 3–5 sections per heart) and satellite cell group ($n=9$ hearts; 9–20 sections per heart).

3.5.9 Analysis of Angiogenesis

The CD31[+] vessels in the entire infarcted area were counted in hearts injected with PBS ($n=3$ hearts per time point 2, 6, and 12 weeks after injection), myoblasts ($n=3$ hearts per time point), and MDSCs ($n=3$ hearts per time point) by a blinded investigator. Capillary density was expressed as the number of CD31[+] structures per mm^2 , as previously described [157].

3.5.10 Statistical Analysis

The cell quantity, cell diameter, cardiac function, capillary density, and apoptosis data are presented in the graphs as mean \pm standard deviation. One-way ANOVA was used for the cell diameter comparisons. Statistical differences in the number of cells, cardiac function, capillary density, and apoptosis data were determined by two-way ANOVA. If statistical differences were observed, *post-hoc* analysis was performed with a Student-Newman-Keuls multiple comparison test.

4.0 TRANSPLANTED MDSCs IMPROVE CARDIAC FUNCTION AFTER MYOCARDIAL INFARCTION BY INDUCING NEOVASCULARIZATION OF ISCHEMIC MYOCARDIUM THROUGH THE SECRETION OF VEGF

4.1 INTRODUCTION

Cell therapy for ischemic hearts has resulted in improved cardiac performance after myocardial infarction (MI), despite the failure of most implanted cell types to extensively regenerate new myocardium [73]. Instead, improvements in cardiac performance after cell transplantation for myocardial infarct repair have been associated with enhanced neovascularization within ischemic myocardium [83, 158-160]. Furthermore, cell types that induced the greatest level of revascularization of ischemic myocardium also demonstrated the greatest improvement in cardiac function [83] (and refer to section 3.0). We have previously shown that MDSCs improved cardiac function more effectively than committed skeletal myoblasts when injected into hearts after MI (see section 3.0). This difference was partially attributed to the ability of MDSCs to induce more neovascularization within the infarct than myoblasts (see section 3.2.9 and Figure 3.6). Only a rare few donor-derived cells incorporated into new blood vessels, indicating that host-derived cells comprised the new vasculature (see section 3.2.10 and Figure 3.6). Taken together, these results led us to hypothesize that

transplanted MDSCs are stimulated by the milieu of ischemic myocardium to induce neovascularization through the release of angiogenic factors.

Yet, it remains unknown how transplanted cells contribute to revascularization and how this affects cardiac function. Because vascular endothelial growth factor (VEGF) is a potent angiogenic factor, we postulated, in this final study, that transplanted MDSCs induce therapeutic angiogenesis through their secretion of VEGF. Our prior results indicated that transplanted MDSCs express VEGF after injection into the myocardium (see section 3.2.11 and Figure 3.7). To further investigate the role of transplanted cell-secreted VEGF, we employed a gain- or loss-of-function approach using skeletal muscle-derived stem cells (MDSC) engineered to express the angiogenic factor VEGF or the anti-angiogenic factor soluble Flt1, a VEGF-specific antagonist. We report here that intramyocardial transplantation of VEGF-expressing and control MDSCs after MI induced angiogenesis and improved cardiac function compared with the injection of control saline. However, these beneficial effects were abolished when transplanted MDSCs expressed soluble Flt1, despite successful engraftment of the cells.

4.2 RESULTS

4.2.1 Hypoxia and Cyclic Stretch Stimulate VEGF Secretion from MDSCs

A potent activator of an angiogenic response from cells is the microenvironment [161]. Indeed, the milieu of ischemic myocardium after MI likely offers a variety of stimuli that can activate an angiogenic response of injected cells, including but not limited to hypoxia, nutrient-deprivation and cyclic load. A well-known initiator of angiogenesis is hypoxia, which upregulates VEGF

[161, 162]. To determine whether MDSCs generate an angiogenic response to hypoxia *in vitro*, we cultured MDSCs in hypoxia (2.5% O₂) for 24 hours and measured their secretion of VEGF in the cell culture supernatant. As expected, MDSCs displayed a 6-fold increase in VEGF secretion when cultured under hypoxia (2.5% O₂) with normal proliferation culture medium (PM) when compared to normoxia and PM (Figure 4.1a and Appendix C), suggesting that MDSCs are induced by hypoxia to secrete VEGF. Furthermore, when the cells were cultured in serum-free medium (SF), VEGF expression by MDSCs was increased 9-fold by hypoxia when compared to normoxia and PM, indicating that a low-nutrient condition enhances the effect of hypoxia (Figure 4.1a and Appendix C). Since the myocardium is subjected to continuous cyclic load, we subjected MDSCs to cyclic stretch *in vitro* to determine whether mechanical forces stimulate a similar response as hypoxia. We observed from these experiments a significant increase (2-fold) in the level of secreted VEGF when compared to the non-stretch control at 10 and 24 hours (Figure 4.1b and Appendix C). Although cyclic stretch does induce a VEGF response from MDSCs, hypoxia appears to be the strongest initiator of VEGF expression by MDSCs. In addition, we have determined that the conditioned medium from MDSCs exposed to cyclic stretch and hypoxia stimulates the proliferation of mouse coronary artery endothelial cells *in vitro* (data not shown), indicating that MDSCs secrete biologically active factors. Indeed, these *in vitro* results corroborate with our previous *in vivo* results documenting that MDSCs expressed VEGF after injection into ischemic myocardium (see section 3.2.11 and Figure 3.7). These results suggest that MDSCs can elicit a strong angiogenic response based on their release of VEGF in response to hypoxic and mechanical stresses *in vitro*.

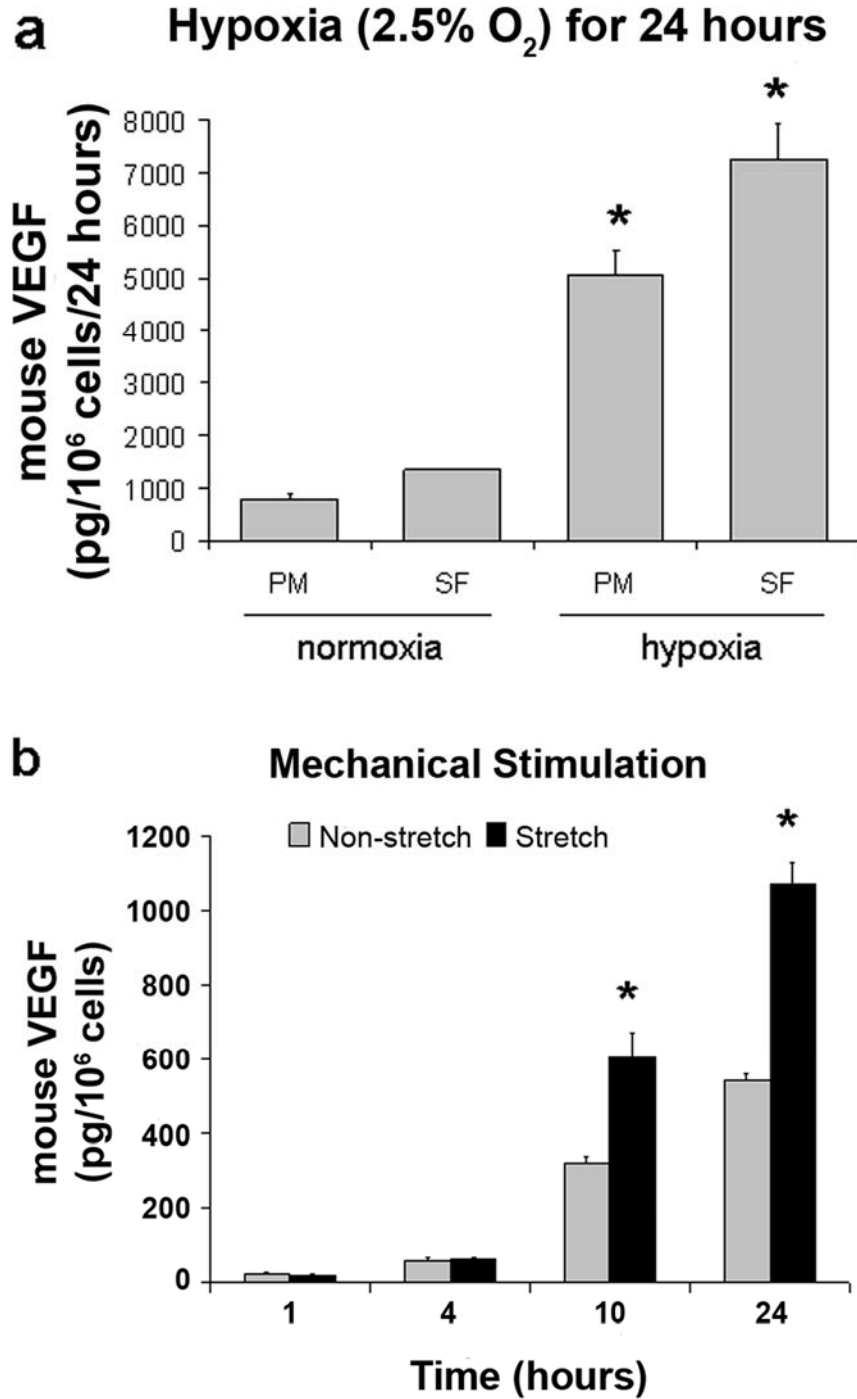


Figure 4.1: Hypoxia and cyclic stretch stimulate stem cells to secrete VEGF.

(a) When exposed to hypoxic condition (2.5% O₂), MDSCs up regulate their secretion of VEGF 6-fold in proliferation medium (PM) and 9-fold in serum-free (SF) culture medium when compared to cells cultured in normoxia (20% O₂) and PM (vs. normoxia and PM or SF, **P* < 0.05). MDSCs demonstrated the highest level of VEGF secretion when cultured under the combination of hypoxia and SF conditions. (b) When exposed to cyclic stretch, MDSCs increase their expression of VEGF 1.9- and 2-fold after exposure to cyclic stretch for 10 and 24 hours, respectively (vs. non-stretch control, **P* < 0.05). This data is also reported in tabular format in Appendix C.

4.2.2 In vivo Study Design

On the basis of these findings *in vitro* and *in vivo*, we hypothesized that the secretion of VEGF by transplanted MDSCs, in response to the milieu of ischemic myocardium, is an important and primary factor through which the transplanted cells evoke angiogenesis and elicit improvements in cardiac function. To test this hypothesis, we employed a gain- and loss-of-function approach to enhance and inhibit the potential therapeutic effects of MDSC-secreted VEGF in a mouse model of MI (Figure 4.2). We used MDSCs genetically engineered with a retrovirus containing the nuclear-localized *LacZ* (nLacZ) gene (MDSC-LacZ) as control MDSCs (Figure 4.2), which would secrete basal levels of VEGF after transplantation into ischemic myocardium. To inhibit the effect of this secreted VEGF, we genetically engineered MDSCs with a retrovirus containing the gene for the VEGF antagonist soluble Flt1 (sFlt-1) (MDSC-FLT), which sequesters MDSC-secreted VEGF (Figure 4.2 and 4.3b). To enhance the effect of VEGF, we transduced MDSCs with a retrovirus containing the human VEGF₁₆₅ gene (MDSC-VEGF) to increase the amount of VEGF secreted by the transplanted cells (Figures 4.2 and 4.3a).

Because the long-term unregulated overexpression of VEGF can induce deleterious *in vivo* side effects, including hemangiomas [163], we attempted to circumvent this concern by decreasing the dosage of VEGF that is delivered by the transplanted cells. We did this by diluting the MDSC-VEGF cells with MDSC-nLacZ cells at 2 different ratios (MDSC-VEGF:total cells): 1:2 ('MDSC-VEGF50') and 1:4 ('MDSC-VEGF25'). After doing this, we measured the level of human VEGF secretion in the MDSC-VEGF50 and MDSC-VEGF25 cell populations. We found that MDSC-VEGF25 secreted half as much VEGF than did the MDSC-VEGF50 cell population (Figure 4.4), indicating that we can effectively control the dosage of VEGF by dilution of the MDSC-VEGF cells with MDSC-LacZ cells.

Model to Test the VEGF Paracrine Effect Hypothesis

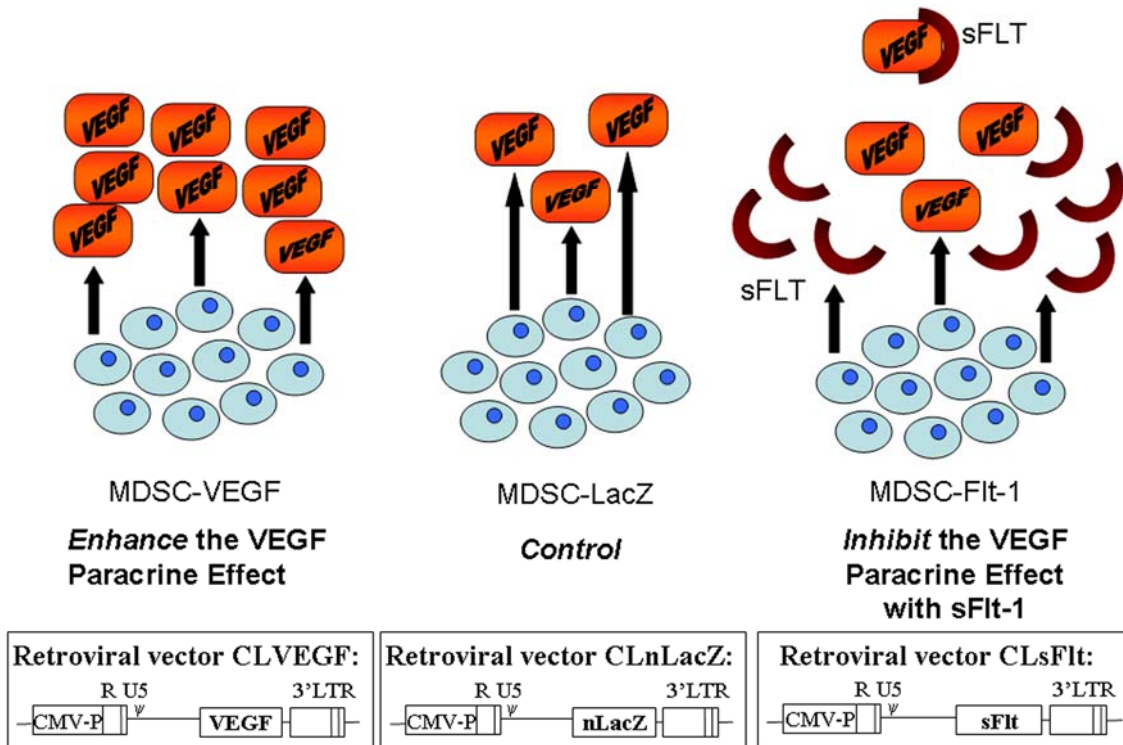


Figure 4.2: Experimental design to test the VEGF paracrine effect hypothesis

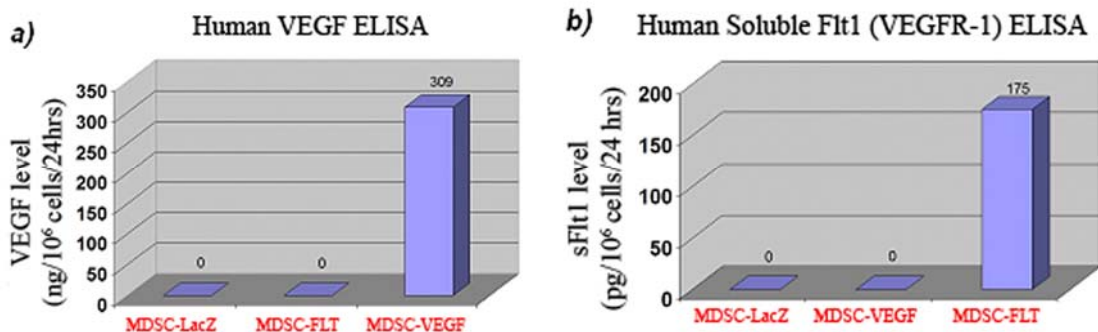


Figure 4.3: Expression of human VEGF and human soluble Flt1 (sFlt) by transduced mouse MDSCs

(a) As detected by a quantitative human VEGF-specific ELISA that does not cross-react with mouse VEGF, MDSCs that were genetically engineered to express the gene encoding human VEGF (MDSC-VEGF) secreted high levels of human VEGF protein (309 ng per 10⁶ MDSCs) into the cell culture supernatant over 24 hours, indicating successful retroviral transduction and transgene expression. As expected, expression of VEGF protein was not detected in the control MDSC-LacZ or MDSC-FLT cell populations. (b) MDSCs engineered to express human sFlt1 secreted 175 pg of sFlt1 protein per 10⁶ cells over 24 hours as detected by a quantitative human sFlt1-specific ELISA that does not cross-react with mouse sFlt1, indicating successful retroviral transduction and transgene expression. The control MDSC-LacZ cells and the MDSC-VEGF cells did not express human sFlt1 transgene.

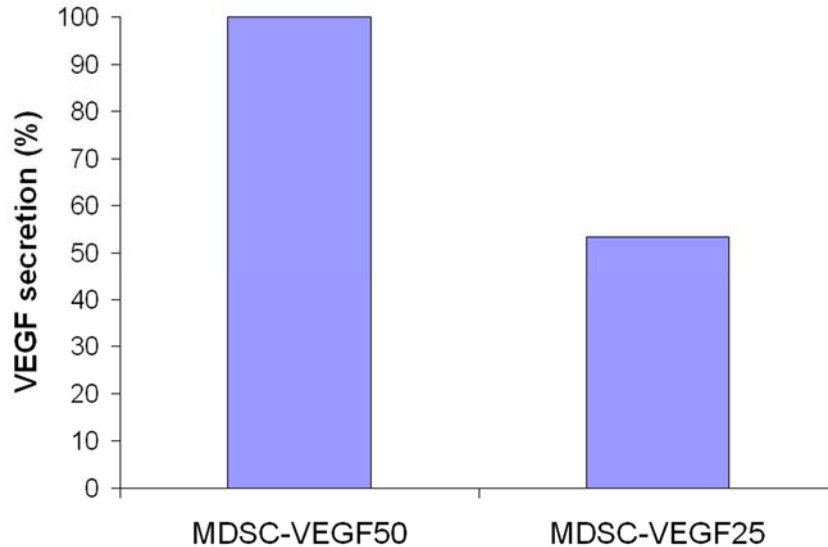


Figure 4.4: Level of human VEGF secretion in the MDSC-VEGF50 and MDSC-VEGF25 cells

As measured by quantitative human VEGF-specific ELISA that does not cross-react with mouse VEGF, the MDSC-VEGF50 cell population secreted twice as much human VEGF as did the MDSC-VEGF25 cell population after 24 hours of culture.

4.2.3 Secretion of VEGF from MDSCs Induces Neovascularization

To assess the level of angiogenesis induced within the infarct 2, 6, and 12 weeks after cell transplantation, we performed immunofluorescent staining for CD31 (PECAM), a marker for blood vessels, and measured the number of CD31-positive capillary structures within the infarct. Comparison of the PBS- and MDSC-FLT-injected hearts with the VEGF-treated hearts revealed that VEGF overexpression in the MDSC-VEGF25 and MDSC-VEGF50 groups enhanced the number of capillaries within the infarcts at all time points (Figure 4.5a and Appendix C). Despite the ability of MDSC-VEGF50 cells to secrete more VEGF than the MDSC-VEGF25 group (Figure 4.4), the finding that MDSC-VEGF50 group did not promote a significantly higher level of neovascularization suggests that a saturated level of VEGF was achieved in these hearts (Figure 4.5a and Appendix C). In contrast, the VEGF antagonist sFlt-1 inhibited the ability of transplanted cells to induce significantly more angiogenesis than the PBS-injected hearts at all

time points (Figure 4.5a and Appendix C). There was a trend that MDSC-FLT injected hearts displayed slightly more angiogenesis than PBS-injected hearts 6 and 12 weeks after MI, indicating that sFlt1 could not block all transplanted cell-induced angiogenesis (Figure 4.5a and Appendix C). Although this finding was not statistically significant, it does suggest either that MDSCs might secrete other factors with limited angiogenic potential or that sFlt1 does not completely sequester all donor cell-secreted VEGF; however, these results still overwhelmingly suggest that transplanted MDSCs induce angiogenesis primarily through the secretion of VEGF. Control MDSC-LacZ-injected hearts also exhibited more angiogenesis than did PBS- and MDSC-FLT-injected hearts; however, as expected, there was less angiogenesis in the control MDSC-LacZ-injected hearts than in either of the VEGF-injected hearts (MDSC-VEGF25 and MDSC-VEGF50) at all time points (Figure 4.5a and Appendix C). Taken together, these results suggest that the secretion of VEGF from transplanted MDSCs is critical for neoangiogenesis to occur within ischemic myocardium.

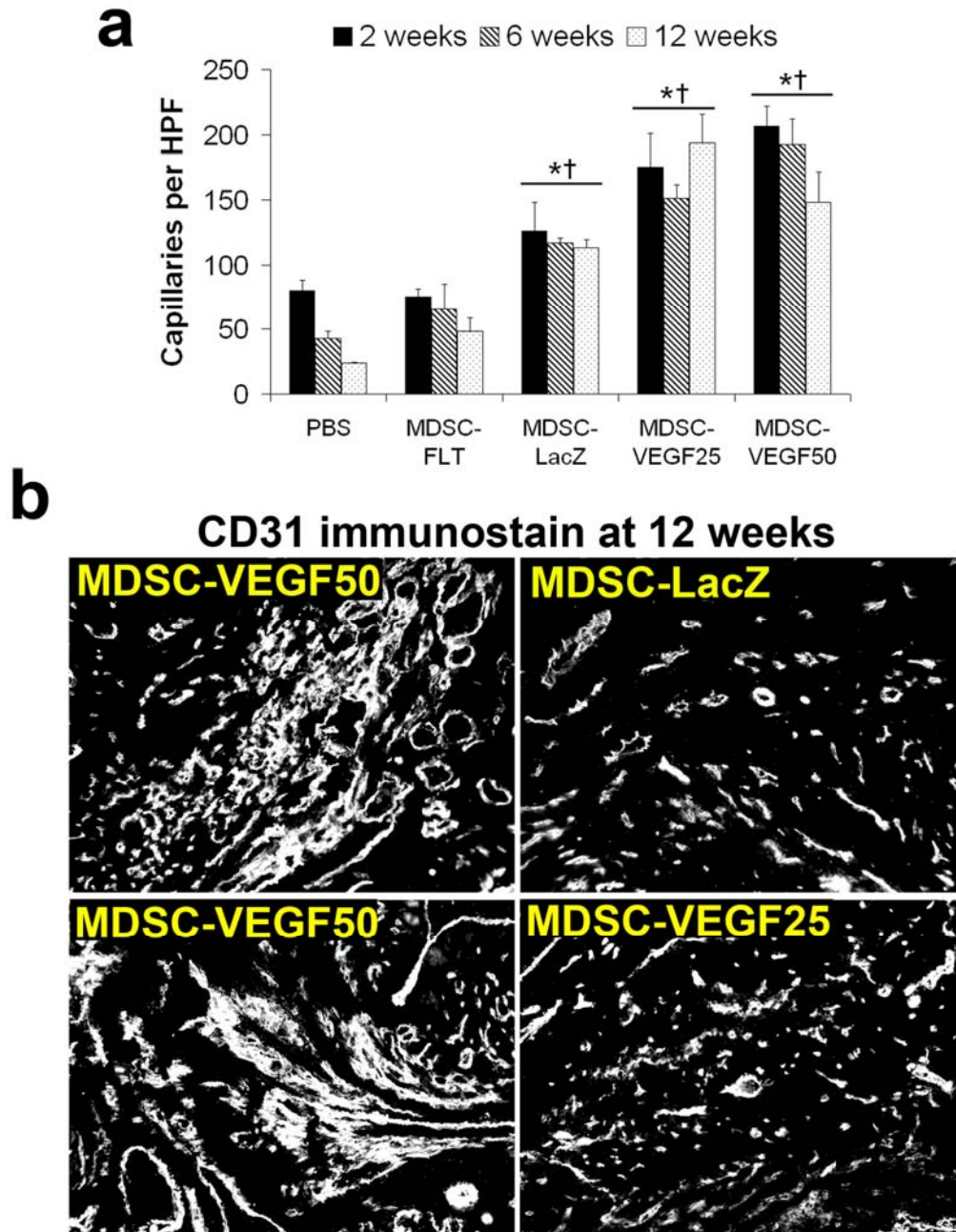


Figure 4.5: Donor cell-induced neovascularization is VEGF-dependent.

(a) The number of blood vessels in the infarct, identified by CD31 immunostain, was highest in the MDSC-LacZ, MDSC-VEGF25, MDSC-VEGF50 groups and significantly more than the PBS- or MDSC-FLT-injected hearts ($* P < 0.01$ vs. PBS, $\dagger P < 0.01$ vs. MDSC-FLT). The hearts injected with MDSC expressing the VEGF antagonist sFlt (MDSC-FLT) contained a lower number of capillaries, which was comparable to the level observed in the control PBS-injected hearts. This data is also reported in tabular format in Appendix C. (b) Unregulated overexpression of VEGF resulted in the potential formation of hemangiomas, a mass of unorganized endothelial cells, as observed in the CD31 immunostain (white), in the MDSC-VEGF50 injected hearts at 12 weeks. However, these abnormal formations were only observed in the MDSC-VEGF50-injected hearts only at 12 weeks but not at earlier time-points. In addition, these findings were not observed in hearts transplanted with stem cells expressing lower levels of the VEGF transgene (MDSC-VEGF25 group) or control MDSC-LacZ, which all displayed normal spatially organized capillaries at all time-points.

Our results indicate that VEGF has a beneficial effect on angiogenesis in the heart; however, its biological effects are dose-dependent [163, 164]. Indeed, at the highest VEGF dosage (MDSC-VEGF50 group), we observed the formation of hemangioma-like structures in hearts injected with MDSC-VEGF50 only at 12 weeks after MI and not at prior time points. However, at lower doses, we observed normal morphology and spatial organization of blood vessels within the myocardial infarct and did not notice the development of any hemangioma-like structures in the MDSC-VEGF25- and MDSC-LacZ-injected hearts at all time-points (Figure 4.5b). These results further confirm earlier findings [163] where continuously high local concentrations of VEGF for long periods of time induced hemangiomas.

4.2.4 Effect of VEGF and sFlt1 on the Transplantation Capacity of MDSCs

To generate an index of cell engraftment, we performed immunofluorescent staining for the skeletal muscle-specific marker fast skeletal myosin heavy chain (fast sk. MHC). Our prior studies have shown that the vast majority of MDSCs transplanted into the heart differentiate into skeletal myocytes that express this skeletal muscle-specific marker, and only a rare few donor-derived cells acquired a cardiac or endothelial phenotype (see sections 2.0 and 3.0). In this study, we also observed that regions of fast sk. MHC reactivity within the heart colocalized with nLacZ (data not shown), another marker for the injected cells. Results from fast sk. MHC immunostaining demonstrate that sFlt-1 had no effect on the engraftment of MDSC-FLT cells in comparison to control MDSC-LacZ (Table 4.1). VEGF overexpression had no effect on the engraftment of MDSC-VEGF25 cells but had an adverse effect on the engraftment of MDSC-VEGF50 group at the 6- and 12-week time points compared to MDSC-LacZ (Table 4.1). These

results suggest that the levels of sFlt-1 and VEGF transgene expression in the MDSC-sFlt-1 and MDSC-VEGF25 groups did not elicit a negative effect on cell engraftment; however, unregulated, long-term, elevated levels of VEGF overexpression in the MDSC-VEGF50 group had decreased donor cell engraftment, potentially caused by VEGF toxicity or by the formation of hemangiomas (Table 4.1).

Table 4.1: Fast sk. MHC graft area (mm²)

	2 weeks	6 weeks	12 weeks
MDSC-LacZ	2.610 ± 0.733	3.035 ± 0.666	2.549 ± 0.779
MDSC-FLT	3.006 ± 0.427	2.993 ± 0.778	2.837 ± 0.813
MDSC-VEGF25	3.050 ± 1.143	2.013 ± 0.853	2.125 ± 1.420
MDSC-VEGF50	4.002 ± 0.305	1.465 ± 0.574*	0.889 ± 0.195*

* $P < 0.05$ vs. 2 week MDSC-VEGF50

4.2.5 Evaluation of Cardiac Function by Echocardiography

To determine whether the gain- and loss-of-function of VEGF affects cardiac performance after MI, we performed echocardiography to measure percent fractional shortening (FS), an index of cardiac contractility. As shown in Figure 4.6, hearts injected with MDSCs engineered to express either LacZ (control, MDSC-LacZ group) or VEGF (MDSC-VEGF25 and MDSCs-VEGF50 groups) showed better cardiac contractility than did control PBS-injected hearts. However, 12 weeks after MI, hearts in the MDSC-VEGF50 group displayed significantly reduced cardiac function (Figure 4.6), perhaps due to deleterious side effects evoked from the formation of hemangiomas (Figure 4.5b), as previously described [163]. Despite this finding, uninhibited expression of VEGF by the transplanted cells resulted in enhanced cardiac performance when compared to control (Figure 4.6). In contrast, hearts injected with MDSCs expressing sFlt1 displayed significantly reduced systolic function (FS) when compared with

hearts injected with LacZ and VEGF-expressing MDSCs (MDSC-LacZ, MDSC-VEGF25, and MDSC-VEGF50 groups) (Figure 4.6). However, comparison of the PBS- and MDSC-FLT-injected hearts revealed no significant difference in FS at any of the tested time points, despite the capacity of the MDSC-FLT cells to engraft to the same extent as control MDSC-LacZ cells (Figure 4.6). Taken together, these results suggest that an improvement in cardiac function elicited by transplanted MDSCs is VEGF-dependent and corresponds with enhanced vascularization of the infarct.

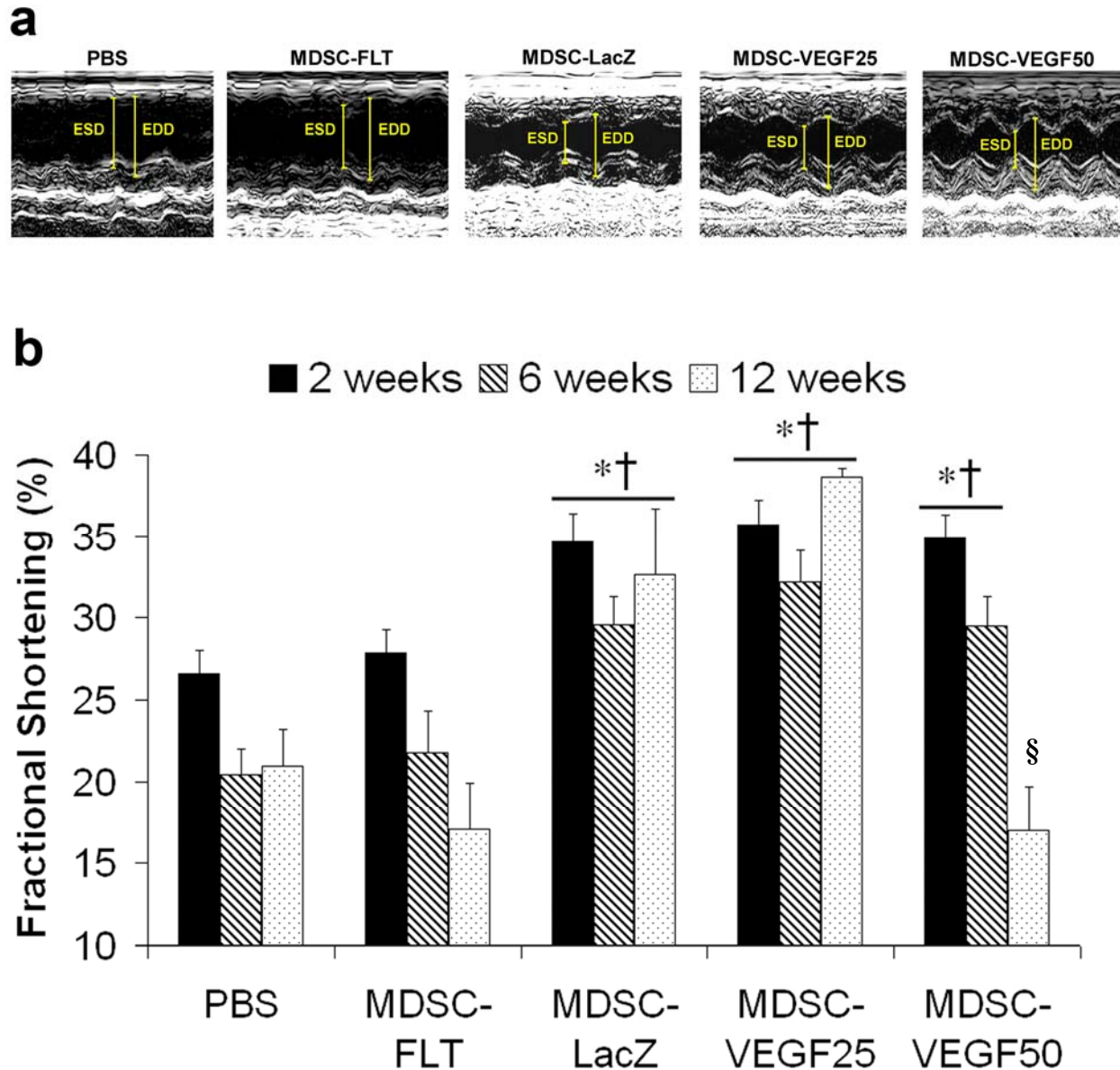


Figure 4.6: Assessment of cardiac function

(a) Representative echocardiographic M-mode images of left ventricles for each group. End-systolic dimensions (ESD) and end-diastolic dimensions (EDD) were measured as indicated in each image to estimate percent fractional shortening (FS). (b) FS, an index of cardiac contractility, was measured at 2, 6, and 12 weeks after infarction. Injection of MDSC-LacZ, MDSC-VEGF25 and MDSC-VEGF50 significantly improved cardiac function ($* P < 0.01$ compared with PBS injection, $\dagger P < 0.01$ compared with MDSC-FLT injection). At 12 weeks after infarction, the MDSC-VEGF50-injected hearts displayed significantly reduced cardiac contractility when compared to the MDSC-LacZ- and MDSC-VEGF25-injected hearts ($\S P < 0.05$ MDSC-VEGF50 group vs. MDSC-LacZ and MDSC-VEGF25 groups at 12 weeks).

4.3 DISCUSSION

These data have important implications for cardiac cell therapy, especially since numerous clinical trials based on autologous skeletal muscle– [13, 14, 19-21, 36, 44, 130, 131], circulating blood–[9], and bone marrow–derived [90, 165] progenitor cells have been initiated without a clear understanding of the mechanism(s) underlying therapeutic benefit. Our results here demonstrate that MDSCs possess a potent capacity for therapeutic angiogenesis based on their ability to secrete VEGF, likely in response to the hypoxic and mechanical stresses that accompany the ischemic milieu of the heart after MI. In addition, this enhanced neovascularization of ischemic myocardium may have a considerable effect on improving cardiac function after MI by bringing blood supply to the myocardium at risk and protecting against cardiomyocyte death and adverse remodeling [83]. This will be further investigated in future studies.

4.4 CONCLUSIONS

In conclusion, our findings suggest that cell-secreted VEGF is critical for inducing therapeutic angiogenesis and functional improvements after myocardial ischemia. These results offer new insights into the mechanism by which cell therapy elicits myocardial infarct repair.

4.5 MATERIALS AND METHODS

4.5.1 Cell Culture and Transduction with Retroviral Vectors

Murine skeletal muscle-derived stem cells were isolated and cultured as previously described by our laboratory [113]. Construction of retroviral vectors containing genes encoding human VEGF, human sFlt-1, or bacterial *nLacZ* was previously described by our laboratory [166]. These cells were transduced separately by the retroviral vectors as previously described [166]. After expansion of transduced cells, cell culture supernatant was assayed for the level of VEGF and sFlt-1 transgene expression by ELISA (R&D Systems, Minneapolis, Minnesota), which were performed according to manufacturer's instructions.

4.5.2 In vitro Stimulation of MDSCs with Hypoxia and Cyclic Stretch

To assess the level of VEGF secretion from MDSCs under conditions of stress, we separately exposed stem cells to cyclic stretch and hypoxia. For hypoxia, MDSCs were plated onto a 6 well plate coated with collagen type I and cultured in proliferation medium (DMEM, 10% fetal bovine serum, 10% horse serum, 1% penicillin/streptomycin, 0.5% chicken embryo extract) until the cells reached ~80% confluence. Nutrient withdrawal was created by replacing the proliferation medium with serum-free DMEM supplemented with 0.1% bovine serum albumin (Sigma, St. Louis, Missouri) for 24 hours. Hypoxic conditions were induced by culturing the cells for 24 hours at 37 °C in an incubator (Heraeus) with an atmosphere of 5% CO₂ and 95% N₂ and a controlled O₂ level of 2.5%. Cyclic stretch was employed with a Flexercell Strain Unit (Flexcell International, Export, Pennsylvania). MDSCs were seeded on a Bioflex culture plate

coated with collagen type I and grown to ~80% confluence. The cells were then subjected to a 10% average surface elongation at a rate of 30 cycles/min for a period of 24 hours. After the completion of all experiments, the cell culture supernatant was collected, flash frozen in liquid N₂ and stored at -80 °C freezer until assayed for mouse VEGF by ELISA (R&D Systems). In all conditions, the attached cells were collected and counted using a hemacytometer.

4.5.3 Myocardial Infarction and Cell Transplantation

All animal experiments and surgical procedures were performed under the approval from The Institutional Animal Care and Use Committee, Children's Hospital of Pittsburgh (Protocol no. 7/03). Acute myocardial infarction was induced in 56 NOD-SCID mice (male, 16 weeks of age, 25–30 grams, NOD.CB17-Prkdc^{SCID}/J, The Jackson Laboratory, Bar Harbor, Maine), as previously described . Immediately after ligation, 3×10^5 cells were transplanted directly into the ischemic region, as previously described (see section 3.5.4). The investigators were blinded as to the contents of the injected solutions: PBS only ($n = 11$ mice), MDSC-LacZ ($n = 11$), MDSC-sFlt-1 ($n = 12$), MDSC-VEGF25 ($n = 11$), or MDSC-VEGF50 ($n = 11$).

4.5.4 Echocardiography

Echocardiography was performed 2, 6, and 12 weeks after cell transplantation by a blinded investigator, as previously described (see section 3.5.7). Two-dimensional images were obtained at the mid-papillary muscle level. EDD was measured from at least 6 consecutive beats using the M-mode tracing. Fractional shortening (FS), an index of cardiac contractility, was calculated as

FS (%) = [(EDD – ESD) ÷ EDD] × 100. Both end-systolic dimensions (ESD) and end-diastolic dimensions (EDD) were determined from short-axis images of the LV.

4.5.5 Tissue Processing and Immunohistochemical Stainings

Mice were sacrificed and their hearts were harvested, frozen in 2-methylbutane precooled in liquid nitrogen, and serially cryosectioned (from the apex to the base of each heart) into sections 7 µm thick. Immunostaining protocols can be found in detail in Appendix D. We performed immunostaining for fast skeletal myosin heavy chain (fast sk. MHC) using a mouse anti-fast sk. MHC antibody (1:400, MY-32 clone, Sigma), as previously described (see sections 2.0 and 3.0). We also performed immunostaining for capillaries using a rat anti-mouse CD31 antibody (1:100, BD Pharmingen) as previously described [166]. To measure infarct vascularization and cell engraftment, digital images of CD31 and fast sk. MHC fluorescence, respectively, in high power fields (HPF) (×20 objective magnification) were acquired throughout the infarct of each heart. We counted the CD31[+] vessels and measured fast sk. MHC[+] area in the images obtained from each group (n = 3 hearts per group per time point [2, 6, and 12 weeks after injection]).

4.5.6 Image Analysis

All fluorescent and brightfield microscopy was performed using a Nikon Eclipse E800 microscope equipped with a Retiga EXi digital camera (Q Imaging, Burnaby, Canada). Images were acquired with Northern Eclipse software (v. 6.0; Empix Imaging, Inc., Cheektowaga, New York). Measurements on images were performed with ImageJ software (v. 1.32j, National Institutes of Health).

4.5.7 Statistical Analysis

All measured data is presented as mean \pm standard error (SE). Statistical differences in the data were determined using a two-way ANOVA. If statistical difference was observed, *post-hoc* analysis was performed using the Tukey multiple comparison test.

5.0 CONCLUSIONS

The findings that we have generated have strong implications given that clinical trials based on skeletal myoblasts have been initiated without a clear understanding of a) the biology of skeletal muscle progenitors for cardiac repair and b) the mechanism by which cell transplantation provides therapeutic benefit. We show here that skeletal muscle contains a stem cell population (MDSCs) that is superior to committed skeletal myoblasts in their capacity for cardiac cell transplantation, and future work to identify such populations in human skeletal muscle is warranted. In addition, we have extensively investigated the mechanism underlying the therapeutic benefit of cardiac cell transplantation. We have shown that MDSCs do not regenerate *de novo* myocardial cells after injection into uninjured (section 2.0) and ischemic (section 3.0) hearts, except for the presence of a rare few donor cells located at the graft-host myocardium border (sections 2.0 and 3.0). Despite this lack of extensive regeneration, we still found that transplanted MDSCs could still effectively repair injured hearts after myocardial infarction (section 3.0). These findings led us to discover that the paracrine effects of transplanted cell-secreted VEGF accounts for the neovascularization and the improvements in cardiac function that are elicited by intramyocardial cell transplantation (section 4.0). Thus we hypothesize that cell transplantation likely provides therapeutic benefit through the paracrine effects of transplanted cell-secreted VEGF rather than the direct differentiation of transplanted cells into

new myocardium. Overall, we believe that this research has contributed significant findings that will help to improve cell-based therapies for cardiac repair.

5.1 FUTURE DIRECTIONS

5.1.1 Identification of Muscle Stem Cells from Human Skeletal Muscle

While our work has given us insight into the biology and therapeutic benefit of mouse MDSC transplantation for cardiac repair, a logical progression of this research would be to identify and isolate a MDSC-like cell population from human skeletal muscle. We could easily evaluate a variety of populations of human skeletal muscle-derived cells for cardiac repair in our established small animal models of myocardial infarction. The identification of a human cell population with properties similar to mouse MDSCs would greatly enhance the efficacy of myoblast transplantation for cardiac repair, since it has been reported in clinical trials that most transplanted human myoblasts rapidly die after injection into the heart [11].

5.1.2 Comparison of Different Adult Stem Cell Types for Cardiac Repair

Although MDSCs appear to be an effective cell type for cardiac repair, it would be interesting to compare MDSCs to other adult stem cell populations (i.e., bone marrow- and circulating blood-derived stem and progenitor cells) and determine which cell type offers the greatest therapeutic potential. If a differential therapeutic effect is observed between different cell types, then it will

be important to determine whether a relationship exists between cardiac function and the engraftment and angiogenic capacity of the transplanted cells.

5.1.3 Cell Therapy for Chronic Models of Ischemic Cardiomyopathy

We have performed this work using a model of acute MI. However, chronic ischemic cardiomyopathy would represent a significant patient population that could benefit from cell therapy [7]. Therefore, future studies should investigate cardiac cell transplantation based on MDSCs in chronic models of myocardial ischemia. In addition, we should incorporate the autologous cell transplantation model and use wild-type and non-immunodeficient mice in future studies. The use of wild-type mice rather than SCID or immune-compromised animal models will allow us to investigate the host immune response after autologous cell transplantation in the heart and its potential effect on cell based therapies.

5.1.4 Alternatives to Cell-based Therapies

We have shown evidence that neovascularization of ischemic myocardium could be the major mechanism by which cardiac cell transplantation provides therapeutic benefit. On the basis of this finding, it would be reasonable to investigate whether the delivery of angiogenic factors by other means could be just as effective as cell transplantation. Gene therapy would be an attractive approach to deliver angiogenic genes to the ischemic myocardium. Additionally, the delivery of angiogenic proteins in combination with injectable biomaterials would be another novel therapy for ischemic myocardium.

APPENDIX A

SUPPLEMENTAL DATA IN TABULAR FORMAT FROM FOR SECTION 2.0

Table A.1: Frequency of donor cells that expressed a hybrid cardiac and skeletal phenotype in each heart

Time-Point	Mouse	Total nLacZ[+], cTnI[+]	nLacZ[+], cTnI[+], fskMHC[+]	nLacZ[+], cTnI[+], fskMHC[-]	Percent Hybrid
2 weeks	1	135	66	69	49%
	2	7	7	0	100%
	3	20	9	11	47%
	Total	162	82	80	51%
4 weeks	4	183	98	85	54%
	5	44	26	18	59%
	6	108	63	45	58%
	Total	335	187	148	56%
8 weeks	7	91	65	26	71%
	8	35	15	20	43%
	9	82	61	21	74%
	Total	208	141	67	68%
12 weeks	10	40	20	20	50%

Table A.2: Frequency of Fusion Events in each MDSC-injected Heart.

Time-point	Mouse	Total nLacZ[+], cTnI[+]	nLacZ[+], cTnI[+], Y-chrom.[+]	nLacZ[+], cTnI[+], Y-chrom.[-]	Percent Y-chrom.[+]
2 weeks	1	15	4	11	27%
	2	N/A	N/A	N/A	N/A
	3	9	3	6	33%
	Total	24	7	17	29%
4 weeks	4	18	4	14	29%
	5	6	3	3	50%
	6	23	7	16	30%
	Total	47	14	33	30%
8 weeks	7	18	12	6	67%
	8	4	1	3	25%
	9	32	16	16	50%
	Total	54	29	25	54%

APPENDIX B

SUPPLEMENTAL DATA IN TABULAR FORM FOR SECTION 3.0

Table B.1: The number of nLacZ[+] cells (mean \pm SD)

	1 week	2 weeks	6 weeks	12 weeks
MDSC	14992 \pm 3529*	17697 \pm 9988*	13544 \pm 3592*	7555 \pm 3797*
myoblast	1402 \pm 1376	18 \pm 12	38 \pm 58	4 \pm 4

* $P < 0.01$ MDSC vs. myoblast

Table B.2: Echocardiographic left ventricular function (mean \pm SD)

	LVEDD (mm)			FAC (%)		
	2 weeks	6 weeks	12 weeks	2 weeks	6 weeks	12 weeks
MDSC	4.8 \pm 0.4	4.6 \pm 0.4* \dagger	4.6 \pm 0.6* \dagger	33.0 \pm 4.3 \P \S	31.1 \pm 3.8 \P \S	28.4 \pm 4.0 \P \S
myoblast	4.6 \pm 0.4	5.0 \pm 0.5	5.2 \pm 0.6*	29.8 \pm 6.6 \P	27.7 \pm 4.4 \P	23.6 \pm 3.0 \P
PBS	4.6 \pm 0.4	5.1 \pm 0.5	5.7 \pm 0.5	23.8 \pm 2.6	19.1 \pm 7.8	15.9 \pm 5.0

* $P < 0.05$ vs. PBS, \dagger $P < 0.05$ vs. myoblast, \P $P < 0.01$ vs. PBS, \S $P < 0.01$ vs. myoblast

Table B.3: The number of nLacZ[+] and cTnI[+] cells (mean ± SD)

	2 weeks	6 weeks	12 weeks
MDSC	446±74*	92±5 †	108±43*
myoblast	5±8	13±19	2±3

* $P < 0.01$ vs. myoblast, † $P < 0.05$ vs. myoblast

Table B.4: The number of donor-derived cells that adopted a cardiac phenotype (mean ± SD)

		2 weeks	6 weeks	12 weeks
MDSC	hybrid	86±9	31±12	53±29
	cardiac-only	360±81*	61±16 †	55±23 †
myoblast	hybrid	4±5	9±14	2±2
	cardiac-only	1±2	4±6	1±1

* $P < 0.01$ vs. hybrid, † $P < 0.01$ vs. 2 week

Table B.5: Capillary density (structures/mm²) (mean ± SD)

	2 weeks	6 weeks	12 weeks
MDSC	335±40 *	440±79 *†‡¶	430±65 *†‡¶
myoblast	297±36 *	234±38 †#	253±27 *#
PBS	241±29	185±32 #	183±26 #

* $P < 0.01$ vs. PBS, † $P < 0.05$ vs. PBS, ‡ $P < 0.01$ vs. myoblast
¶ $P < 0.01$ vs. 2 week, # $P < 0.05$ vs. 2 week

APPENDIX C

SUPPLEMENTAL DATA IN TABULAR FORM FOR SECTION 4.0

Table C.1: Secretion of mouse VEGF (pg/10⁶ cells) from MDSCs in response to cyclic stretch (mean ± SE)

	1 hour	4 hours	10 hours	24 hours
Non-stretch	24 ± 1	55 ± 8	318 ± 20	539 ± 19
Cyclic Stretch	18 ± 2	61 ± 3	605 ± 67*	1071 ± 58*

* $P < 0.05$ versus non-stretch control

Table C.2: Secretion of mouse VEGF (pg/10⁶ cells/24 hrs) from MDSCs in response to hypoxia (2.5% O₂) (mean ± SE)

	Proliferation Medium	Serum-free Medium
Normoxia	79 ± 9	134 ± 3
Hypoxia	505 ± 47*	727 ± 68*

* $P < 0.05$ versus normoxia

Table C.3: CD31⁺ capillaries per HPF (×200) within infarct

	2 weeks	6 weeks	12 weeks
PBS	81 ± 8	43 ± 5	24 ± 1
MDSC-FLT	76 ± 6	66 ± 20	48 ± 10
MDSC-LacZ	126 ± 22*†	117 ± 4*†	113 ± 6*†
MDSC-VEGF25	175 ± 26*†	151 ± 11*†	194 ± 22*†
MDSC-VEGF50	206 ± 16*†	193 ± 20*†	148 ± 24*†

* $P < 0.01$ vs. PBS, † $P < 0.01$ vs. MDSC-FLT

APPENDIX D

STEP BY STEP IMMUNOHISTOCHEMISTRY STAINING PROTOCOLS

Table D.1: Immunohistochemistry Staining Protocols, Part 1

Multi-Label Stain	Cardiac α -MHC /Dystrophin	LacZ/ Cardiac α -MHC/ Dystrophin	LacZ/ Cardiac Troponin I/ Fast Skeletal MHC	LacZ/ Cardiac Troponin I/ Y-chromosome FISH
Fixation	Cold Acetone (2 min.; Sigma)	2% Formaldehyde (2 min.; Sigma)	2% Formaldehyde (2 min.; Sigma)	Cold 4% Formalin (5 min.; Sigma)
Histological Stain	N/A	X-Gal Solution (37 °C, Overnight)	X-Gal Solution (37 °C, Overnight)	X-Gal Solution (37 °C, Overnight)
Blocking Reagents	Mouse IgG Blocking Reagent (60 min.; MOM Kit, Vector)	Mouse IgG Blocking Reagent (60 min.; MOM Kit, Vector)	10% Rabbit Serum (RS) (60 min.; Vector)	10% Rabbit Serum (RS) (60 min.; Vector)
1°	Mouse Anti- α -MHC (ATCC) (1:2 in MOM Diluent; 30 min.)	Mouse Anti- α -MHC (ATCC) (1:2 in MOM Diluent; 30 min.)	Goat Anti-cTnI (Scripps) (1:25,000 in 2.5% RS; 2 hrs.)	Goat Anti-cTnI (Scripps) (1:25,000 in 2.5% RS; 2 hrs.)
2°	Anti-Mouse IgG-biotinylated (10 min.; MOM Kit, Vector)	Anti-Mouse IgG-biotinylated (10 min.; MOM Kit, Vector)	Anti-Goat IgG-Cy3 (Sigma) (1:100 in 2.5% RS; 60 min.)	Anti-Goat IgG-biotinylated (1:150 in 2.5% RS, 60 min.; Vector)
3°	Streptavidin-Cy3 (Sigma) (1:200 in PBS; 10 minutes)	Streptavidin-Cy3 (Sigma) (1:200 in PBS; 10 min.)	Mouse IgG Blocking Reagent (60 min.; MOM Kit; Vector)	Streptavidin, Oregon Green™, 488 Conjugate (1:500; 10 min.) (Molecular Probes)
4°	Rabbit Anti-Dystrophin (1:1,000 in 2.5% HS; Overnight) (Gift from T. Partridge)	Rabbit Anti-Dystrophin (1:1,000 in 2.5% HS; Overnight) (Gift from T. Partridge)	Mouse Anti-Fast Skeletal MHC (1:400 in MOM Diluent; 30 min.) (Sigma)	Mouse Y-chromosome FISH
5°	Anti-Rabbit IgG-FITC (1:100 in PBS; 90 min.; Sigma)	Anti-Rabbit IgG-FITC (1:100 in PBS; 90 min.; Sigma)	Anti-Mouse IgG-biotinylated (10 min.; MOM Kit, Vector)	
6°			Streptavidin, Oregon Green™, 488 Conjugate (1:1,000; 10 min.) (Molecular Probes)	

Table D.2: Immunohistochemistry Staining Protocols, Part 2

Multi-Label Stain	nLacZ/ Cardiac Troponin I/ Y-Chromosome FISH	nLacZ/ Connexin43/ Cardiac Troponin I/ Fast Skeletal MHC	CD31	nLacZ / CD31	nLacZ/ VEGF/ Fast Skeletal MHC	VEGF / CD31
Fixation	Cold 4% Formalin (5 min; Sigma)	4% Paraformaldehyde (5 min; Sigma)	4% Paraformaldehyde (5 min; Sigma)	4% Paraformaldehyde (5 min; Sigma)	4% Paraformaldehyde (5 min; Sigma)	Cold Acetone (2 min; Sigma)
Histological Stain	X-Gal Solution (37 °C, Overnight)	X-Gal Solution (37 °C, Overnight)	N/A	X-Gal Solution (37 °C, Overnight)	X-Gal Solution (37 °C, Overnight)	N/A
Blocking Reagents	10% Rabbit Serum (RS) (60 min; Vector)	10% Donkey Serum (DS) (60 min; Jackson Immuno Research)	10% DS (60 min; Jackson Immuno Research)	5% RS (30 min; VECTASTAIN; Vector)	10% DS (60 min; Jackson Immuno Research)	10% DS (60 min; Jackson Immuno Research)
1°	Goat Anti-cTnI (1:25,000 in 2.5% RS; 2 hrs; Scripps)	Rabbit Anti-Mouse Connexin43 (4 µg/ml in 2.5% DS; Overnight at 4 °C; Chemicon)	Rat Anti-Mouse CD31 (1:100 in 2.5% DS; 30 min; BD Pharmingen)	Rat Anti-Mouse CD31 (1:100 in 1.5% RS; 30 min; BD Pharmingen)	Goat Anti-Mouse VEGF (1:100 in 2.5% DS; Overnight at 4 °C; Santa Cruz)	Goat Anti-Mouse VEGF (1:100 in 2.5% DS; 2 hrs; Santa Cruz)
2°	Anti-Goat IgG- Biotinylated (1:150 in 2.5% RS; 60 min; Vector)	Anti-Rabbit IgG-Alexa Fluor 488 (1:200 in 2.5% DS; 60 min; Molecular Probes)	Anti-Rat IgG-Alexa Fluor 555 (1:200 in 2.5% DS; 60 min; Molecular Probes)	Anti-Rat IgG- Biotinylated (1:200 in 1.5% RS; 30 min; VECTASTAIN; Vector)	Anti-Goat IgG-Alexa Fluor 555 (1:200 in 2.5% DS; 60 min; Molecular Probes)	Anti-Goat IgG-Alexa Fluor 488 (1:200 in 2.5% DS; 60 min; Molecular Probes)
3°	Streptavidin, Oregon Green™, 488 Conjugate (1:500; 10 min; Molecular Probes)	Goat Anti-cTnI (1:25,000 in 2.5% DS; 2 hrs; Scripps)		VECTASTAIN ABC Reagent (30 min; VECTASTAIN; Vector)	Mouse IgG Blocking Reagent (60 min; MOM Kit; Vector)	Rat Anti-Mouse CD31 (1:100 in 2.5% DS; 30 min; BD Pharmingen)
4°	Y-Chromosome FISH	Anti-Goat IgG-Alexa Fluor 555 (1:200 in 2.5% DS; 60 min; Molecular Probes)		DAB Substrate for Peroxidase (1 min; Vector)	Mouse Anti-Fast Skeletal MHC (1:400 in MOM Diluent; 30 min; Sigma)	Anti-Rat IgG-Alexa Fluor 555 (1:200 in 2.5% DS; 60 min; Molecular Probes)
5°		Mouse IgG Blocking Reagent (60 min; MOM Kit; Vector)			Anti-Mouse IgG-Alexa Fluor 488 (1:200 in MOM Diluent; 60 min; Molecular Probes)	
6°		Mouse Anti-Fast Skeletal MHC (1:400 in MOM Diluent; 30 min; Sigma)				
7°		Anti-Mouse IgG-Alexa Fluor 647 (1:200 in MOM Diluent; 60 min; Molecular Probes)				

BIBLIOGRAPHY

1. Association, A.H., ed. *Heart Disease and Stroke Statistics-2004 Update.*, ed. A.H. Association. 2003: Dallas, Texas.
2. Association, A.H., *Heart Disease and Stroke Statistics-2003 Update.* 2002, Dallas, Texas: American Heart Association.
3. Sakai, T., Y. Ling, T.R. Payne, and J. Huard, *The use of ex vivo gene transfer based on muscle-derived stem cells for cardiovascular medicine.* Trends Cardiovasc Med, 2002. **12**(3): p. 115-20.
4. Association, A.H., *2001 Heart and Stroke Statistical Update.* 2000, Dallas, Texas: American Heart Association.
5. Hughes, S., *Cardiac stem cells.* J Pathol, 2002. **197**(4): p. 468-78.
6. Laflamme, M.A. and C.E. Murry, *Regenerating the heart.* Nat Biotechnol, 2005. **23**(7): p. 845-56.
7. Caplice, N.M., B.J. Gersh, and J.R. Alegria, *Cell therapy for cardiovascular disease: what cells, what diseases and for whom?* Nat Clin Pract Cardiovasc Med, 2005. **2**(1): p. 37-43.
8. Chiu, R.C., A. Zibaitis, and R.L. Kao, *Cellular cardiomyoplasty: myocardial regeneration with satellite cell implantation.* Ann Thorac Surg, 1995. **60**(1): p. 12-8.
9. Assmus, B., V. Schachinger, C. Teupe, M. Britten, R. Lehmann, N. Dobert, F. Grunwald, A. Aicher, C. Urbich, H. Martin, D. Hoelzer, S. Dimmeler, and A.M. Zeiher, *Transplantation of Progenitor Cells and Regeneration Enhancement in Acute Myocardial Infarction (TOPCARE-AMI).* Circulation, 2002. **106**(24): p. 3009-17.
10. Chachques, J.C., C. Acar, J. Herreros, J.C. Trainini, F. Prosper, N. D'Attellis, J.N. Fabiani, and A.F. Carpentier, *Cellular cardiomyoplasty: clinical application.* Ann Thorac Surg, 2004. **77**(3): p. 1121-30.
11. Menasche, P., *Cellular transplantation: hurdles remaining before widespread clinical use.* Curr Opin Cardiol, 2004. **19**(2): p. 154-61.

12. Menasche, P., *Myoblast transfer in heart failure*. Surg Clin North Am, 2004. **84**(1): p. 125-39.
13. Menasche, P., A.A. Hagege, M. Scorsin, B. Pouzet, M. Desnos, D. Duboc, K. Schwartz, J.T. Vilquin, and J.P. Marolleau, *Myoblast transplantation for heart failure*. Lancet, 2001. **357**(9252): p. 279-80.
14. Menasche, P., A.A. Hagege, J.T. Vilquin, M. Desnos, E. Abergel, B. Pouzet, A. Bel, S. Sarateanu, M. Scorsin, K. Schwartz, P. Bruneval, M. Benbunan, J.P. Marolleau, and D. Duboc, *Autologous skeletal myoblast transplantation for severe postinfarction left ventricular dysfunction*. J Am Coll Cardiol, 2003. **41**(7): p. 1078-83.
15. Pagani, F.D., H. DerSimonian, A. Zawadzka, K. Wetzel, A.S. Edge, D.B. Jacoby, J.H. Dinsmore, S. Wright, T.H. Aretz, H.J. Eisen, and K.D. Aaronson, *Autologous skeletal myoblasts transplanted to ischemia-damaged myocardium in humans. Histological analysis of cell survival and differentiation*. J Am Coll Cardiol, 2003. **41**(5): p. 879-88.
16. Perin, E.C., H.F. Dohmann, R. Borojevic, S.A. Silva, A.L. Sousa, C.T. Mesquita, M.I. Rossi, A.C. Carvalho, H.S. Dutra, H.J. Dohmann, G.V. Silva, L. Belem, R. Vivacqua, F.O. Rangel, R. Esporcatte, Y.J. Geng, W.K. Vaughn, J.A. Assad, E.T. Mesquita, and J.T. Willerson, *Transendocardial, autologous bone marrow cell transplantation for severe, chronic ischemic heart failure*. Circulation, 2003. **107**(18): p. 2294-302.
17. Perin, E.C., H.F. Dohmann, R. Borojevic, S.A. Silva, A.L. Sousa, G.V. Silva, C.T. Mesquita, L. Belem, W.K. Vaughn, F.O. Rangel, J.A. Assad, A.C. Carvalho, R.V. Branco, M.I. Rossi, H.J. Dohmann, and J.T. Willerson, *Improved exercise capacity and ischemia 6 and 12 months after transendocardial injection of autologous bone marrow mononuclear cells for ischemic cardiomyopathy*. Circulation, 2004. **110**(11 Suppl 1): p. II213-8.
18. Silva, G.V., E.C. Perin, H.F. Dohmann, R. Borojevic, S.A. Silva, A.L. Sousa, J.A. Assad, W.K. Vaughn, C.T. Mesquita, L. Belem, A.C. Carvalho, H.J. Dohmann, E. Barroso do Amaral, J. Coutinho, R. Branco, E. Oliveira, and J.T. Willerson, *Catheter-based transendocardial delivery of autologous bone-marrow-derived mononuclear cells in patients listed for heart transplantation*. Tex Heart Inst J, 2004. **31**(3): p. 214-9.
19. Siminiak, T., D. Fiszer, O. Jerzykowska, B. Grygielska, N. Rozwadowska, P. Kalmucki, and M. Kurpisz, *Percutaneous trans-coronary-venous transplantation of autologous skeletal myoblasts in the treatment of post-infarction myocardial contractility impairment: the POZNAN trial*. Eur Heart J, 2005. **26**(12): p. 1188-95.
20. Siminiak, T., R. Kalawski, D. Fiszer, O. Jerzykowska, J. Rzezniczak, N. Rozwadowska, and M. Kurpisz, *Autologous skeletal myoblast transplantation for the treatment of postinfarction myocardial injury: phase I clinical study with 12 months of follow-up*. Am Heart J, 2004. **148**(3): p. 531-7.

21. Smits, P.C., R.J. van Geuns, D. Poldermans, M. Bountiukos, E.E. Onderwater, C.H. Lee, A.P. Maat, and P.W. Serruys, *Catheter-based intramyocardial injection of autologous skeletal myoblasts as a primary treatment of ischemic heart failure: clinical experience with six-month follow-up*. J Am Coll Cardiol, 2003. **42**(12): p. 2063-9.
22. Scorsin, M., F. Marotte, A. Sabri, O. Le Dref, M. Demirag, J.L. Samuel, L. Rappaport, and P. Menasche, *Can grafted cardiomyocytes colonize peri-infarct myocardial areas?* Circulation, 1996. **94**(9 Suppl): p. II337-40.
23. Leor, J., M. Patterson, M.J. Quinones, L.H. Kedes, and R.A. Kloner, *Transplantation of fetal myocardial tissue into the infarcted myocardium of rat. A potential method for repair of infarcted myocardium?* Circulation, 1996. **94**(9 Suppl): p. II332-6.
24. Reinecke, H., M. Zhang, T. Bartosek, and C.E. Murry, *Survival, integration, and differentiation of cardiomyocyte grafts: a study in normal and injured rat hearts*. Circulation, 1999. **100**(2): p. 193-202.
25. Li, R.K., Z.Q. Jia, R.D. Weisel, D.A. Mickle, J. Zhang, M.K. Mohabeer, V. Rao, and J. Ivanov, *Cardiomyocyte transplantation improves heart function*. Ann Thorac Surg, 1996. **62**(3): p. 654-60; discussion 660-1.
26. Soonpaa, M.H., G.Y. Koh, M.G. Klug, and L.J. Field, *Formation of nascent intercalated disks between grafted fetal cardiomyocytes and host myocardium*. Science, 1994. **264**(5155): p. 98-101.
27. Etzion, S., A. Battler, I.M. Barbash, E. Cagnano, P. Zarin, Y. Granot, L.H. Kedes, R.A. Kloner, and J. Leor, *Influence of embryonic cardiomyocyte transplantation on the progression of heart failure in a rat model of extensive myocardial infarction*. J Mol Cell Cardiol, 2001. **33**(7): p. 1321-30.
28. Watanabe, E., D.M. Smith, Jr., J.B. Delcarpio, J. Sun, F.W. Smart, C.H. Van Meter, Jr., and W.C. Claycomb, *Cardiomyocyte transplantation in a porcine myocardial infarction model*. Cell Transplant, 1998. **7**(3): p. 239-46.
29. Koh, G.Y., M.H. Soonpaa, M.G. Klug, and L.J. Field, *Long-term survival of AT-1 cardiomyocyte grafts in syngeneic myocardium*. Am J Physiol, 1993. **264**(5 Pt 2): p. H1727-33.
30. Klug, M.G., M.H. Soonpaa, G.Y. Koh, and L.J. Field, *Genetically selected cardiomyocytes from differentiating embryonic stem cells form stable intracardiac grafts*. J Clin Invest, 1996. **98**(1): p. 216-24.
31. Li, R.K., Z.Q. Jia, R.D. Weisel, F. Merante, and D.A. Mickle, *Smooth muscle cell transplantation into myocardial scar tissue improves heart function*. J Mol Cell Cardiol, 1999. **31**(3): p. 513-22.

32. Sakai, T., R.K. Li, R.D. Weisel, D.A. Mickle, E.J. Kim, S. Tomita, Z.Q. Jia, and T.M. Yau, *Autologous heart cell transplantation improves cardiac function after myocardial injury*. *Ann Thorac Surg*, 1999. **68**(6): p. 2074-80; discussion 2080-1.
33. Hutcheson, K.A., B.Z. Atkins, M.T. Hueman, M.B. Hopkins, D.D. Glower, and D.A. Taylor, *Comparison of benefits on myocardial performance of cellular cardiomyoplasty with skeletal myoblasts and fibroblasts*. *Cell Transplant*, 2000. **9**(3): p. 359-68.
34. Dib, N., E.B. Diethrich, A. Campbell, N. Goodwin, B. Robinson, J. Gilbert, D.W. Hobohm, and D.A. Taylor, *Endoventricular transplantation of allogenic skeletal myoblasts in a porcine model of myocardial infarction*. *J Endovasc Ther*, 2002. **9**(3): p. 313-9.
35. Dib, N., P. McCarthy, A. Campbell, M. Yeager, F.D. Pagani, S. Wright, W.R. MacLellan, G. Fonarow, H.J. Eisen, R.E. Michler, P. Binkley, D. Buchele, R. Korn, M. Ghazoul, J. Dinsmore, S.R. Opie, and E. Diethrich, *Feasibility and safety of autologous myoblast transplantation in patients with ischemic cardiomyopathy*. *Cell Transplant*, 2005. **14**(1): p. 11-9.
36. Dib, N., R.E. Michler, F.D. Pagani, S. Wright, D.J. Kereiakes, R. Lengerich, P. Binkley, D. Buchele, I. Anand, C. Swingen, M.F. Di Carli, J.D. Thomas, W.A. Jaber, S.R. Opie, A. Campbell, P. McCarthy, M. Yeager, V. Dilsizian, B.P. Griffith, R. Korn, S.K. Kreuger, M. Ghazoul, W.R. MacLellan, G. Fonarow, H.J. Eisen, J. Dinsmore, and E. Diethrich, *Safety and feasibility of autologous myoblast transplantation in patients with ischemic cardiomyopathy: four-year follow-up*. *Circulation*, 2005. **112**(12): p. 1748-55.
37. Dorfman, J., M. Duong, A. Zibaitis, M.P. Pelletier, D. Shum-Tim, C. Li, and R.C. Chiu, *Myocardial tissue engineering with autologous myoblast implantation*. *J Thorac Cardiovasc Surg*, 1998. **116**(5): p. 744-51.
38. Dowell, J.D., M. Rubart, K.B. Pasumarthi, M.H. Soonpaa, and L.J. Field, *Myocyte and myogenic stem cell transplantation in the heart*. *Cardiovasc Res*, 2003. **58**(2): p. 336-50.
39. Horackova, M., R. Arora, R. Chen, J.A. Armour, P.A. Cattini, R. Livingston, and Z. Byczko, *Cell Transplantation for the Treatment of Acute Myocardial Infarction: The Unique Capacity for Repair by Skeletal Muscle Satellite Cells*. *Am J Physiol Heart Circ Physiol*, 2004.
40. Kessler, P.D. and B.J. Byrne, *Myoblast cell grafting into heart muscle: cellular biology and potential applications*. *Annu Rev Physiol*, 1999. **61**: p. 219-42.
41. Koh, G.Y., M.G. Klug, M.H. Soonpaa, and L.J. Field, *Differentiation and long-term survival of C2C12 myoblast grafts in heart*. *J Clin Invest*, 1993. **92**(3): p. 1548-54.

42. Menasche, P., *Skeletal muscle satellite cell transplantation*. Cardiovasc Res, 2003. **58**(2): p. 351-7.
43. Menasche, P., *Skeletal myoblast transplantation for cardiac repair*. Expert Rev Cardiovasc Ther, 2004. **2**(1): p. 21-8.
44. Menasche, P., *Skeletal myoblast for cell therapy*. Coron Artery Dis, 2005. **16**(2): p. 105-10.
45. Murry, C.E., M.L. Whitney, and H. Reinecke, *Muscle cell grafting for the treatment and prevention of heart failure*. J Card Fail, 2002. **8**(6 Suppl): p. S532-41.
46. Murry, C.E., R.W. Wiseman, S.M. Schwartz, and S.D. Hauschka, *Skeletal myoblast transplantation for repair of myocardial necrosis*. J Clin Invest, 1996. **98**(11): p. 2512-23.
47. Pouzet, B., J.T. Vilquin, A.A. Hagege, M. Scorsin, E. Messas, M. Fiszman, K. Schwartz, and P. Menasche, *Factors affecting functional outcome after autologous skeletal myoblast transplantation*. Ann Thorac Surg, 2001. **71**(3): p. 844-50; discussion 850-1.
48. Reinecke, H., E. Minami, V. Poppa, and C.E. Murry, *Evidence for fusion between cardiac and skeletal muscle cells*. Circ Res, 2004. **94**(6): p. e56-60.
49. Reinecke, H. and C.E. Murry, *Transmural replacement of myocardium after skeletal myoblast grafting into the heart. Too much of a good thing?* Cardiovasc Pathol, 2000. **9**(6): p. 337-44.
50. Robinson, S.W., P.W. Cho, H.I. Levitsky, J.L. Olson, R.H. Hruban, M.A. Acker, and P.D. Kessler, *Arterial delivery of genetically labelled skeletal myoblasts to the murine heart: long-term survival and phenotypic modification of implanted myoblasts*. Cell Transplant, 1996. **5**(1): p. 77-91.
51. Rubart, M., M.H. Soonpaa, H. Nakajima, and L.J. Field, *Spontaneous and evoked intracellular calcium transients in donor-derived myocytes following intracardiac myoblast transplantation*. J Clin Invest, 2004. **114**(6): p. 775-83.
52. Scorsin, M., A. Hagege, J.T. Vilquin, M. Fiszman, F. Marotte, J.L. Samuel, L. Rappaport, K. Schwartz, and P. Menasche, *Comparison of the effects of fetal cardiomyocyte and skeletal myoblast transplantation on postinfarction left ventricular function*. J Thorac Cardiovasc Surg, 2000. **119**(6): p. 1169-75.
53. Sim, E.K., S. Jiang, L. Ye, Y.L. Lim, O.C. Ooi, and K.H. Haider, *Skeletal myoblast transplant in heart failure*. J Card Surg, 2003. **18**(4): p. 319-27.

54. Suzuki, K., N.J. Brand, S. Allen, M.A. Khan, A.O. Farrell, B. Murtuza, R.E. Oakley, and M.H. Yacoub, *Overexpression of connexin 43 in skeletal myoblasts: Relevance to cell transplantation to the heart*. J Thorac Cardiovasc Surg, 2001. **122**(4): p. 759-66.
55. Suzuki, K., N.J. Brand, R.T. Smolenski, J. Jayakumar, B. Murtuza, and M.H. Yacoub, *Development of a novel method for cell transplantation through the coronary artery*. Circulation, 2000. **102**(19 Suppl 3): p. III359-64.
56. Suzuki, K., B. Murtuza, L. Heslop, J.E. Morgan, R.T. Smolenski, N. Suzuki, T.A. Partridge, and M.H. Yacoub, *Single fibers of skeletal muscle as a novel graft for cell transplantation to the heart*. J Thorac Cardiovasc Surg, 2002. **123**(5): p. 984-92.
57. Suzuki, K., B. Murtuza, R.T. Smolenski, I.A. Sammut, N. Suzuki, Y. Kaneda, and M.H. Yacoub, *Cell transplantation for the treatment of acute myocardial infarction using vascular endothelial growth factor-expressing skeletal myoblasts*. Circulation, 2001. **104**(12 Suppl 1): p. I207-12.
58. Suzuki, K., B. Murtuza, N. Suzuki, R.T. Smolenski, and M.H. Yacoub, *Intracoronary infusion of skeletal myoblasts improves cardiac function in doxorubicin-induced heart failure*. Circulation, 2001. **104**(12 Suppl 1): p. I213-7.
59. Suzuki, K., R.T. Smolenski, J. Jayakumar, B. Murtuza, N.J. Brand, and M.H. Yacoub, *Heat shock treatment enhances graft cell survival in skeletal myoblast transplantation to the heart*. Circulation, 2000. **102**(19 Suppl 3): p. III216-21.
60. Taylor, D.A., *Cellular cardiomyoplasty with autologous skeletal myoblasts for ischemic heart disease and heart failure*. Curr Control Trials Cardiovasc Med, 2001. **2**(5): p. 208-210.
61. Taylor, D.A., B.Z. Atkins, P. Hungspreugs, T.R. Jones, M.C. Reedy, K.A. Hutcheson, D.D. Glower, and W.E. Kraus, *Regenerating functional myocardium: improved performance after skeletal myoblast transplantation*. Nat Med, 1998. **4**(8): p. 929-33.
62. Min, J.Y., Y. Yang, K.L. Converso, L. Liu, Q. Huang, J.P. Morgan, and Y.F. Xiao, *Transplantation of embryonic stem cells improves cardiac function in postinfarcted rats*. J Appl Physiol, 2002. **92**(1): p. 288-96.
63. Yamashita, J., H. Itoh, M. Hirashima, M. Ogawa, S. Nishikawa, T. Yurugi, M. Naito, and K. Nakao, *Flk1-positive cells derived from embryonic stem cells serve as vascular progenitors*. Nature, 2000. **408**(6808): p. 92-6.
64. Agbulut, O., M.L. Menot, Z. Li, F. Marotte, D. Paulin, A.A. Hagege, C. Chomienne, J.L. Samuel, and P. Menasche, *Temporal patterns of bone marrow cell differentiation following transplantation in doxorubicin-induced cardiomyopathy*. Cardiovasc Res, 2003. **58**(2): p. 451-9.

65. Gneocchi, M., H. He, O.D. Liang, L.G. Melo, F. Morello, H. Mu, N. Noiseux, L. Zhang, R.E. Pratt, J.S. Ingwall, and V.J. Dzau, *Paracrine action accounts for marked protection of ischemic heart by Akt-modified mesenchymal stem cells*. Nat Med, 2005. **11**(4): p. 367-8.
66. Mangi, A.A., N. Noiseux, D. Kong, H. He, M. Rezvani, J.S. Ingwall, and V.J. Dzau, *Mesenchymal stem cells modified with Akt prevent remodeling and restore performance of infarcted hearts*. Nat Med, 2003. **9**(9): p. 1195-201.
67. Pittenger, M.F., A.M. Mackay, S.C. Beck, R.K. Jaiswal, R. Douglas, J.D. Mosca, M.A. Moorman, D.W. Simonetti, S. Craig, and D.R. Marshak, *Multilineage potential of adult human mesenchymal stem cells*. Science, 1999. **284**(5411): p. 143-7.
68. Toma, C., M.F. Pittenger, K.S. Cahill, B.J. Byrne, and P.D. Kessler, *Human mesenchymal stem cells differentiate to a cardiomyocyte phenotype in the adult murine heart*. Circulation, 2002. **105**(1): p. 93-8.
69. Wang, J.S., D. Shum-Tim, J. Galipeau, E. Chedrawy, N. Eliopoulos, and R.C. Chiu, *Marrow stromal cells for cellular cardiomyoplasty: feasibility and potential clinical advantages*. J Thorac Cardiovasc Surg, 2000. **120**(5): p. 999-1005.
70. Tomita, S., R.K. Li, R.D. Weisel, D.A. Mickle, E.J. Kim, T. Sakai, and Z.Q. Jia, *Autologous transplantation of bone marrow cells improves damaged heart function*. Circulation, 1999. **100**(19 Suppl): p. II247-56.
71. Wang, J.S., D. Shum-Tim, E. Chedrawy, and R.C. Chiu, *The coronary delivery of marrow stromal cells for myocardial regeneration: pathophysiologic and therapeutic implications*. J Thorac Cardiovasc Surg, 2001. **122**(4): p. 699-705.
72. Agbulut, O., S. Vandervelde, N. Al Attar, J. Larghero, S. Ghostine, B. Leobon, E. Robidel, P. Borsani, M. Le Lorc'h, A. Bissery, C. Chomienne, P. Bruneval, J.P. Marolleau, J.T. Vilquin, A. Hagege, J.L. Samuel, and P. Menasche, *Comparison of human skeletal myoblasts and bone marrow-derived CD133+ progenitors for the repair of infarcted myocardium*. J Am Coll Cardiol, 2004. **44**(2): p. 458-63.
73. Balsam, L.B., A.J. Wagers, J.L. Christensen, T. Kofidis, I.L. Weissman, and R.C. Robbins, *Haematopoietic stem cells adopt mature haematopoietic fates in ischaemic myocardium*. Nature, 2004. **428**(6983): p. 668-73.
74. Hirschi, K.K. and M.A. Goodell, *Hematopoietic, vascular and cardiac fates of bone marrow-derived stem cells*. Gene Ther, 2002. **9**(10): p. 648-52.
75. Jackson, K.A., S.M. Majka, H. Wang, J. Pocius, C.J. Hartley, M.W. Majesky, M.L. Entman, L.H. Michael, K.K. Hirschi, and M.A. Goodell, *Regeneration of ischemic cardiac muscle and vascular endothelium by adult stem cells*. J Clin Invest, 2001. **107**(11): p. 1395-402.

76. Kajstura, J., M. Rota, B. Whang, S. Cascapera, T. Hosoda, C. Bearzi, D. Nurzynska, H. Kasahara, E. Zias, M. Bonafe, B. Nadal-Ginard, D. Torella, A. Nascimbene, F. Quaini, K. Urbanek, A. Leri, and P. Anversa, *Bone marrow cells differentiate in cardiac cell lineages after infarction independently of cell fusion*. *Circ Res*, 2005. **96**(1): p. 127-37.
77. Kamihata, H., H. Matsubara, T. Nishiue, S. Fujiyama, Y. Tsutsumi, R. Ozono, H. Masaki, Y. Mori, O. Iba, E. Tateishi, A. Kosaki, S. Shintani, T. Murohara, T. Imaizumi, and T. Iwasaka, *Implantation of bone marrow mononuclear cells into ischemic myocardium enhances collateral perfusion and regional function via side supply of angioblasts, angiogenic ligands, and cytokines*. *Circulation*, 2001. **104**(9): p. 1046-52.
78. Murry, C.E., M.H. Soonpaa, H. Reinecke, H. Nakajima, H.O. Nakajima, M. Rubart, K.B. Pasumarthi, J.I. Virag, S.H. Bartelmez, V. Poppa, G. Bradford, J.D. Dowell, D.A. Williams, and L.J. Field, *Haematopoietic stem cells do not transdifferentiate into cardiac myocytes in myocardial infarcts*. *Nature*, 2004. **428**(6983): p. 664-8.
79. Orlic, D., J. Kajstura, S. Chimenti, F. Limana, I. Jakoniuk, F. Quaini, B. Nadal-Ginard, D.M. Bodine, A. Leri, and P. Anversa, *Mobilized bone marrow cells repair the infarcted heart, improving function and survival*. *Proc Natl Acad Sci U S A*, 2001. **98**(18): p. 10344-9.
80. Orlic, D., J. Kajstura, S. Chimenti, D.M. Bodine, A. Leri, and P. Anversa, *Transplanted adult bone marrow cells repair myocardial infarcts in mice*. *Ann N Y Acad Sci*, 2001. **938**: p. 221-9; discussion 229-30.
81. Orlic, D., J. Kajstura, S. Chimenti, I. Jakoniuk, S.M. Anderson, B. Li, J. Pickel, R. McKay, B. Nadal-Ginard, D.M. Bodine, A. Leri, and P. Anversa, *Bone marrow cells regenerate infarcted myocardium*. *Nature*, 2001. **410**(6829): p. 701-5.
82. Itescu, S., A.A. Kocher, and M.D. Schuster, *Myocardial neovascularization by adult bone marrow-derived angioblasts: strategies for improvement of cardiomyocyte function*. *Heart Fail Rev*, 2003. **8**(3): p. 253-8.
83. Kocher, A.A., M.D. Schuster, M.J. Szabolcs, S. Takuma, D. Burkhoff, J. Wang, S. Homma, N.M. Edwards, and S. Itescu, *Neovascularization of ischemic myocardium by human bone-marrow-derived angioblasts prevents cardiomyocyte apoptosis, reduces remodeling and improves cardiac function*. *Nat Med*, 2001. **7**(4): p. 430-6.
84. Asahara, T., T. Murohara, A. Sullivan, M. Silver, R. van der Zee, T. Li, B. Witzenbichler, G. Schatteman, and J.M. Isner, *Isolation of putative progenitor endothelial cells for angiogenesis*. *Science*, 1997. **275**(5302): p. 964-7.
85. Shi, Q., S. Rafii, M.H. Wu, E.S. Wijelath, C. Yu, A. Ishida, Y. Fujita, S. Kothari, R. Mohle, L.R. Sauvage, M.A. Moore, R.F. Storb, and W.P. Hammond, *Evidence for circulating bone marrow-derived endothelial cells*. *Blood*, 1998. **92**(2): p. 362-7.

86. Takahashi, T., C. Kalka, H. Masuda, D. Chen, M. Silver, M. Kearney, M. Magner, J.M. Isner, and T. Asahara, *Ischemia- and cytokine-induced mobilization of bone marrow-derived endothelial progenitor cells for neovascularization*. *Nat Med*, 1999. **5**(4): p. 434-8.
87. Beltrami, A.P., L. Barlucchi, D. Torella, M. Baker, F. Limana, S. Chimenti, H. Kasahara, M. Rota, E. Musso, K. Urbanek, A. Leri, J. Kajstura, B. Nadal-Ginard, and P. Anversa, *Adult cardiac stem cells are multipotent and support myocardial regeneration*. *Cell*, 2003. **114**(6): p. 763-76.
88. Martin, C.M., A.P. Meeson, S.M. Robertson, T.J. Hawke, J.A. Richardson, S. Bates, S.C. Goetsch, T.D. Gallardo, and D.J. Garry, *Persistent expression of the ATP-binding cassette transporter, Abcg2, identifies cardiac SP cells in the developing and adult heart*. *Dev Biol*, 2004. **265**(1): p. 262-75.
89. Oh, H., S.B. Bradfute, T.D. Gallardo, T. Nakamura, V. Gaussin, Y. Mishina, J. Pocius, L.H. Michael, R.R. Behringer, D.J. Garry, M.L. Entman, and M.D. Schneider, *Cardiac progenitor cells from adult myocardium: homing, differentiation, and fusion after infarction*. *Proc Natl Acad Sci U S A*, 2003. **100**(21): p. 12313-8.
90. Strauer, B.E., M. Brehm, T. Zeus, M. Kosterling, A. Hernandez, R.V. Sorg, G. Kogler, and P. Wernet, *Repair of infarcted myocardium by autologous intracoronary mononuclear bone marrow cell transplantation in humans*. *Circulation*, 2002. **106**(15): p. 1913-8.
91. Bischoff, R., *Proliferation of muscle satellite cells on intact myofibers in culture*. *Dev Biol*, 1986. **115**(1): p. 129-39.
92. Atkins, B.Z., M.T. Hueman, J. Meuchel, K.A. Hutcheson, D.D. Glower, and D.A. Taylor, *Cellular cardiomyoplasty improves diastolic properties of injured heart*, in *J Surg Res*. 1999. p. 234-42.
93. Atkins, B.Z., M.T. Hueman, J.M. Meuchel, M.J. Cottman, K.A. Hutcheson, and D.A. Taylor, *Myogenic cell transplantation improves in vivo regional performance in infarcted rabbit myocardium*. *J Heart Lung Transplant*, 1999. **18**(12): p. 1173-80.
94. Thompson, R.B., S.M. Emani, B.H. Davis, E.J. van den Bos, Y. Morimoto, D. Craig, D. Glower, and D.A. Taylor, *Comparison of intracardiac cell transplantation: autologous skeletal myoblasts versus bone marrow cells*. *Circulation*, 2003. **108 Suppl 1**: p. II264-71.
95. Atkins, B.Z., C.W. Lewis, W.E. Kraus, K.A. Hutcheson, D.D. Glower, and D.A. Taylor, *Intracardiac transplantation of skeletal myoblasts yields two populations of striated cells in situ*. *Ann Thorac Surg*, 1999. **67**(1): p. 124-9.

96. Yoon, P.D., R.L. Kao, and G.J. Magovern, *Myocardial regeneration. Transplanting satellite cells into damaged myocardium*. *Tex Heart Inst J*, 1995. **22**(2): p. 119-25.
97. Reinecke, H., V. Poppa, and C.E. Murry, *Skeletal muscle stem cells do not transdifferentiate into cardiomyocytes after cardiac grafting*. *J Mol Cell Cardiol*, 2002. **34**(2): p. 241-9.
98. Qu, Z., L. Balkir, J.C. van Deutekom, P.D. Robbins, R. Pruchnic, and J. Huard, *Development of approaches to improve cell survival in myoblast transfer therapy*. *J Cell Biol*, 1998. **142**(5): p. 1257-67.
99. Tremblay, J.P., F. Malouin, R. Roy, J. Huard, J.P. Bouchard, A. Satoh, and C.L. Richards, *Results of a triple blind clinical study of myoblast transplantations without immunosuppressive treatment in young boys with Duchenne muscular dystrophy*. *Cell Transplant*, 1993. **2**(2): p. 99-112.
100. Huard, J., R. Roy, B. Guerette, S. Verreault, G. Tremblay, and J.P. Tremblay, *Human myoblast transplantation in immunodeficient and immunosuppressed mice: evidence of rejection*. *Muscle Nerve*, 1994. **17**(2): p. 224-34.
101. Mendell, J.R., J.T. Kissel, A.A. Amato, W. King, L. Signore, T.W. Prior, Z. Sahenk, S. Benson, P.E. McAndrew, R. Rice, and et al., *Myoblast transfer in the treatment of Duchenne's muscular dystrophy*. *N Engl J Med*, 1995. **333**(13): p. 832-8.
102. Fan, Y., M. Maley, M. Beilharz, and M. Grounds, *Rapid death of injected myoblasts in myoblast transfer therapy*. *Muscle Nerve*, 1996. **19**(7): p. 853-60.
103. Beauchamp, J.R., J.E. Morgan, C.N. Pagel, and T.A. Partridge, *Dynamics of myoblast transplantation reveal a discrete minority of precursors with stem cell-like properties as the myogenic source*. *J Cell Biol*, 1999. **144**(6): p. 1113-22.
104. Beauchamp, J.R., J.E. Morgan, C.N. Pagel, and T.A. Partridge, *Quantitative studies of efficacy of myoblast transplantation*. *Muscle Nerve*, 1994. **18** (Suppl): p. 261.
105. Beauchamp, J.R., C.N. Pagel, and T.A. Partridge, *A dual-marker system for quantitative studies of myoblast transplantation in the mouse*. *Transplantation*, 1997. **63**(12): p. 1794-7.
106. Miller, J.B., L. Schaefer, and J.A. Dominov, *Seeking muscle stem cells*. *Curr Top Dev Biol*, 1999. **43**: p. 191-219.
107. Gussoni, E., Y. Soneoka, C.D. Strickland, E.A. Buzney, M.K. Khan, A.F. Flint, L.M. Kunkel, and R.C. Mulligan, *Dystrophin expression in the mdx mouse restored by stem cell transplantation*. *Nature*, 1999. **401**(6751): p. 390-4.

108. Cornelison, D.D. and B.J. Wold, *Single-cell analysis of regulatory gene expression in quiescent and activated mouse skeletal muscle satellite cells*. Dev Biol, 1997. **191**(2): p. 270-83.
109. Baroffio, A., M. Hamann, L. Bernheim, M.L. Bochaton-Piallat, G. Gabbiani, and C.R. Bader, *Identification of self-renewing myoblasts in the progeny of single human muscle satellite cells*. Differentiation, 1996. **60**(1): p. 47-57.
110. Huard, J., J.P. Bouchard, R. Roy, F. Malouin, G. Dansereau, C. Labrecque, N. Albert, C.L. Richards, B. Lemieux, and J.P. Tremblay, *Human myoblast transplantation: preliminary results of 4 cases*. Muscle Nerve, 1992. **15**(5): p. 550-60.
111. Tambara, K., Y. Sakakibara, G. Sakaguchi, F. Lu, G.U. Premaratne, X. Lin, K. Nishimura, and M. Komeda, *Transplanted skeletal myoblasts can fully replace the infarcted myocardium when they survive in the host in large numbers*. Circulation, 2003. **108 Suppl 1**: p. II259-63.
112. Jankowski, R.J., B.M. Deasy, and J. Huard, *Muscle-derived stem cells*. Gene Ther, 2002. **9**(10): p. 642-7.
113. Qu-Petersen, Z., B. Deasy, R. Jankowski, M. Ikezawa, J. Cummins, R. Pruchnic, J. Mytinger, B. Cao, C. Gates, A. Wernig, and J. Huard, *Identification of a novel population of muscle stem cells in mice: potential for muscle regeneration*. J Cell Biol, 2002. **157**(5): p. 851-64.
114. Lee, J.Y., Z. Qu-Petersen, B. Cao, S. Kimura, R. Jankowski, J. Cummins, A. Usas, C. Gates, P. Robbins, A. Wernig, and J. Huard, *Clonal isolation of muscle-derived cells capable of enhancing muscle regeneration and bone healing*. J Cell Biol, 2000. **150**(5): p. 1085-100.
115. Cao, B., B. Zheng, R.J. Jankowski, S. Kimura, M. Ikezawa, B. Deasy, J. Cummins, M. Epperly, Z. Qu-Petersen, and J. Huard, *Muscle stem cells differentiate into haematopoietic lineages but retain myogenic potential*. Nat Cell Biol, 2003. **5**(7): p. 640-6.
116. Leung, D.W., G. Cachianes, W.J. Kuang, D.V. Goeddel, and N. Ferrara, *Vascular endothelial growth factor is a secreted angiogenic mitogen*. Science, 1989. **246**(4935): p. 1306-9.
117. Keck, P.J., S.D. Hauser, G. Krivi, K. Sanzo, T. Warren, J. Feder, and D.T. Connolly, *Vascular permeability factor, an endothelial cell mitogen related to PDGF*. Science, 1989. **246**(4935): p. 1309-12.
118. Hoffman, E.P., R.H. Brown, Jr., and L.M. Kunkel, *Dystrophin: the protein product of the Duchenne muscular dystrophy locus*. Cell, 1987. **51**(6): p. 919-28.

119. Towbin, J.A. and N.E. Bowles, *The failing heart*. Nature, 2002. **415**(6868): p. 227-33.
120. Badorff, C., G.H. Lee, B.J. Lamphear, M.E. Martone, K.P. Campbell, R.E. Rhoads, and K.U. Knowlton, *Enteroviral protease 2A cleaves dystrophin: evidence of cytoskeletal disruption in an acquired cardiomyopathy*. Nat Med, 1999. **5**(3): p. 320-6.
121. Xiong, D., G.H. Lee, C. Badorff, A. Dorner, S. Lee, P. Wolf, and K.U. Knowlton, *Dystrophin deficiency markedly increases enterovirus-induced cardiomyopathy: A genetic predisposition to viral heart disease*. Nat Med, 2002. **8**(8): p. 872-7.
122. Danialou, G., A.S. Comtois, R. Dudley, G. Karpati, G. Vincent, C. Des Rosiers, and B.J. Petrof, *Dystrophin-deficient cardiomyocytes are abnormally vulnerable to mechanical stress-induced contractile failure and injury*. Faseb J, 2001. **15**(9): p. 1655-7.
123. Kamogawa, Y., S. Biro, M. Maeda, M. Setoguchi, T. Hirakawa, H. Yoshida, and C. Tei, *Dystrophin-deficient myocardium is vulnerable to pressure overload in vivo*. Cardiovasc Res, 2001. **50**(3): p. 509-15.
124. Yue, Y., Z. Li, S.Q. Harper, R.L. Davisson, J.S. Chamberlain, and D. Duan, *Microdystrophin gene therapy of cardiomyopathy restores dystrophin-glycoprotein complex and improves sarcolemma integrity in the mdx mouse heart*. Circulation, 2003. **108**(13): p. 1626-32.
125. Yue, Y., J.W. Skimming, M. Liu, T. Strawn, and D. Duan, *Full-length dystrophin expression in half of the heart cells ameliorates beta-isoproterenol-induced cardiomyopathy in mdx mice*. Hum Mol Genet, 2004. **13**(15): p. 1669-75.
126. Gregorevic, P., M.J. Blankinship, J.M. Allen, R.W. Crawford, L. Meuse, D.G. Miller, D.W. Russell, and J.S. Chamberlain, *Systemic delivery of genes to striated muscles using adeno-associated viral vectors*. Nat Med, 2004. **10**(8): p. 828-34.
127. Koh, G.Y., M.H. Soonpaa, M.G. Klug, H.P. Pride, B.J. Cooper, D.P. Zipes, and L.J. Field, *Stable fetal cardiomyocyte grafts in the hearts of dystrophic mice and dogs*. J Clin Invest, 1995. **96**(4): p. 2034-42.
128. Laugwitz, K.L., A. Moretti, J. Lam, P. Gruber, Y. Chen, S. Woodard, L.Z. Lin, C.L. Cai, M.M. Lu, M. Reth, O. Platoshyn, J.X. Yuan, S. Evans, and K.R. Chien, *Postnatal isl1+ cardioblasts enter fully differentiated cardiomyocyte lineages*. Nature, 2005. **433**(7026): p. 647-53.
129. Matsuura, K., T. Nagai, N. Nishigaki, T. Oyama, J. Nishi, H. Wada, M. Sano, H. Toko, H. Akazawa, T. Sato, H. Nakaya, H. Kasanuki, and I. Komuro, *Adult cardiac Sca-1-positive cells differentiate into beating cardiomyocytes*. J Biol Chem, 2004. **279**(12): p. 11384-91.

130. Hagege, A.A., C. Carrion, P. Menasche, J.T. Vilquin, D. Duboc, J.P. Marolleau, M. Desnos, and P. Bruneval, *Viability and differentiation of autologous skeletal myoblast grafts in ischaemic cardiomyopathy*. Lancet, 2003. **361**(9356): p. 491-2.
131. Herreros, J., F. Prosper, A. Perez, J.J. Gavira, M.J. Garcia-Velloso, J. Barba, P.L. Sanchez, C. Canizo, G. Rabago, J.M. Marti-Climent, M. Hernandez, N. Lopez-Holgado, J.M. Gonzalez-Santos, C. Martin-Luengo, and E. Alegria, *Autologous intramyocardial injection of cultured skeletal muscle-derived stem cells in patients with non-acute myocardial infarction*. Eur Heart J, 2003. **24**(22): p. 2012-20.
132. Hoffman, E.P., J.E. Morgan, S.C. Watkins, and T.A. Partridge, *Somatic reversion/suppression of the mouse mdx phenotype in vivo*. J Neurol Sci, 1990. **99**(1): p. 9-25.
133. Wang, X., H. Willenbring, Y. Akkari, Y. Torimaru, M. Foster, M. Al-Dhalimy, E. Lagasse, M. Finegold, S. Olson, and M. Grompe, *Cell fusion is the principal source of bone-marrow-derived hepatocytes*. Nature, 2003. **422**(6934): p. 897-901.
134. Alvarez-Dolado, M., R. Pardal, J.M. Garcia-Verdugo, J.R. Fike, H.O. Lee, K. Pfeffer, C. Lois, S.J. Morrison, and A. Alvarez-Buylla, *Fusion of bone-marrow-derived cells with Purkinje neurons, cardiomyocytes and hepatocytes*. Nature, 2003. **425**(6961): p. 968-73.
135. Nygren, J.M., S. Jovinge, M. Breitbach, P. Sawen, W. Roll, J. Hescheler, J. Taneera, B.K. Fleischmann, and S.E. Jacobsen, *Bone marrow-derived hematopoietic cells generate cardiomyocytes at a low frequency through cell fusion, but not transdifferentiation*. Nat Med, 2004. **10**(5): p. 494-501.
136. Terada, N., T. Hamazaki, M. Oka, M. Hoki, D.M. Mastalerz, Y. Nakano, E.M. Meyer, L. Morel, B.E. Petersen, and E.W. Scott, *Bone marrow cells adopt the phenotype of other cells by spontaneous cell fusion*. Nature, 2002. **416**(6880): p. 542-5.
137. Vassilopoulos, G., P.R. Wang, and D.W. Russell, *Transplanted bone marrow regenerates liver by cell fusion*. Nature, 2003. **422**(6934): p. 901-4.
138. Ying, Q.L., J. Nichols, E.P. Evans, and A.G. Smith, *Changing potency by spontaneous fusion*. Nature, 2002. **416**(6880): p. 545-8.
139. Pavlath, G.K., K. Rich, S.G. Webster, and H.M. Blau, *Localization of muscle gene products in nuclear domains*. Nature, 1989. **337**(6207): p. 570-3.
140. Leobon, B., I. Garcin, P. Menasche, J.T. Vilquin, E. Audinat, and S. Charpak, *Myoblasts transplanted into rat infarcted myocardium are functionally isolated from their host*. Proc Natl Acad Sci U S A, 2003. **100**(13): p. 7808-11.
141. Qu, Z. and J. Huard, *Matching host muscle and donor myoblasts for myosin heavy chain improves myoblast transfer therapy*. Gene Ther, 2000. **7**(5): p. 428-37.

142. Huard, J., G. Acsadi, A. Jani, B. Massie, and G. Karpati, *Gene transfer into skeletal muscles by isogenic myoblasts*. Hum Gene Ther, 1994. **5**(8): p. 949-58.
143. Skuk, D., M. Goulet, B. Roy, and J.P. Tremblay, *Efficacy of myoblast transplantation in nonhuman primates following simple intramuscular cell injections: toward defining strategies applicable to humans*. Exp Neurol, 2002. **175**(1): p. 112-26.
144. Skuk, D., B. Roy, M. Goulet, P. Chapdelaine, J.P. Bouchard, R. Roy, F.J. Dugre, J.G. Lachance, L. Deschenes, S. Helene, M. Sylvain, and J.P. Tremblay, *Dystrophin expression in myofibers of Duchenne muscular dystrophy patients following intramuscular injections of normal myogenic cells*. Mol Ther, 2004. **9**(3): p. 475-82.
145. Hodgetts, S.I. and M.D. Grounds, *Irradiation of dystrophic host tissue prior to myoblast transfer therapy enhances initial (but not long-term) survival of donor myoblasts*. J Cell Sci, 2003. **116**(Pt 20): p. 4131-46.
146. Lee-Pullen, T.F., A.L. Bennett, M.W. Beilharz, M.D. Grounds, and L.M. Samuels, *Superior survival and proliferation after transplantation of myoblasts obtained from adult mice compared with neonatal mice*. Transplantation, 2004. **78**(8): p. 1172-6.
147. Seale, P., L.A. Sabourin, A. Girgis-Gabardo, A. Mansouri, P. Gruss, and M.A. Rudnicki, *Pax7 is required for the specification of myogenic satellite cells*. Cell, 2000. **102**(6): p. 777-86.
148. Lee, S.H., P.L. Wolf, R. Escudero, R. Deutsch, S.W. Jamieson, and P.A. Thistlethwaite, *Early expression of angiogenesis factors in acute myocardial ischemia and infarction*. N Engl J Med, 2000. **342**(9): p. 626-33.
149. Cherwek, D.H., M.B. Hopkins, M.J. Thompson, B.H. Annex, and D.A. Taylor, *Fiber type-specific differential expression of angiogenic factors in response to chronic hindlimb ischemia*. Am J Physiol Heart Circ Physiol, 2000. **279**(3): p. H932-8.
150. Zhang, M., D. Methot, V. Poppa, Y. Fujio, K. Walsh, and C.E. Murry, *Cardiomyocyte grafting for cardiac repair: graft cell death and anti-death strategies*. J Mol Cell Cardiol, 2001. **33**(5): p. 907-21.
151. Halevy, O., B.G. Novitch, D.B. Spicer, S.X. Skapek, J. Rhee, G.J. Hannon, D. Beach, and A.B. Lassar, *Correlation of terminal cell cycle arrest of skeletal muscle with induction of p21 by MyoD*. Science, 1995. **267**(5200): p. 1018-21.
152. Jankowski, R.J., B.M. Deasy, B. Cao, C. Gates, and J. Huard, *The role of CD34 expression and cellular fusion in the regeneration capacity of myogenic progenitor cells*. J Cell Sci, 2002. **115**(Pt 22): p. 4361-74.

153. Jain, M., H. DerSimonian, D.A. Brenner, S. Ngoy, P. Teller, A.S. Edge, A. Zawadzka, K. Wetzel, D.B. Sawyer, W.S. Colucci, C.S. Apstein, and R. Liao, *Cell therapy attenuates deleterious ventricular remodeling and improves cardiac performance after myocardial infarction*. *Circulation*, 2001. **103**(14): p. 1920-7.
154. Rissanen, T.T., I. Vajanto, M.O. Hiltunen, J. Rutanen, M.I. Kettunen, M. Niemi, P. Leppanen, M.P. Turunen, J.E. Markkanen, K. Arve, E. Alhava, R.A. Kauppinen, and S. Yla-Herttuala, *Expression of vascular endothelial growth factor and vascular endothelial growth factor receptor-2 (KDR/Flk-1) in ischemic skeletal muscle and its regeneration*. *Am J Pathol*, 2002. **160**(4): p. 1393-403.
155. Germani, A., A. Di Carlo, A. Mangoni, S. Straino, C. Giacinti, P. Turrini, P. Biglioli, and M.C. Capogrossi, *Vascular endothelial growth factor modulates skeletal myoblast function*. *Am J Pathol*, 2003. **163**(4): p. 1417-28.
156. Takuma, S., K. Suehiro, C. Cardinale, T. Hozumi, H. Yano, J. Shimizu, S. Mullis-Jansson, R. Sciacca, J. Wang, D. Burkhoff, M.R. Di Tullio, and S. Homma, *Anesthetic inhibition in ischemic and nonischemic murine heart: comparison with conscious echocardiographic approach*. *Am J Physiol Heart Circ Physiol*, 2001. **280**(5): p. H2364-70.
157. Kawata, H., K. Yoshida, A. Kawamoto, H. Kurioka, E. Takase, Y. Sasaki, K. Hatanaka, M. Kobayashi, T. Ueyama, T. Hashimoto, and K. Dohi, *Ischemic preconditioning upregulates vascular endothelial growth factor mRNA expression and neovascularization via nuclear translocation of protein kinase C epsilon in the rat ischemic myocardium*. *Circ Res*, 2001. **88**(7): p. 696-704.
158. Angoulvant, D., S. Fazel, and R.K. Li, *Neovascularization derived from cell transplantation in ischemic myocardium*. *Mol Cell Biochem*, 2004. **264**(1-2): p. 133-42.
159. Silva, G.V., S. Litovsky, J.A. Assad, A.L. Sousa, B.J. Martin, D. Vela, S.C. Coulter, J. Lin, J. Ober, W.K. Vaughn, R.V. Branco, E.M. Oliveira, R. He, Y.J. Geng, J.T. Willerson, and E.C. Perin, *Mesenchymal stem cells differentiate into an endothelial phenotype, enhance vascular density, and improve heart function in a canine chronic ischemia model*. *Circulation*, 2005. **111**(2): p. 150-6.
160. Davani, S., A. Marandin, N. Mersin, B. Royer, B. Kantelip, P. Herve, J.P. Etievent, and J.P. Kantelip, *Mesenchymal progenitor cells differentiate into an endothelial phenotype, enhance vascular density, and improve heart function in a rat cellular cardiomyoplasty model*. *Circulation*, 2003. **108 Suppl 1**: p. II253-8.
161. Giordano, F.J. and R.S. Johnson, *Angiogenesis: the role of the microenvironment in flipping the switch*. *Curr Opin Genet Dev*, 2001. **11**(1): p. 35-40.

162. Shweiki, D., A. Itin, D. Soffer, and E. Keshet, *Vascular endothelial growth factor induced by hypoxia may mediate hypoxia-initiated angiogenesis*. *Nature*, 1992. **359**(6398): p. 843-5.
163. Lee, R.J., M.L. Springer, W.E. Blanco-Bose, R. Shaw, P.C. Ursell, and H.M. Blau, *VEGF gene delivery to myocardium: deleterious effects of unregulated expression*. *Circulation*, 2000. **102**(8): p. 898-901.
164. Carmeliet, P., *VEGF gene therapy: stimulating angiogenesis or angioma-genesis?* *Nat Med*, 2000. **6**(10): p. 1102-3.
165. Stamm, C., B. Westphal, H.D. Kleine, M. Petzsch, C. Kittner, H. Klinge, C. Schumichen, C.A. Nienaber, M. Freund, and G. Steinhoff, *Autologous bone-marrow stem-cell transplantation for myocardial regeneration*. *Lancet*, 2003. **361**(9351): p. 45-6.
166. Peng, H., V. Wright, A. Usas, B. Gearhart, H.C. Shen, J. Cummins, and J. Huard, *Synergistic enhancement of bone formation and healing by stem cell-expressed VEGF and bone morphogenetic protein-4*. *J Clin Invest*, 2002. **110**(6): p. 751-9.